

Waste Management Institute  
Marine Sciences Research Center  
State University of New York  
Stony Brook, New York 11794

The Fixation of Incineration Residues:

Phase II

Interim Report - May, 1987

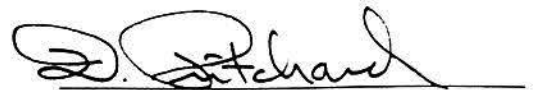
Prepared for

New York State Legislative Commission on the  
Water Resource Needs of Long Island

Working Paper #28

Reference 87-3

Approved for Distribution

A handwritten signature in black ink, appearing to read "D. Pritchard", written over a horizontal line.

D. Pritchard, Acting Director

## ABSTRACT

Incineration residues obtained from operational facilities in the New York Metropolitan area were successfully stabilized with additives including Portland cement, lime, sodium carbonate, and sand to form blocks. The high compressive strengths of these blocks indicated that the blocks would be suitable for marine disposal and for use by the construction industry.

Elemental analysis of stabilized incineration residues showed that the blocks were enriched in lead, zinc, copper and iron. Chemical testing showed that leachate from stabilized incineration residues did not exceed EPA limits for toxicity. Furthermore, seawater tank leaching studies showed that metals such as lead, zinc and copper were effectively retained by the stabilized blocks. Calcium leaching data from the tank studies indicates that the blocks would have a potentially long lifetime in the sea.

Laboratory block fabrication techniques were successfully transferred to existing commercial block making technologies. On three occasions, successful block making runs with incineration residue were completed using conventional machines at an operating block factory. Accelerated block curing resulted in strengths adequate for handling and stacking of blocks by automatic block handling equipment.

Results of chemical, physical and biological studies show that stabilized incineration residue is compatible with the marine environment. Tank leaching studies show that metals are effectively retained by the blocks. Block strengths were shown to increase with increasing seawater exposure and bioassay studies show that stabilized incineration residues do not appear toxic to marine organisms. On the basis of these results, an artificial habitat was constructed using stabilized incineration residue in Conscience Bay, Long Island Sound.

Blocks of stabilized incineration residue, Portland cement and sand were found to possess compressive strengths suitable for use by the construction industry. Engineering evaluations and plans to construct a boathouse using stabilized incineration residue blocks continue.

## Table of Contents

<u>Section</u>	<u>Page</u>
Abstract.....	ii
List of Figures.....	ix
List of Tables.....	xi
Acknowledgements.....	xvii
1 Introduction/Overview.....	1
1.1 Project Description.....	1
1.2 Project Objectives.....	1
1.3 Accomplishments.....	2
1.4 Conclusions.....	3
2 Incineration Waste Characteristics.....	5
2.1 Incineration Residues.....	5
2.2 Bulk Properties.....	5
2.2.1 Particle-size Analysis.....	5
2.2.2 Moisture Content.....	6
2.2.3 Loss on Ignition.....	6
2.2.4 pH.....	16
3 Chemical Properties of Incineration Waste.....	19
3.1 Incineration Ash Digestions for Elemental Analysis....	19
3.1.1 Sample Preparation.....	19
3.1.2 Digest Analysis.....	20
3.1.3 Results and Discussion.....	21
3.2 EP, TCLP, and Seawater Shaking Leachate Tests.....	26
3.2.1 Methods.....	26
3.2.1a EPA Toxicant Extraction Procedure.....	26
3.2.1b EPA Toxicant Characteristic Leaching Procedure.....	28
3.2.1c Seawater Shaking Extraction Procedure....	28
3.2.2 Leachate Analysis.....	28
3.2.3 Results and Discussion.....	30

<u>Section</u>	<u>Page</u>
3.2.3a pH.....	30
3.2.3b Particle Size.....	34
3.2.3c Comparison of Leaching Results with EPA Regulatory Limits for EP Toxicity....	35
3.3 Sequential Extraction of Particulate Incineration Ash.	37
3.3.1 Introduction.....	37
3.3.2 Methods.....	38
3.3.2a Acid Digestions.....	39
3.3.2b Metal Analysis.....	39
3.3.3 Results and Discussion.....	39
3.3.3a Short-term and Long-term Leachability for Particulate Ash.....	41
4 Large Scale Block Production.....	44
4.1 Process for Concrete Block Fabrication.....	44
4.2 Benefits of Construction Sized Block Unit.....	44
4.3 Block Fabrication at Barrasso and Sons, Inc.....	49
4.4 Block Fabrication Investigations at Alpena, December, 1986.....	52
4.4.1 Block Making Equipment.....	58
4.4.1a Block Machines.....	58
4.4.1b Steam Curing.....	58
5 Compressive Strength Testing of Incineration Ash Blocks....	59
5.1 Introduction.....	59
5.2 Methods.....	59
5.2.1 Compressive Strength Testing.....	59
5.2.2 Resistance to Impact.....	59
5.3 Results and Discussion.....	60
5.3.1 Compressive Strengths of Barrasso January 1986 Blocks.....	60
5.3.2 Compressive Strengths of Barrasso September 1986 Blocks.....	60
5.3.3 Compressive Strengths of Alpena Test Bricks....	67



<u>Section</u>	<u>Page</u>
5.3.3a Bottom Ash.....	67
5.3.3b Composite Ash.....	67
5.3.4 Effects of Additives on Brick Strength.....	70
5.3.4a Sand.....	70
5.3.4b Portland type II Cement.....	70
5.3.5 Compressive Strength of Alpena Blocks.....	71
5.3.6 Resistance to Impact.....	71
5.3.7 Effects of Seawater on Block Strength.....	74
5.3.7a Westchester Proctors.....	74
5.3.7b Barrasso Blocks.....	74
5.3.7c Alpena Blocks.....	74
5.4 Nondestructive Testing of Incinerator Waste Blocks....	84
5.4.1 Introduction.....	84
5.4.2 Methods.....	85
5.4.3 Results and Discussion.....	95
6 Minerology: Compositions and Alterations.....	130
6.1 Apparatus and Procedures.....	130
6.1.1 X-ray Diffraction Analysis.....	130
6.2 Results.....	131
6.2.1 Incineration Residues.....	131
6.2.2 Barrasso Fabricated Blocks.....	131
6.2.3 Effects of Seawater Submersion on Barrasso Blocks.....	131
6.2.4 Alpena Fabricated Blocks.....	131
6.3 Discussion.....	135
6.3.1 Barrasso Blocks.....	137
6.3.2 Alpena Blocks.....	137
7 Leaching Properties of Stabilized Incineration Ash Blocks..	138
7.1 Block Digestions for Elemental Analysis.....	138
7.1.1 Sample Preparation.....	138

7.1.2 Digest Analysis by Atomic Absorption Spectrophotometry.....	138
7.1.3 Results and Discussion.....	138
7.2 EP, TCLP, and Modified ASTM Leaching Tests.....	140
7.2.1 Sample Preparation.....	140
7.2.2 Leachate Analysis.....	140
7.2.3 Results and Discussion.....	142
7.2.3a pH.....	146
7.2.3b Effects of Stabilization of Incineration Residues on Metal Leaching.....	146
7.2.3c Comparison of Leaching Results with EPA Regulatory Limit for EP Toxicity and Drinking Water.....	147
7.3 Seawater Tank Dissolution Study.....	149
7.3.1 Materials and Methods.....	149
7.3.1a Experimental Design.....	149
7.3.1b Leachate Analysis.....	151
7.3.1c Leachable Fraction Analysis.....	151
7.3.1d Estimation of Pore Water pH.....	153
7.3.2 Results.....	153
7.3.2a Determination of Metal Fluxes.....	153
7.3.2b Calcium Release.....	153
7.3.2c Calcium Flux.....	157
7.3.2d Magnesium Uptake.....	158
7.3.2e Magnesium Flux.....	158
7.3.2f Copper, Lead, and Cadmium Release.....	162
7.3.2g Copper, Lead, and Cadmium Flux.....	162
7.3.3 Application of Results to a Diffusion Model....	166
7.3.3a Diffusion Model.....	166
7.3.3b Calcium Diffusion Coefficients.....	167
7.3.3c Copper Diffusion Coefficients.....	169
7.3.4 Calcium Discussion.....	169
7.3.4a Source of Leachable Calcium.....	173

<u>Section</u>	<u>Page</u>
7.3.4b pH.....	173
7.3.4c Magnesium in Seawater.....	176
7.3.4d Temperature.....	177
7.3.5 Copper, Lead, and Cadmium Discussion.....	178
7.3.5a pH.....	179
7.3.5b Cement.....	179
7.4 Sequential Extraction of Stabilized Incineration Ash..	180
7.4.1 Methods.....	180
7.4.2 Results and Discussion.....	180
7.4.2a Short-term and Long-term Leachability for Stabilized Incineration Ash.....	180
7.4.2b Matrix Associated Metals.....	184
 8 Bioassays For Potential Toxicity of Incineration Waste in the Sea.....	185
8.1 Toxicity Assays With Cultures of Marine Plants.....	185
8.1.1 Materials and Methods.....	185
8.1.1a Incinerator Ash Leachates.....	185
8.1.1b Bioassay Method.....	186
8.1.1c Statistical Analysis.....	188
8.1.2 Results.....	188
8.1.2a Westchester Ash Leachates.....	189
8.1.2b Huntington Ash Leachates.....	189
8.1.3 Conclusions.....	194
8.2 Chronic Exposure to Incineration Waste Suspension.....	195
8.2.1 Methods.....	195
8.2.2 Tissue Digestion Methods.....	198
 9 Utilization of Stabilized Incineration Waste Blocks.....	200
9.1 Boathouse Construction.....	200
9.1.1 Chemical Evaluation of MSRC Soils.....	200
9.1.1a Methods.....	200
9.1.1b Results and Discussion.....	203

Section

Page

9.1.2 Radon Emanating From Incineration Ash: Results From City, Huntington, and Westchester Ashes and Blocks.....	203
9.1.2a Introduction.....	203
9.1.2b Sample Preparation.....	207
9.1.2c Methods.....	208
9.1.2d Results and Discussion.....	208
9.2 Artificial Reef Construction.....	210
9.2.1 Model Estimate of Marine Disposal Impacts.....	210
9.2.1a Limitations of the Model Estimate.....	214
10 References.....	217

## List of Figures

<u>Figure</u>		<u>Page</u>
2.1a	Grain size distribution curve for Westchester ash .....	8
2.1b	Grain size distribution curve for Westchester ash .....	9
2.1c	Grain size distribution curve for Westchester ash .....	10
3.1	Sequential chemical extraction of particulate incineration residue .....	43
4.1	Simplified schematic of block processing .....	45
4.2	Besser Vibrapac block machine .....	46
4.3	Experimental blocks produced at Alpena, Michigan .....	47
4.4	Steam kiln used to cure coal waste blocks, Alpena, Michigan .....	48
5.1	Compressive strength of Barrasso January 1986 blocks versus time .....	63
5.2	Compressive strength of Barrasso September 1986 blocks versus time .....	66
5.3	Inspect resistance versus compressive strength for Alpena blocks .....	76
5.4	Compressive strength versus seawater submersion time for Westchester proctors .....	79
5.5	Compressive strength versus seawater submersion time for Barrasso blocks .....	82
5.6	Testing schedule .....	88
5.7	Block diagram of ultrasonic testing system .....	92
5.8	Digitized reference and sample signals .....	94
5.9	Block diagram of testing procedure .....	97
5.10a	Density time series for individual samples and means .....	102
5.10b	Density time series for individual samples and means .....	104
5.11a	Velocity time series for individual samples and means .....	106
5.11b	Velocity time series for individual samples and means .....	108
5.12a	Elastic modulus time series for individual samples and means .....	110
5.12b	Elastic modulus time series for individual samples and means .....	112

## List of Figures

<u>Figure</u>		<u>Page</u>
5.13	Compressive strength versus time .....	118
5.14	Elastic modulus versus time .....	120
5.15	Compressive strength versus elastic modulus .....	122
5.16	Velocity versus density .....	124
5.17	Velocity versus density for sample #30 .....	127
7.1	Cumulative release of calcium from stabilized incineration ash in seawater .....	155
7.2	Cumulative release of calcium and uptake of magnesium for stabilized incineration ash blocks .....	161
7.3	Cumulative release of copper from stabilized incineration ash blocks in seawater .....	165
7.4	Pore water pH versus time for stabilized incineration ash in seawater .....	175
7.5	Sequential extraction of stabilized incineration waste ....	183
8.1	Schematic diagram of agitator mechanism .....	197
9.1	Soil sample collection sites at the MSRC boathouse .....	202
9.2	The metal:iron ratio for MSRC soil metals .....	206
9.3	Diagram showing the downstream dispersion of leachate from a stabilized incineration ash reef configuration .....	213

## List of Tables

<u>Table</u>		<u>Page</u>
2.1	Westchester ash cumulative frequency analysis .....	11
2.2	Westchester ash particle size analysis .....	13
2.3	Moisture content of Westchester ash samples .....	15
2.4	Loss on ignition for Westchester ash samples .....	17
2.5	pH values for Westchester ash samples .....	18
3.1	Elemental concentrations of NBS 1633a standard fly ash and % recovery, HF-H <sub>3</sub> BO <sub>3</sub> -AAS method .....	22
3.2	Metal concentrations in incineration residues .....	23
3.3	Metal concentrations in other incineration residues .....	25
3.4	Measured pH values for particulate incineration residues in EP, TCLP and seawater shaking leaching tests and amount of acetic acid added in EP test .....	27
3.5	Metal concentrations in EP leachate of incineration residues .....	31
3.6	Metal concentrations in TCLP leachate of incineration residues .....	32
3.7	Metal concentrations in seawater shaking leachate of incineration residues .....	33
3.8	Compressive strength of EP, TCLP and seawater shaking leachate concentrations from particulate incineration residues with EP regulatory limits for EP toxicity .....	36
3.9	Sequential extraction of metals from particulate incineration ash .....	40
4.1	Mix designs and color coding of Barrasso blocks (1/86) ....	50
4.2	Mix designs and color coding of Barrasso blocks (9/86) ....	53
4.3	Mix designs for Alpena bricks (12/86) .....	55
4.4	Mix designs for Alpena blocks (12/86) .....	57
5.1	Compressive strengths of Barrasso January 1986 hollow masonry blocks .....	61
5.2	Compressive strengths of Barrasso September 1986 blocks ...	64
5.3	Compressive strengths of Alpena 12/86 bricks .....	68

## List of Tables

<u>Table</u>		<u>Page</u>
5.4	Compressive strengths of Alpena (8 x 8 x 16 inch) blocks ..	72
5.5	Alpena block (8 x 8 x 16 in) weights, densities, and impact resistance after 1 day cure .....	73
5.6	Seawater submersion test of Westchester proctors .....	77
5.7	Compressive strength of seawater submerged (9/86) Barrasso blocks .....	80
5.8	Seawater submersion test for Alpena reef block .....	83
5.9	Chronological NDE data for individual samples 28, 29, and 30 and their group mean .....	99
5.10	Chronological NDE data for individual samples 25, 26, and 27 and their group mean .....	100
5.11	Individual parameter values for chronological test groups: values on days of compressive tests.....	113
5.12	Mean parameters and standard deviations for chronological test groups: values on days of compressive tests .....	114
5.13	Initial mean NDE parameter values for chronological test groups on day 1 .....	115
6.1	Mineral composition of Westchester incineration ash samples .....	132
6.2	Mineral composition of seawater submerged and air-cured hollow masonry units fabricated at Barrasso & Sons, Inc. ..	133
6.3	Mineral composition of Alpena fabricated hollow masonry blocks .....	134
7.1	Metal concentrations in stabilized incineration ash blocks	
7.2	Measured pH values from stabilized incineration ash blocks in EP, TCLP and seawater shaking leaching tests and amount of acetic acid added in EP test .....	139
7.3	Metal concentrations in EP leachate of stabilized incineration ash blocks .....	141
7.4	Metal concentrations in TCLP leachate of stabilized incineration ash blocks .....	143



## List of Tables

<u>Table</u>		<u>Page</u>
5.4	Compressive strengths of Alpena (8 x 8 x 16 inch) blocks ..	72
5.5	Alpena block (8 x 8 x 16 in) weights, densities, and impact resistance after 1 day cure .....	73
5.6	Seawater submersion test of Westchester proctors .....	77
5.7	Compressive strength of seawater submerged (9/86) Barrasso blocks .....	80
5.8	Seawater submersion test for Alpena reef block .....	83
5.9	Chronological NDE data for individual samples 28, 29, and 30 and their group mean .....	99
5.10	Chronological NDE data for individual samples 25, 26, and 27 and their group mean .....	100
5.11	Individual parameter values for chronological test groups: values on days of compressive tests.....	113
5.12	Mean parameters and standard deviations for chronological test groups: values on days of compressive tests .....	114
5.13	Initial mean NDE parameter values for chronological test groups on day 1 .....	115
6.1	Mineral composition of Westchester incineration ash samples .....	132
6.2	Mineral composition of seawater submerged and air-cured hollow masonry units fabricated at Barrasso & Sons, Inc. ..	133
6.3	Mineral composition of Alpena fabricated hollow masonry blocks .....	134
7.1	Metal concentrations in stabilized incineration ash blocks .	139
7.2	Measured pH values from stabilized incineration ash blocks in EP, TCLP and seawater shaking leaching tests and amount of acetic acid added in EP test .....	141
7.3	Metal concentrations in EP leachate of stabilized incineration ash blocks .....	143
7.4	Metal concentrations in TCLP leachate of stabilized incineration ash blocks .....	144

## List of Tables

<u>Table</u>		<u>Page</u>
7.5	Metal concentrations in seawater shaking leachate of stabilized incineration ash blocks .....	145
7.6	Comparison of EP, TCLP and seawater shaking leachate concentrations from stabilized incineration ash blocks with EPA regulatory limits for EP toxicity and drinking water .....	148
7.7	Formulations and bulk characteristics of stabilized incineration ash blocks .....	150
7.8	Sampling intervals and measured pH values in tank study ..	152
7.9	Measured concentration and calculated flux of calcium in tank study .....	156
7.10	Measured concentration and calculated flux of magnesium in tank study .....	159
7.11	Measured concentration and calculated flux of copper in tank study .....	163
7.12	Variables used in eqs. 7.6 and 7.7 for calculating effective diffusion coefficients for calcium .....	168
7.13	Effective distance ( $x_c$ ) of the diffusion zone for calcium ..	170
7.14	Variables used in eqs. 7.6 and 7.7 for calculating effective diffusion coefficients for copper .....	171
7.15	Effective distance ( $x_c$ ) of the diffusion zone for copper ..	172
7.16	Sequential extraction of metals from stabilized incineration ash .....	181
8.1	Bioassay with <u>Thalassiosira</u> , Westchester MSW, batch 1 .....	190
8.2	Bioassay with <u>Thalassiosira</u> , Westchester MSW, batch 2 .....	191
8.3	Bioassay with <u>Prorocentrum</u> , Westchester MSW, batch 3 .....	192
8.4	Bioassay with <u>Thalassiosira</u> , Huntington MSW, batch 1 .....	193
8.5	Elemental concentrations and percent recoveries from NBS standard tissue digests .....	199
9.1	Elemental analysis (ug/g) of soil .....	204

## List of Tables

<u>Table</u>		<u>Page</u>
9.2	$^{222}\text{Rn}$ emanation from, and $^{226}\text{Ra}$ gamma activity of, ash and aggregate samples .....	209
9.3	Approximate supported radon content of a building 60' x 90' x 20' .....	211
9.4	Model calculations of dispersion distance (L) for copper .....	215

## PARTICIPANTS IN THIS STUDY

This report reflects the work of many members of the State University of New York at Stony Brook, New York 11794 and our subcontractors. Those participating in the study are listed below.

Frank J. Roethel  
Vincent T. Breslin  
Victor Schaeperkoetter  
Mary Ann Lau  
Peter M. J. Woodhead  
Ruth Gregg  
Kyeong Park  
Herbert Carleton  
Joseph Muratore  
Nathan Epler  
Jeffrey Mantus  
Alan Milligan

### Subcontractors

Barrasso and Sons, Inc. Islip Terrace, N.Y.  
George Hampton  
Frank Scafuri

Besser Company, Alpena, Michigan.  
Lucas Pfeiffenberger  
Robert Rohn  
Michael Gentry  
Glen Campbell

## ACKNOWLEDGMENTS

Our sincere thanks to Signal Environmental Systems, the Town of Huntington and the New York City Department of Sanitation for their cooperation and making available the incineration residue utilized in this investigation. We are pleased to acknowledge the help of Mr. George Proios, New York State Commission on Water Resource Needs of Long Island for his valuable comments and active involvement in this investigation. We are especially indebted to Senator Caesar Trunzo whose early interest and participation in this investigation was directly associated with the funding of this project by the New York State Legislature.

## Section 1

### INTRODUCTION/OVERVIEW

#### 1.1 PROJECT DESCRIPTION

This interim report is part of an ongoing investigation into the feasibility of stabilizing incineration residue produced by waste-to-energy facilities. This study is undertaken by the Waste Management Institute (WMI) of the Marine Sciences Research Center (MSRC) under the sponsorship of the New York State Legislature. The Legislative Commission for the Water Resource Needs for Long Island represents the lead agency for this study. This comprehensive report describes in detail the studies made from April 1986 through April 1987, which culminated in the successful placement of the first artificial marine habitat fabricated using incineration residue in the waters of Conscience Bay, Long Island Sound.

This report is the third issued under this investigation to evaluate the feasibility of stabilizing incineration residue and evaluating potential marine and land disposal options. The disposal of incineration wastes in an environmentally acceptable manner is particularly difficult in the highly urbanized areas of the industrial northeast states. In this region, as in others, land for waste disposal is not available locally and the potential for groundwater pollution exists. As a result, alternatives for incineration residue disposal are needed.

#### 1.2 PROJECT OBJECTIVES

The overall objective of this investigation is to explore the feasibility and environmental effects of both marine and terrestrial disposal of stabilized incineration residues (SIR). The program has led to the construction of a small artificial habitat in the waters of Conscience Bay and the production of hollow masonry blocks possessing strengths acceptable for use by the construction industry. The objectives of the second phase of the investigation, which this report addresses, was to examine in depth the chemical characteristics of stabilized incineration residue, develop

non-destructive engineering methods to evaluate the structural properties of SIR blocks, to adapt existing concrete construction methods to SIR block fabrication and to investigate questions of environmental acceptability of SIR in both marine and terrestrial disposal applications.

### 1.3 ACCOMPLISHMENTS

Block Production. On three occasions, using the facilities at Barrasso and Sons, Islip Terrace, N.Y. and the Besser Co., Alpena, Michigan, blocks (8 x 8 x 16 inch) were successfully machine formed with concrete block equipment and a variety of incineration residues and additives were examined for their suitability to fabricate block. Accelerated block curing procedures were developed using selected additives and steam kilns. Some blocks developed strengths within one day of curing which were greater than those attained previously in one month of ambient curing. The strengths developed were adequate for handling and stacking by automatic block factory handling equipment. Accelerated curing allowed for significant cost reductions by eliminating the need for storing/curing space. Accelerated curing also afforded independence from environmental factors such as rain and low winter temperatures.

Technology Transfer. The new fabrication techniques were successfully transferred to the commercial factory through experimental block production runs with 20 tons of incineration residues, using the conventional plant and machines at the operating block factory that would ultimately be used for full scale reef-block production.

Habitat Construction. Cured reef blocks were transported by road and sea to the project demonstration site. On 27 April 1987, approximately 30 stabilized incineration residue blocks along with 30 standard cement blocks were submerged in 30 feet of water in Conscience Bay, Long Island Sound.

Chemical Testing. Block elemental composition was determined using a variety of techniques. Mineral phases and mineralogical changes were determined using scanning electron microscopy and x-ray diffraction. Long term leaching studies yielded leaching rates for major and minor block

components. These data were used to calculate effective diffusion coefficients for calcium and copper. Calcium diffusion coefficients were useful in calculating the expected lifetime of stabilized incineration residues in seawater.

Physical Testing. Ongoing laboratory experiments have confirmed several trends on the effects of seawater submersion on test blocks. The compressive strengths of submerged stabilized incineration residue blocks were found to increase with time. Non-destructive ultrasonic testing procedures were developed which showed a positive correlation between block strength and sound velocity.

Biological Testing. Bioassay of stabilized incineration residue elutriates in seawater had no significant effects upon marine phytoplankton cultures. Experiments to evaluate the potential uptake of block components by the mussel midulus edulus were initiated and are currently ongoing.

#### 1.4 CONCLUSIONS

Blocks of stabilized waste can be produced with conventional concrete block machines. Residue from waste-to-energy facilities stabilized with Portland cement can readily be processed into blocks by conventional concrete block factory machines. Accelerated curing developed block strengths sufficient to allow automatic factory handling for immediate transport and disposal.

Equipment has the capacity for processing incineration wastes. The materials capacity of commercial block machines and associated equipment are large enough to handle the daily combustion wastes from a waste-to-energy facility.

Block materials appear compatible with the marine environment. Diverse data from laboratory and field investigations of the physical, chemical, and biological interactions of a variety of stabilized incineration residue mixes in seawater have all suggested that in the form of solid blocks, the material is compatible with the marine environment. During prolonged seawater



exposure, where blocks have been in flowing seawater tanks for more than one year, the physical integrity has been maintained and material strength increased. Leaching of major components decreased with time and minor components were retained by the blocks. The blocks do not appear to be toxic to organisms in the sea.

Demonstration habitat will be studied for potential impacts. With the establishment of a small marine habitat, the program's major task will focus on the effects of the habitat on the marine environment.

Artificial reefs would enhance productivity and fishing. As potentially valuable resource materials for artificial fishing reef construction, stabilized incineration residue blocks may modify the local environment to increase biological productivity and raise the catches of finfishes, crabs, and lobsters.

Structural integrity suitable for construction materials. Blocks of incineration residue, Portland cement and sand were fabricated at the Besser facility and were shown to possess strengths suitable for use by the construction industry. Engineering evaluations and plans to construct a boathouse using stabilized incineration residue blocks continue.

## Section 2

### INCINERATION WASTE CHARACTERISTICS

#### 2.1 INCINERATION RESIDUES

Incineration residues were sampled on four occasions from the Signal-Resco resource recovery facility located in Westchester County, N.Y. for use in the stabilization studies. Incineration residues analyzed and discussed in this section are labeled according to their respective collection dates. The August 1985 composite ash was collected during Phase One of this study. The January 1986 composite ash was collected to maintain sufficient quantities of composite ash for on-going laboratory studies. Additional residues were collected on two separate occasions for use in large scale block manufacturing. The September 1986 composite ash was sampled for use at Barasso and Sons, Inc. (Islip Terrace, N.Y.) for stabilization into hollow masonry blocks, and November 1986 composite ash and bottom ash were collected for shipment to the Besser Company, Alpena, Michigan for stabilization into hollow masonry blocks (Section 4).

Two ash types were collected during November 1986: bottom ash, and composite ash. Composite ash is a mixture of bottom ash and fly ash. For the particle-size analysis described below, a third type of ash, crushed, was also analyzed. Crushed ash was created at the Besser Company, Alpena, Michigan, from bottom ash retained by a 3/8" sieve. This material was crushed mechanically and resieved to less than 3/8".

#### 2.2 BULK PROPERTIES

##### 2.2.1 Particle-size Analysis

The distribution of particle sizes in the incineration residues was determined by sieving a sample of approximately 3 kg for the January 1986 sample, 5 kg for the September 1986 ash, 1.5 kg for the November 1986 composite ash and 5 kg for November 1986 bottom ash. The analysis followed ASTM D422-63 using a series of U.S. Standard Sieves: 3 in, 1.5 in, 0.75 in, Numbers 4, 10,

18, 40, 60, 100 and 200. The residues were sieved dry and shaken by hand for the three larger sized sieves. The sieved residue was then transferred into the smaller sieves and placed into a Ro-Tap sieve shaker and mechanically shaken.

Results of the grain size analysis are shown in Figure 2.1 and Table 2.1. The grain size distributions for the six ash samples are predominantly in the sand size range ( $<4.75$  mm,  $>0.075$  mm) with lesser amounts in the gravel ( $>4.75$  mm) and silt or clay sizes ( $<0.075$  mm). The August 1985 composite sample was the finest with 4.47% of the ash in the gravel range, 89.2% of the ash falling in the sand range and 6.27% in the silt or clay range. In contrast the January 1986 ash sample contained 28.9% of the ash in the gravel range, 67.31% in the sand size range, and 3.79% in the silt or clay size range.

Mean grain sizes of the collected residues are shown in Table 2.2. All 1986 samples are significantly larger than the August 1985 sample; mean grain size ranges from 1.02 mm to 2.03 mm for the September 1986 composite ash and January 1986 composite ash, respectively, while the August 1985 composite sample had a mean grain size of only 0.482 mm. The November 1986 crushed sample had a mean grain size value of 1.79 mm.

#### 2.2.2 Moisture Content

Moisture content was determined in replicate ( $n=5$ ) on 10 gram samples of fresh residue following each collection event. Samples were dried to constant weight in an oven at  $110^{\circ} \pm 5^{\circ}\text{C}$ .

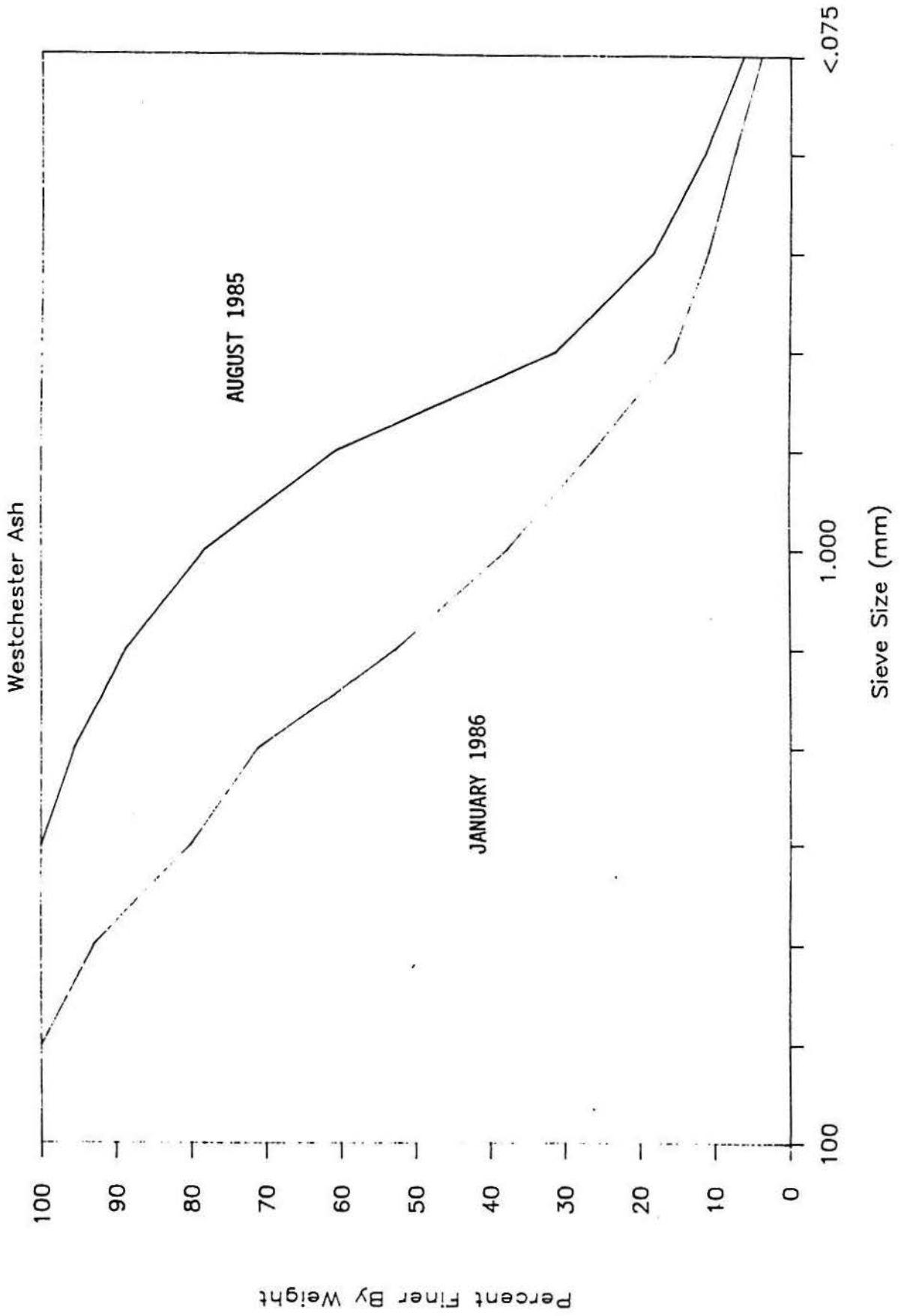
Results are shown in Table 2.3. Moisture contents ranged from 2.25% for August 1985 composite ash to 15.3% for the November 1986 composite ash. For the November 1986 composite sample one measurement was taken on a 400 gram sample at the Besser Company. Since there is only one measurement for this sample, no standard deviation is reported.

#### 2.2.3 Loss on Ignition

The dried samples of residue used for determination of moisture content

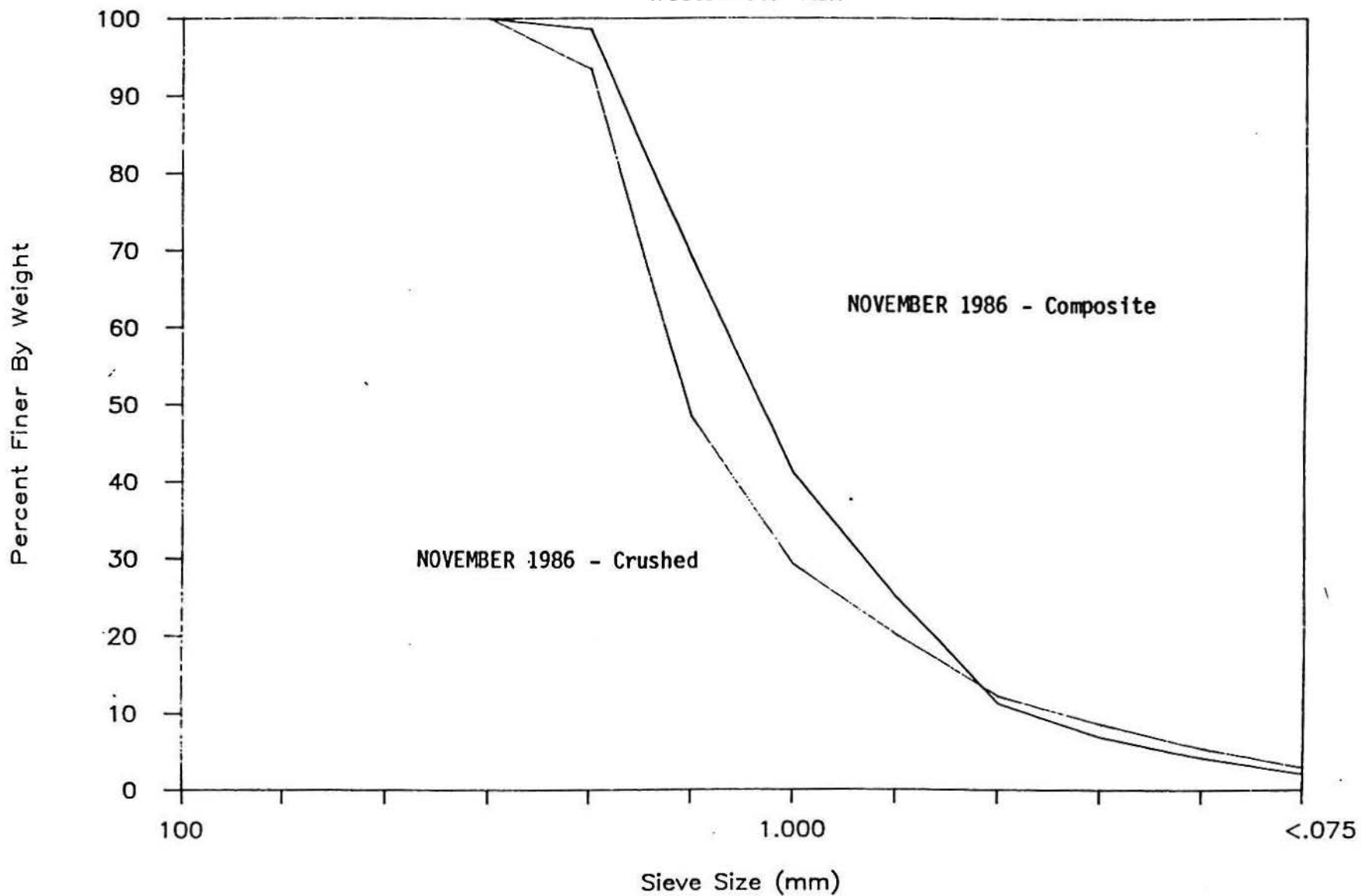
Figures 2.1a-c Grain size distribution curve for Westchester ash.

# GRAIN SIZE ANALYSIS



# GRAIN SIZE ANALYSIS (cont.)

Westchester Ash



# GRAIN SIZE ANALYSIS (cont.)

Westchester Ash

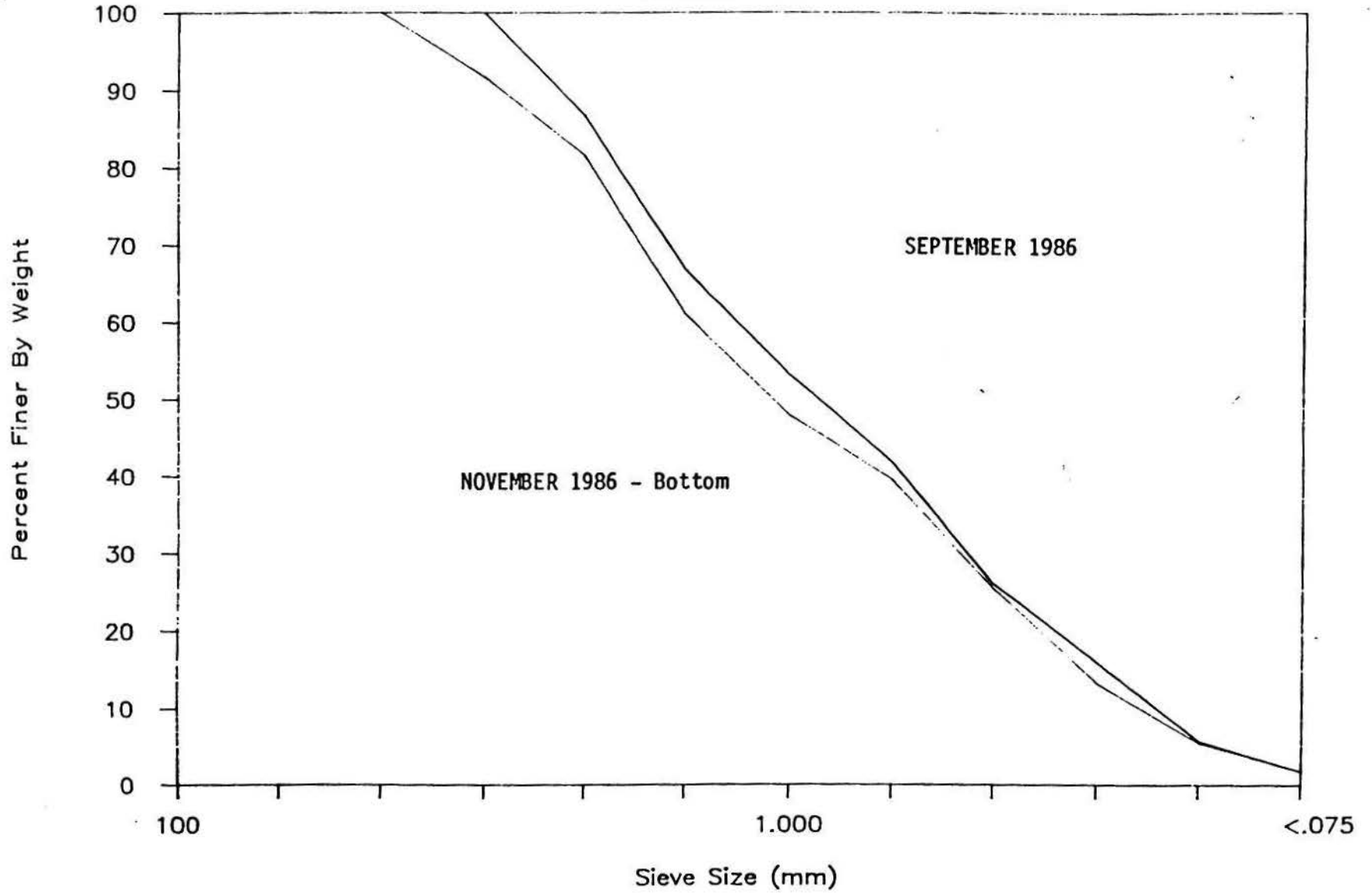


Table 2.1. Weschester Ash Cumulative Frequency Analysis.

SIEVE NUMBER	OPENING SIZE	(mm)	August 85 COMPOSITE ASH		January 86 COMPOSITE ASH		September 86 COMPOSITE ASH	
			% RETAINED	CUM FREQ	% RETAINED	CUM FREQ	% RETAINED	CUM FREQ
	.75"	19.050			7.07	100.0		
	.50"	12.700			12.90	92.9		
	.375"	9.525	4.47	100.0	8.93	80.0	13.23	100.0
4	4.75 mm	4.750	6.87	95.5	18.38	71.1	19.79	86.8
10	2.00 mm	2.000	10.56	88.7	14.95	52.7	13.73	67.0
18	1.00 mm	1.000	17.36	78.1	11.45	37.8	11.40	53.2
40	425 $\mu$ m	0.425	29.46	60.8	10.76	26.3	15.71	41.8
60	250 $\mu$ m	0.250	12.92	31.3	4.52	15.6	10.17	26.1
100	150 $\mu$ m	0.150	6.92	18.4	3.56	11.1	10.22	16.0
200	75 $\mu$ m	0.075	5.18	11.5	3.70	7.5	3.95	5.7
	<75 $\mu$ m	<.075	6.27	6.3	3.79	3.8	1.78	1.8
TOTAL WEIGHT			100%		100%		100%	



Table 2.1. (continued).

SIEVE NUMBER	OPENING SIZE	(mm)	November 86 BOTTOM ASH		November 86 COMPOSITE ASH		November 86 CRUSHED ASH	
			% RETAINED	CUM FREQ	% RETAINED	CUM FREQ	% RETAINED	CUM FREQ
	.75"	19.050						
	.50"	12.700	8.32	100.0				
	.375"	9.525	10.13	91.7	1.41	100.0	6.54	100.0
4	4.75 mm	4.750	20.41	81.6	29.40	98.6	44.96	93.5
10	2.00 mm	2.000	13.23	61.1	28.07	69.2	19.23	48.5
18	1.00 mm	1.000	8.40	47.9	15.98	41.1	9.10	29.3
40	425 $\mu\text{m}$	0.425	13.99	39.5	13.76	25.1	7.91	20.2
60	250 $\mu\text{m}$	0.250	12.29	25.5	4.44	11.4	3.69	12.3
100	150 $\mu\text{m}$	0.150	7.76	13.2	2.72	6.9	3.14	8.6
200	75 $\mu\text{m}$	0.075	3.73	5.5	2.10	4.2	2.52	5.4
	<75 $\mu\text{m}$	<.075	1.74	1.74	2.12	2.12	2.90	2.9
TOTAL WEIGHT			100%		100%		100%	

Table 2.2. Weschester Ash Particle Size Analysis.

SIEVE NUMBER	OPENING SIZE	August 85 COMPOSITE ASH		January 86 COMPOSITE ASH		September 86 COMPOSITE ASH	
		GRAMS RETAINED	% RETAINED	GRAMS RETAINED	% RETAINED	GRAMS RETAINED	% RETAINED
	.75"			205.52	7.07		
	.50"			375.22	12.90		
	.375"	47.2	4.47	259.73	8.93	766.4	13.23
4	4.75 mm	72.5	6.87	534.53	18.38	1146.5	19.79
10	2.00 mm	111.4	10.56	434.93	14.95	795.3	13.73
18	1.00 mm	183.1	17.36	332.99	11.45	660.3	11.40
40	425 $\mu$ m	310.8	29.46	312.93	10.76	910.2	15.71
60	250 $\mu$ m	136.3	12.92	131.62	4.52	589.4	10.17
100	150 $\mu$ m	73.0	6.92	103.44	3.56	592.3	10.22
200	75 $\mu$ m	54.6	5.18	107.53	3.70	229.1	3.95
	<75 $\mu$ m	66.1	6.27	110.29	3.79	103.2	1.78
TOTAL WEIGHT		1055.0	100%	2908.7	100%	5792.7	100%
MEAN GRAIN SIZE (mm) =		0.482		2.03		1.02	

Table 2.2. (continued).

SIEVE NUMBER	OPENING SIZE	November 86 BOTTOM ASH		November 86 COMPOSITE ASH		November 86 CRUSHED ASH	
		GRAMS RETAINED	% RETAINED	GRAMS RETAINED	% RETAINED	GRAMS RETAINED	% RETAINED
	.75"						
	.50"	442.5	8.32				
	.375"	538.9	10.13	21.8	1.41	77.5	6.54
4	4.75 mm	1086.0	20.41	455.7	29.40	532.5	44.96
10	2.00 mm	704.0	13.23	435.1	28.07	227.7	19.23
18	1.00 mm	446.9	8.40	247.7	15.98	107.8	9.10
40	425 $\mu$ m	744.2	13.99	213.3	13.76	93.7	7.91
60	250 $\mu$ m	653.9	12.29	68.8	4.44	43.7	3.69
100	150 $\mu$ m	412.9	7.76	42.1	2.72	37.2	3.14
200	75 $\mu$ m	198.2	3.73	32.6	2.10	29.9	2.52
	<75 $\mu$ m	92.7	1.74	32.8	2.12	34.3	2.90
TOTAL WEIGHT		5320.1	100%	1549.9	100%	1184.3	100%
MEAN GRAIN SIZE (mm) =		1.32		1.41		1.79	

Table 2.3. Moisture content of the Westchester ash samples.

Ash Type	Moisture <sup>a</sup> Content (%)	Standard Dev.
August 85 COMPOSITE ASH	2.25 <sup>a</sup>	± 0.12
January 86 COMPOSITE ASH	14.1	± 1.14
September 86 COMPOSITE ASH	9.98	± 1.06
November 86 BOTTOM ASH	9.92 <sup>b</sup>	± 0.41
November 86 COMPOSITE ASH	15.3 <sup>c</sup>	

a. Moisture content (%) was determined at 105°C

b. n = 3

c. n = 1

were also used to measure loss on ignition (LOI). Samples were ignited in a covered crucible in a muffle furnace at controlled temperatures. Separate determinations were made for LOI at two temperatures,  $500^{\circ} \pm 50^{\circ}\text{C}$  and  $900^{\circ} \pm 50^{\circ}\text{C}$ .

Loss on ignition is useful because it offers a rough approximation of the amount of organic matter present in the ash. Results however, may also reflect loss of water of crystallization, loss of volatile organic matter before combustion, and decomposition of mineral salts during combustion. LOI is frequently determined at temperatures of between 900 to 1,000°C. In this study, LOI was also determined at 500°C since biogenic organics are burned off at this temperature. The biogenic carbon content of the residues is of interest in these studies.

Table 2.4 illustrates that the LOI values for the 1986 samples were significantly higher than 1985, both at 500°C and at 900°C. Loss on ignition values at 500°C ranged from 1.83% for August 1985 composite ash to 5.92% for November 1986 bottom ash. These values increased to 3.89% and 6.96% for August 1985 composite ash and November 1986 bottom ash at 900°C, respectively. These values are well under the ASTM C618 requirement of a maximum allowable loss on ignition of 12% for coal fly ash used in Portland cement concrete (ASTM, 1974).

#### 2.2.4 pH

The pH of incineration residue-distilled-deionized water mixtures (approximately 1:1 w/v) at 10 minutes was determined using an Orion Research Model 701A pH meter attached to a standard glass electrode.

All distilled-deionized water-incineration ash mixtures were alkaline (Table 2.5). pH of the incineration ash-distilled-deionized water mixtures ranged from 8.84 for November 1986 bottom ash to 12.7 for August 1985 composite ash.

Table 2.4. Loss on Ignition for the Westchester ash samples.

Ash Type	at 500°C % LOI ±(S.D.)	at 900°C % LOI ±(S.D.)
August 85 COMPOSITE ASH	1.83 ± (0.19)	3.89 ± (0.25)
January 86 COMPOSTIE ASH	5.04 ± (0.57)	6.44 ± (0.63)
September 86 COMPOSITE ASH	5.60 ± (1.54)	6.57 ± (1.81)
November 86 BOTTOM ASH	5.92 ± (0.97)	6.96 ± (1.24)
November 86 COMPOSITE ASH	5.23 ± (0.34)	6.51 ± (0.33)

Table 2.5. pH values for the Westchester ash samples.

Ash Type	pH <sup>a</sup>
August 1985 COMPOSITE ASH	12.7
January 1986 COMPOSITE ASH	11.5
September 1986 COMPOSITE ASH	10.4
November 1986 BOTTOM ASH	8.84
November 1986 COMPOSITE ASH	10.5

a. Incineration Ash-distilled-deionized water mixtures (1:1 w/v) at 10 minutes

## Section 3

## CHEMICAL PROPERTIES OF INCINERATION WASTE

## 3.1 INCINERATION ASH DIGESTIONS FOR ELEMENTAL ANALYSIS

Analysis of hydrofluoric-boric acid ( $\text{HF-H}_3\text{BO}_3$ ) digests by atomic absorption spectroscopy was used to determine the elemental composition of incineration residues. This method was a modification of the procedure reported by Silberman and Fisher (1979). It utilizes the ability of HF to breakdown silicious materials;  $\text{H}_3\text{BO}_3$  is used to complex remaining fluoride ions and to dissolve insoluble metal fluorides formed during digestion.

## 3.1.1 Sample Preparation

All glass and plasticware used were acid washed prior to use. Glassware was soaked in 10% HCl-10%  $\text{HNO}_3$  (Baker Analyzed<sup>®</sup>; J.T. Baker Chemical Co., Phillipsburg, NJ) for at least 24 h, rinsed with distilled-deionized (DID) water, soaked in 1% Ultrex<sup>®</sup> nitric acid (J.T. Baker Chemical Co.) for at least 24 h, and again rinsed several times with DID water. Plasticware was soaked in a solution of 10%  $\text{HNO}_3$  (Baker Analyzed<sup>®</sup>) for at least 24 h and rinsed with DID water. Acid cleaned glass and plasticware were then air dried in a laminar flow hood and stored in plastic bags prior to use. Acid washed volumetric flasks were wrapped in parafilm to prevent contamination.

Ash from three operational New York State facilities was utilized in the characterization studies. The Southwest Brooklyn plant operated by the City of New York, the Signal-Resco facility in Westchester County, and the Town of Huntington incinerator located in East Northport were selected. Ash was collected from each site and returned to our facility in steel 55 gallon drums. Ash samples were oven-dried at  $110^\circ\text{C} \pm 5^\circ\text{C}$  for 24 hours and sieved to obtain different size fractions for acid digestion (Table 3.2). New York City fly ash ( $\text{C}_1$  and  $\text{C}_2$ ) was collected in November 1985. Composite ash, a combination of bottom and fly ash was collected at the Westchester and Huntington facilities. Huntington composite ash ( $\text{H}_1$  and  $\text{H}_2$ ) was collected in October 1985. Westchester composite ash was collected on two separate occasions.  $\text{W}_1$  and



$W_2$  were collected in August 1985 while  $W_3$  and  $W_4$  were collected in September 1986.

Approximately 0.5 g ( $\pm 0.0001$ ) samples of each of these materials and National Bureau of Standards (NBS) 1633-a coal fly ash were weighed into 125 ml plastic polyethylene bottles followed by the addition of 10 ml of DID water and 10 ml of concentrated HF (Fisher Scientific Company, Fair Lawn, NJ). The mixtures were then shaken mechanically for 24 hours. Seventy mls of saturated  $H_3BO_3$  (Fisher Scientific Company) at 45°C was added and the samples were again agitated for 24 hours, followed by ultrasonication for 1 hour. The digests were filtered through 0.45  $\mu m$  Millipore<sup>®</sup> (Millipore Corp., Bedford, MA) filter papers. The filtrates were transferred to 100 ml glass volumetric flasks, brought to volume with saturated  $H_3BO_3$  (25°C), then stored in a refrigerator at 5°C prior to analysis.

### 3.1.2 Digest Analysis

Replicate samples (n=3) of each incineration ash were analyzed for calcium, magnesium, aluminum, iron, copper, lead, zinc, cadmium, nickel, manganese, chromium, cobalt, arsenic and mercury by atomic absorption spectrophotometry.

All Ca and Mg analyses were performed using an air-acetylene flame on the Perkin Elmer Model 5000 Atomic Absorption Spectrophotometer (AAS; Perkin-Elmer, Norwalk, CT) without background correction. Samples and standards were prepared in 0.5% (w/v)  $La^{+3}$  solution, added as lanthanum oxide ('Baker'  $La_2O_3$ ), to enhance the sensitivity of the analysis by suppressing interferences caused by the presence of other ions.

Analysis of Fe, Cu, Zn, Mn, Ni was also performed using an air-acetylene flame without background correction. Aluminum was determined using a nitrous oxide-acetylene flame without background correction. Concentration of Pb, Cd, Cr, Co, and As was determined using the Perkin Elmer Model 5000 AAS equipped with a HGA-500 graphite atomizer and AS-40 autosampler with background correction. All standards were serial dilutions of Fisher Certified atomic absorption standards (Fisher Scientific Company) and were prepared in the same

matrix present in the samples to be analyzed. Concentration of Pb in HF (10%)-H<sub>3</sub>BO<sub>3</sub> (80%) solution was so high that standard solutions and samples were prepared in 0.1% Ultrex<sup>®</sup> HNO<sub>3</sub> solution for Pb analysis. Ammonium phosphate [(NH<sub>4</sub>)<sub>2</sub>HPO<sub>4</sub>] (1% w/v) was used for Cd analysis and 0.1% Ni (w/v) as Ni(NO<sub>3</sub>)<sub>2</sub> (1:1) was used for As analysis to allow for the use of higher charring temperatures (Ediger, 1975).

Mercury was determined using the MHS-10 hydride generator attached to the Perkin Elmer Model 5000 AAS. Using the MHS-10, Hg was converted in dilute acid solution to its hydride by the addition of excess sodium borohydride (NaBH<sub>4</sub>, 3% w/v) and sodium hydroxide (NaOH, 1% w/v). Nitrogen gas was used to flush the vaporous hydride into a quartz tube through which the AAS beams were focused. Mercury standard solutions were stabilized by an addition of 0.1% (w/v) potassium iodide (KI) solution to minimize the adsorption of Hg onto the wall of glass volumetric flasks used for making standard solutions.

### 3.1.3 Results and Discussion

Elemental analysis of NBS 1633-a standard coal fly ash was conducted to determine the accuracy and precision of the analytical methods (Table 3.1). The HF-H<sub>3</sub>BO<sub>3</sub> digestion followed by AAS analysis yielded 90 to 100% recovery for Ca, Mg, Al, Fe, Cu, Zn, Cd, Mn and As. Exceptions were Pb (88%), Cr (88%), Co (108%), and Ni (129%). Mercury concentration in the NBS digest solution was lower than the detection limit (1 μg L<sup>-1</sup>) of the analytical method (MHS-10).

The elemental concentrations of the incineration residues used to fabricate the stabilized blocks, are presented in Table 3.2. For the purpose of classification, major constituents are defined as those elements present in concentrations > 1 mg g<sup>-1</sup>; minor constituents are those in the range 100 μg g<sup>-1</sup> - 1 mg g<sup>-1</sup>; and trace elements are those present in concentrations < 100 μg g<sup>-1</sup> (Roethel, 1981).

Major elements found in particulate incineration residues include Ca, Mg, Al, Fe, Pb, Zn, and Mn. Copper was found in major amounts in Westchester composite ash (W1, W2, W3, W4) and Huntington composite ash (H1, H2) but in minor amounts in New York City fly ash (C1, C2). Minor elements in all three

Table 3.1 Elemental concentrations of NBS 1633a standard fly ash and % recovery, HF-H<sub>3</sub>BO<sub>3</sub>-AAS method.

Element	NBS Reported	Measured	% Recovery <sup>a</sup>
Ca (%)	1.11 (0.01) <sup>b</sup>	1.11 (0.08)	100
Mg (%)	0.455 (0.01)	0.44 (0.02)	100
Al (%)	14 <sup>c</sup>	13 (0.2)	93
Fe (%)	9.4 (0.1)	8.7 (0.2)	93
Cu ( $\mu\text{g g}^{-1}$ )	118 (3)	110 (1)	93
Pb ( $\mu\text{g g}^{-1}$ )	72.4 (0.4)	63.8 (1.8)	88
Zn ( $\mu\text{g g}^{-1}$ )	210 (10)	195 (5)	100
Cd ( $\mu\text{g g}^{-1}$ )	1.00 (0.15)	0.92 (0.05)	100
Mn ( $\mu\text{g g}^{-1}$ )	190 <sup>c</sup>	174 (4)	92
Ni ( $\mu\text{g g}^{-1}$ )	127 (4)	164 (4)	129
Cr ( $\mu\text{g g}^{-1}$ )	196 (6)	173 (2)	88
Co ( $\mu\text{g g}^{-1}$ )	46 <sup>c</sup>	50 (1)	109
As ( $\mu\text{g g}^{-1}$ )	145 (15)	143 (7)	100
Hg ( $\mu\text{g g}^{-1}$ )	0.16 (0.01)	BDL <sup>d</sup>	

<sup>a</sup> % recovery considered to be 100% if measured value was within the range of NBS reported mean  $\pm$  standard deviation. Where  $<$  or  $>$  100%, calculation was based on mean values.

<sup>b</sup> Values in paranthesis denote standard deviation (n=6).

<sup>c</sup> Value is not certified by NBS.

<sup>d</sup> BDL means below detection limit ( $1 \mu\text{g L}^{-1}$  for Hg).

Table 3.2 Metal concentrations in incineration residues.

	Ca <sup>d</sup> (%)	Mg (%)	Al (%)	Fe (%)	Cu (%)	Pb (%)	Zn (%)	Cd ( $\mu\text{g/g}$ )	Mn (%)	Ni ( $\mu\text{g/g}$ )	Cr ( $\mu\text{g/g}$ )	Co ( $\mu\text{g/g}$ )	As ( $\mu\text{g/g}$ )	Hg ( $\mu\text{g/g}$ )
W1 <sup>a</sup>	16	1.8	5.6	2.0	0.19	0.31	0.75	85	0.17	130	130	22	21	0.99
SD <sup>b</sup>	0.6	0.0	0.1	0.02	0.01	0.02	0.01	10	0.001	3	1	1	2	0.30
W2	6.5	1.2	3.4	12	1.4	0.14	0.74	10	0.12	120	170	13	7.5	8.8
	1.9	0.6	1.2	10	1.4	0.10	0.89	5	0.03	60	80	4	2.8	0.3
W3	ND	0.12	2.5	3.4	0.13	0.32	1.93	ND	0.12	108	177	48	ND	ND
		0.01	0.1	0.2	0.01	0.01	0.17		0.01	18	26	11		
W4	ND	0.12	3.1	3.7	0.16	0.45	3.28	ND	0.23	103	195	51	ND	ND
		0.02	1.2	1.6	0.67	0.17	0.77		0.08	5	9	5		
H1	6.5	0.89	6.1	6.0	0.19	0.14	0.44	25	0.12	170	89	20	27	BDL <sup>c</sup>
	0.1	0.10	0.1	0.1	0.01	0.01	0.01	0.2	0.001	1	2	1	1	
H2	5.5	0.92	4.4	11	0.048	0.062	0.13	8.8	0.10	74	150	13	11	BDL
	0.9	0.26	1.0	2	0.018	0.028	0.04	3.5	0.03	7	40	1	4	
C1	5.8	0.95	6.3	1.6	0.073	0.87	2.5	1300	0.15	150	180	26	120	0.13
	1.5	0.42	0.9	0.02	0.011	0.10	0.3	30	0.006	3	6	1	2	2.13
C2	6.0	1.1	9.8	1.8	0.062	0.77	3.8	780	0.082	120	170	19	60	0.24
	0.1	0.01	0.4	0.2	0.004	0.07	1.3	30	0.003	3	10	1	4	1.61

<sup>a</sup> Particle size ranges used are;

W1 : < 200  $\mu\text{m}$ , H1 : < 150 $\mu\text{m}$ , C1 : < 75  $\mu\text{m}$ ,  
W2 and H2 : 2.00 mm - 4.75 mm, C2 : 250 $\mu\text{m}$  - 4.75 mm.

W3 : <150  $\mu\text{m}$

W4 : <75  $\mu\text{m}$

<sup>b</sup> Values denote the standard deviation of replicate samples (n=3).

<sup>c</sup> BDL means below detection limit; 1 ( $\mu\text{g L}^{-1}$ ) for Hg.

<sup>d</sup> ND elements were not determined.

types of incineration ashes included Cr and Ni while Co, As, and Hg were trace elements. C1 and C2 were enriched in Cd (major to minor element), while Cd was present as a trace element in W1, W2, H1, and H2.

The chemical composition of the incineration residues will depend largely on the waste sources and plant designs. The ultimate source of metals in the ash materials of any municipal refuse combustion process is the urban refuse being burned (Law and Gordon, 1979). Urban refuse can be divided into two major components: a combustible fraction (paper, cardboards, plastics, fabrics and etc.) and a noncombustible fraction (ferrous metals, nonferrous metals, glass, ceramics and etc.). Metals including Pb, Zn, Cd, Mn, and Cr in incinerator effluents may originate in noncombustible sources in addition to the contribution from combustible materials. Aluminum, Fe, Ni, and Co may also have significant noncombustible sources. The primary sources of Ca, Mg, Cu, and Hg may be the combustible components of refuse.

Organic content in municipal solid waste (MSW) incineration residues (LOI, Section 2) depends on the degree of burnout. The degree of burnout is determined by several factors including furnace combustion temperatures, the amount of air injected into the furnace, the degree of turbulence, the uniformity of the burning bed, and the residence time of MSW in the furnace. The capacity of the electrostatic precipitators influence the composition of incinerated solid waste by-products, particularly the percent fly ash. Differences in waste sources and plant designs result in the observed variation in elemental concentration among incineration residues.

Metal concentrations in residues from other incinerators (Alexandria Municipal Incinerator and Solid Waste Reduction Center in Washington D. C., U. S. Bureau of Mine facility at College Park, Maryland and Signal Environmental System facilities) are listed in Table 3.3. Calcium is found to be more abundant in residues used in this study than other residues listed in Table 3.3. From Table 3.2 and 3.3, it is evident that incineration residues are enriched with metals of environmental concern such as Pb, Cu, Zn and Cd. Moreover, Cd and Pb in the fly ash samples (C1 and C2) used in this study are 5 to 40 times higher than was found in the other fly ashes shown in Table 3.3. Metals volatilized in the furnace are adsorbed onto the fly ash particle

Table 3.3 Metal concentrations in other incineration residues.

Element	Alexandria <sup>a</sup>	SWRC <sup>a</sup>	USBM <sup>b</sup>	SES <sup>c</sup>	
	<u>fly ash</u>	<u>fly ash</u>	<u>fly ash</u>	<u>fly</u>	<u>bottom</u>
Ca (%)	4.3 (1.0) <sup>d</sup>	5.0 (0.2)	5.9 (1.3)	5.45	5.05
Mg (%)	1.3 (0.5)	1.3 (0.3)	0.98 (0.11)	NA <sup>e</sup>	NA
Al (%)	10.9 (1.1)	13.5 (0.4)	11 (2)	7.0	3.3
Fe (%)	5.2 (1.2)	2.5 (0.1)	2.7 (1.0)	1.75	1.32
Cu (%)	0.098 (0.044)	0.095 (0.022)	0.083 (0.031)	NA	NA
Pb (%)	0.40 (0.13)	NA	0.53 (0.47)	0.52	0.09
Zn (%)	1.08 (0.14)	2.4 (0.2)	0.87 (0.38)	NA	NA
Cd ( $\mu\text{g g}^{-1}$ )	42 (24)	185 (8)	NA	470	<100
Mn (%)	0.43 (0.18)	0.21 (0.02)	0.15 (0.10)	NA	NA
Ni ( $\mu\text{g g}^{-1}$ )	740 (100)	NA	200 (105)	NA	NA
Cr ( $\mu\text{g g}^{-1}$ )	1330 (170)	780 (50)	670 (190)	400	500
Co ( $\mu\text{g g}^{-1}$ )	35 (5)	27 (2)	NA	NA	NA
As ( $\mu\text{g g}^{-1}$ )	40 (13)	59 (5)	NA	NA	NA

<sup>a</sup> Alexandria Municipal Incinerator and Solid Waste Reduction Center (SWRC) in Washington D.C., respectively (Greenberg *et al.*, 1978).

<sup>b</sup> U.S. Bureau of Mines (USBM) facility at College Park in Maryland (Lawrence *et al.*, 1972).

<sup>c</sup> Signal Environmental System (SES) facilities (Surgi, 1986).

<sup>d</sup> Mean (Standard deviation).

<sup>e</sup> NA indicates data not available.



surfaces downstream of the combustion area as the flue gas temperature decreases resulting in the enrichment of metals in the fly ash fraction (Roethel et al., 1986; Neal and Schubel, 1987).

3.2 EP, TCLP AND SEAWATER SHAKING LEACHING TESTS

The EPA Toxicant Extraction Procedure (EP), EPA Toxicant Characteristic Leaching Procedure (TCLP) and Seawater Shaking Extraction Procedure were performed on particulate incineration residues to evaluate their leaching behavior in seawater and acidic solutions.

3.2.1 Methods

Particle sizes used for leaching tests are listed in Table 3.4. Particulate ash samples were sieved to achieve two different size ranges listed in Table 3.4. Larger and smaller particle sizes were selected to represent the bottom and fly ash fractions, respectively.

3.2.1a EPA Toxicant Extraction Procedure (EP)

The methods described in the Federal Register (1980), U. S. Environmental Protection Agency (EPA) Toxicant Extraction Procedure (40 CFR 261.24), were used to evaluate the leaching characteristics of incineration residues. Forty grams of each material (Table 3.4) were added to HDPE bottles containing 640 ml of DID water. Acetic acid (0.5 N, Baker Analyzed<sup>®</sup> ACS Reagent grade) was added to each bottle at 15, 30 and 60 minute intervals until achieving a pH of 5 (±0.2). The EP Toxicant protocol calls for the addition of not more than 4 ml of acid for every gram of solid. After mechanically shaking for 24 hours, pH of the solution was measured with a Digital Ionalyzer<sup>®</sup> Model 701-A pH/mv meter (Orion Research Inc., Cambridge, MA). Additional acid, up to 160 ml per bottle which contained 40 g samples, was added when necessary. Table 3.4 lists the final pH values and the total amount of acid added to each sample. The elutriates were filtered through a 0.45 μm Millipore<sup>®</sup> filter paper and the volume of filtrates was adjusted to 800 ml with DID water. Filtered samples were acidified to pH < 2 using Ultrex<sup>®</sup> HNO<sub>3</sub> and stored (< 3 months) at 5°C prior to analysis.

Table 3.4 Measured pH values for particulate incineration residues in EP, TCLP and Seawater Shaking leaching tests and amount of acetic acid added in EP test.

Residues	Particle Size	EP		TCLP	Seawater
		pH	Acid <sup>a</sup>	pH	pH
Westchester					
Composite Ash : W1	< 150 $\mu$ m	9.25	160	7.72	10.9
W2	2.0 - 4.75 mm	5.06	35	4.80	9.08
Huntington					
Composite Ash : H1	< 150 $\mu$ m	5.59	160	5.77	7.09
H2	2.0 - 4.75 mm	5.09	33	4.81	7.36
New York City					
Fly Ash : C1	< 75 $\mu$ m	5.16	160	5.12	9.17
C2	250 $\mu$ m - 1.0 mm	5.12	105	5.16	8.38

<sup>a</sup> Total amount of acetic acid (0.5 N, ACS Reagent grade) added in 40 grams of samples (mls).



### 3.2.1b EPA Toxicant Characteristic Leaching Procedure (TCLP)

In the Federal Register (Vol. 51, 1986), U. S. EPA proposed the use of a new procedure, TCLP, for identifying wastes as hazardous based on their likelihood to leach toxic contaminants. Forty grams of each sample (Table 3.4) and 20 times its weight (800 ml) of the appropriate extraction fluid was shaken using an end-over-end agitator at 30 ( $\pm 2$ ) rpm for 18 hours. The appropriate extraction fluid was determined from the pH of the mixture of 5.0 g of sub-sample and 96.5 ml of DID water. Extraction fluid No. 2 was used since the pH of all sample material-DID water mixtures exceeded the minimum pH, 5.00. The extraction fluid was prepared by diluting 5.7 ml glacial acetic acid (ACS Reagent grade Fisher Scientific Company) with DID water to a volume of 1 liter (pH 2.88  $\pm 0.05$ ). Following the 18 hour extraction, pH of the solution was measured (Table 3.4). The solution was filtered through a 0.45  $\mu\text{m}$  Millipore<sup>®</sup> filter paper, acidified to pH < 2 using Ultrex<sup>®</sup> HNO<sub>3</sub> and stored (< 3 months) at 5°C prior to analysis.

### 3.2.1c Seawater Shaking Extraction Procedure

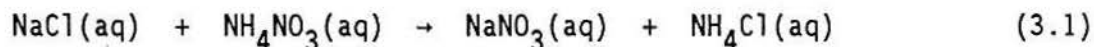
Samples were also leached using a modification of the method of the American Society for Testing Materials (ASTM) Proposed Method for Leaching of Waste Materials, Part A: Water Shake Extraction Procedure (ASTM, 1980). The modification consisted of using filtered (0.45  $\mu\text{m}$ ) seawater in place of DID water as the extraction fluid. For this procedure, three replicates of 75 g of each material (Table 3.4) were placed into high density polyethylene (HDPE) bottles with 300 ml of filtered (0.45  $\mu\text{m}$ ) seawater. Samples were then placed on a mechanical shaker for 48 hours. After measuring pH (Table 3.4), the elutriates were filtered through 0.45  $\mu\text{m}$  Millipore<sup>®</sup> filter papers, acidified to pH < 2 using Ultrex<sup>®</sup> HNO<sub>3</sub> and stored (< 3 months) at 5°C prior to analysis.

### 3.2.2 Leachate Analysis

Calcium and magnesium in the leachates determined using the EP, TCLP and Seawater Shaking tests were analyzed using flame Atomic Absorption Spectrophotometry [AAS] (Section 3.1.2). Zinc, copper and manganese in EP and

TCLP leachates were also determined with an air-acetylene flame on the Perkin Elmer Model 5000 AAS without background correction. Manganese in EP leachate of W1 (see Table 3.4) was analyzed using the AAS equipped with a HGA-500 graphite atomizer and AS-40 Autosampler with background correction. Lead in EP and TCLP leachates of some incineration ash samples (W1, H1, and H2 for EP leachate; W1 and H1 for TCLP leachate) was determined using flameless AAS. Analysis of Al, Fe, Cd, Ni, Cr, Co, and As in EP and TCLP leachates were also performed using flameless AAS. All standards for the analysis of EP and TCLP leachates were dilutions of Fisher Certified atomic absorption standards that were made up in the same matrix present in the samples to be analyzed. For Cd analysis, samples and standards were prepared in 1%  $(\text{NH}_4)_2\text{HPO}_4$  (w/v) and for As analysis, 0.1% Ni (w/v) as  $\text{Ni}(\text{NO}_3)_2$  (1:1) was used to allow the use of higher charring temperatures (Ediger, 1975).

For analysis of Seawater Shaking leachates, Fe, Cu, Pb, Cd, Mn, Ni, Cr, and Co were determined using flameless AAS using a matrix modifier (ammonium nitrate,  $\text{NH}_4\text{NO}_3$ ; Aldrich Chemical Company, Inc., Milwaukee, WI) to remove sodium and chloride ions present in the seawater matrix. Ediger *et al.* (1974) have shown that an addition of  $\text{NH}_4\text{NO}_3$  in seawater could convert sodium chloride ( $\text{NaCl}$ ) into sodium nitrate ( $\text{NaNO}_3$ ) and ammonium chloride ( $\text{NH}_4\text{Cl}$ ) via the following reaction:



The sublimation temperature of  $\text{NH}_4\text{Cl}$  is  $335^\circ\text{C}$ , and  $\text{NH}_4\text{NO}_3$  and  $\text{NaNO}_3$  start to decompose at  $210^\circ\text{C}$  and  $380^\circ\text{C}$  respectively, while the boiling temperature of  $\text{NaCl}$  is  $1413^\circ\text{C}$ . Therefore, by adding  $\text{NH}_4\text{NO}_3$  to seawater, the sodium and chloride could be volatilized out of the graphite furnace at charring temperatures near  $500^\circ\text{C}$ .

Serial dilutions of Fisher Certified atomic absorption standards were prepared with reagent concentrations equivalent to those in the samples to be analyzed. Copper standards were made up in the (1+100) diluted seawater with 0.2% Ultrex<sup>®</sup>  $\text{HNO}_3$  while (1+10) diluted seawater was used to prepare standard solutions for analysis of Fe, Pb, Ni, and Co. Both (1+10) and (1+100) diluted seawaters were used for analysis of Cd, Mn and Cr: (1+100) for Mn determination

in H1, H2, and C2 samples; (1+100) for Cr analysis of W1 and C1; (1+100) for Cd analysis of H1, C1, and C2. Cadmium samples and standards were diluted with 1% (w/v)  $(\text{NH}_4)_2\text{HPO}_4$  solution to allow for the use of higher charring temperatures.

Analyses of Hg in EP, TCLP, and Seawater Shaking leachates were performed with the use of the MHS-10 hydride generator attached to the Perkin-Elmer Model 5000 AAS (Section 3.1.2). Arsenic in Seawater Shaking leachate was determined using the MHS-10 hydride generator attached to the Perkin-Elmer Model 5000 AAS with an air-acetylene flame.

### 3.2.3 Results and Discussion

Metal concentrations in EP, TCLP, and Seawater Shaking leachates from particulate incineration ashes, are shown in Table 3.5 through 3.7. pH of the extraction fluid and sample particle size are two important factors controlling the leaching behavior of incineration residues; smaller particle size (due to the metal enrichment and larger surface area) and low pH (acidic condition) favor the leaching of heavy metals. In general, metal concentrations in the Seawater Shaking leachates were lower than those in the EP and TCLP leachates.

#### 3.2.3a pH

The TCLP leaching test does not require continuous pH adjustment. Despite the difference in leaching procedures, there was only a small difference in the final pH values between EP and TCLP leachates (Table 3.4). pH's of TCLP solutions were generally lower than those of EP with the exception of H1. The higher metal concentrations in TCLP relative to EP leachate is attributable to the lower pH of TCLP leachates.

The percent of total metal released from particulate incineration residues was higher in EP and TCLP leachates, than in Seawater Shaking leachate. To compare EP and TCLP leachates versus Seawater Shaking leachate, it is necessary to consider difference in the ratio of total liquid volume to sample weight ( $\text{ml g}^{-1}$ ): the ratio is 20:1 for EP and TCLP, and 4:1 for ASTM procedure (Seawater Shaking). When normalizing the metal concentration in solution ( $\mu\text{g ml}^{-1}$ ) to total metal concentration of the materials ( $\mu\text{g g}^{-1}$ ), the percent

Table 3.5 Metal concentrations in EP leachate of incineration residues.

	Ca (g/L)	Mg (mg/L)	Al (mg/L)	Fe (mg/L)	Cu (mg/L)	Pb (mg/L)	Zn (mg/L)	Cd (mg/L)	Mn (mg/L)	Ni ( $\mu\text{g/L}$ )	Cr ( $\mu\text{g/L}$ )	Co ( $\mu\text{g/L}$ )	As ( $\mu\text{g/L}$ )	Hg ( $\mu\text{g/L}$ )
W1 <sup>a</sup>	2.2	150	0.099	BDL <sup>c</sup>	0.20	BDL	0.055	0.003	0.006	4.0	210	BDL	BDL	BDL
SD <sup>b</sup>	0.04	40	0.004		0.02		0.014	0.001	0.001	0.8	4			
W2	0.44	30	1.1	0.51	1.2	5.2	7.8	0.18	0.45	39	7.0	8.9	BDL	7.0
	0.04	2	0.04	0.02	0.5	1.4	1.6	0.004	0.02	6	0.1	2.5		0.9
H1	2.0	70	0.48	0.10	1.4	0.054	32	0.31	15	340	2.5	38	3.7	BDL
	0.02	1	0.06	0.02	0.03	0.001	0.5	0.002	0.2	10	0.2	2	0.2	
H2	0.32	21	0.41	12	1.3	0.028	19	0.034	2.6	93	BDL	6.5	BDL	BDL
	0.02	1	0.01	0.2	0.3	0.012	10	0.004	0.2	12		1.1		
C1	0.96	280	13	0.24	7.7	12	1100	48	9.2	710	88	100	14	4.7
	0.01	10	0.5	0.04	0.1	0.5	10	1	0.4	30	5	4	1	0.4
C2	0.87	180	11	0.43	1.8	6.8	880	34	6.2	330	46	76	18	BDL
	0.12	5	0.4	0.06	1.6	2.1	30	1	0.7	40	3	10	2	

<sup>a</sup> Particle size ranges and pH values are listed in Table 3.4.

<sup>b</sup> Values denote the standard deviation of replicate samples (n=3).

<sup>c</sup> BDL means below detection limit.

: 0.05 ( $\mu\text{g L}^{-1}$ ) for Cr and As,

0.5 ( $\mu\text{g L}^{-1}$ ) for Fe, Pb and Co, and

2 ( $\mu\text{g L}^{-1}$ ) for Hg.

Table 3.6 Metal concentrations in TCLP leachate of incineration residues.

	Ca (g/L)	Mg (mg/L)	Al (mg/L)	Fe (mg/L)	Cu (mg/L)	Pb (mg/L)	Zn (mg/L)	Cd (mg/L)	Mn (mg/L)	Ni (µg/L)	Cr (µg/L)	Co (µg/L)	As (µg/L)	Hg (µg/L)
W1 <sup>a</sup>	2.3	220	1.1	BDL <sup>c</sup>	0.30	0.016	1.9	0.011	0.52	53	220	13	1.5	BDL
SD <sup>b</sup>	0.07	4	0.2		0.000	0.002	0.2	0.0001	0.04	2	5	1	0.4	
W2	0.85 0.09	93 3	33 4	24 7	1.3 0.1	38 4	23 2	0.43 0.05	2.3 0.1	390 70	200 20	86 10	39 4	7.3 0.9
H1	2.0 0.02	29 0.2	0.76 0.01	0.13 0.02	1.7 0.05	0.065 0.005	34 0.4	0.29 0.005	15 0.1	390 6	4.4 0.8	66 10	4.0 0.3	BDL
H2	0.91 0.03	72 5	10 0.2	27 3	1.7 0.02	7.0 3.0	31 2	0.11 0.01	9.0 0.6	380 20	52 8	63 8	9.7 1.4	BDL
C1	1.0 0.01	290 1	12 0.1	0.38 0.02	9.8 0.1	18 0.4	1300 10	47 1	9.6 0.1	920 6	110 3	130 7	14 1	4.2 0.6
C2	0.89 0.02	19 7	26 2	5.3 0.4	0.39 0.07	10 0.4	1000 30	31 1	7.3 0.2	480 14	280 10	100 10	48 9	BDL

<sup>a</sup> Particle size ranges and pH values are listed in Table 3.4.

<sup>b</sup> Values denote the standard deviation of replicate samples (n=3).

<sup>c</sup> BDL means below detection limit.

: 0.5 ( $\mu\text{g L}^{-1}$ ) for Fe, and  
2 ( $\mu\text{g L}^{-1}$ ) for Hg.

Table 3.7 Metal concentrations in Seawater Shaking leachate of incineration residues.

	Ca (g/L)	Mg (g/L)	Fe ( $\mu\text{g/L}$ )	Cu (mg/L)	Pb ( $\mu\text{g/L}$ )	Cd ( $\mu\text{g/L}$ )	Mn (mg/L)	Ni ( $\mu\text{g/L}$ )	Cr ( $\mu\text{g/L}$ )	Co ( $\mu\text{g/L}$ )	As ( $\mu\text{g/L}$ )	Hg ( $\mu\text{g/L}$ )
W1 <sup>a</sup>	1.7	-1.0 <sup>c</sup>	BDL <sup>d</sup>	0.46	BDL	BDL	BDL	2.3	340	BDL	2.5	BDL
SD <sup>b</sup>	0.08	0.0002		0.02				1.0	10		0.2	
W2	0.85	-0.22	BDL	0.15	BDL	20	0.066	6.6	2.7	BDL	BDL	BDL
	0.07	0.03		0.02		1	0.013	2.2	1.5			
H1	0.92	0.10	11	0.84	25	220	1.4	130	1.8	10	3.2	BDL
	0.06	0.03	7	0.04	4	20	0.1	6	0.6	2	0.5	
H2	0.30	0.053	33	0.38	BDL	38	1.1	86	BDL	5.4	BDL	BDL
	0.02	0.018	9	0.01		3	0.06	4		3.4		
C1	0.45	0.30	19	0.002	64	430	0.14	20	410	BDL	4.5	BDL
	0.01	0.03	3	0.001	7	20	0.007	2	10		0.6	
C2	0.40	0.37	31	0.026	410	350	1.5	19	BDL	BDL	12	BDL
	0.03	0.02	12	0.005	7	10	0.1	1			0.1	

<sup>a</sup> Particle size ranges and pH values are listed in Table 3.4.

<sup>b</sup> Values denote the standard deviation of replicate samples (n=3).

<sup>c</sup> Negative sign means the Mg concentration in the leachate was lower than that of seawater (0.45  $\mu\text{m}$ ) blank.

<sup>d</sup> BDL means below detection limit.

- : 0.5 ( $\mu\text{g L}^{-1}$ ) for Cd and Cr,
- 1 ( $\mu\text{g L}^{-1}$ ) for Fe, Co and As,
- 2 ( $\mu\text{g L}^{-1}$ ) for Mn and Hg, and
- 5 ( $\mu\text{g L}^{-1}$ ) for Pb.

metal released from EP and TCLP leachates become 5 times larger relative to those of Seawater Shaking leachate. Higher metal release in EP and TCLP leachates is attributable to the low pH of the extraction fluid in EP and TCLP (Table 3.4), which shows that metals were leached under acidic (relative to the Seawater Shaking test) conditions for EP and TCLP leaching tests, while Seawater Shaking test was conducted at alkaline pH.

For finer ash particles, several acid additions were required to adjust the pH of the solution to 5.0. The tendency of increasing pH with time when adjusting pH in EP solutions may be due to the dissolution of mineral phases such as calcite ( $\text{CaCO}_3$ ) and anhydrite ( $\text{CaSO}_4$ ) present in the incineration residues (Roethel *et al.*, 1986). Alkalinity produced by hydration reactions in the form of calcium hydroxide [ $\text{Ca}(\text{OH})_2$ ] can neutralize the added acid (Neville, 1983). Elemental analysis of two different particle sizes showed that smaller particles contained more Ca than larger ones, particularly in Westchester composite ash samples (Table 3.2). Larger surface area to volume ratios enhances the release of alkaline species. That finer samples required more acid to obtain pH of Ca. 5.0, may be due to both the higher Ca content in finer particles and the larger surface area available for alkalinity release.

Chromium behavior in the leachates was unique in that chromium release increased with increasing solution pH. Theis and Richter (1979), using coal fly ash, showed that Cr solubility, unlike other metals (Cu, Pb, Zn, Cd, and Ni), increased at pH values above 7.5 due to the formation of soluble hydroxo complexes such as  $\text{Cr}(\text{OH})_4^-$ . The formation of soluble complexes in solution of higher pH may account for the higher Cr concentration in samples of higher pH; Seawater Shaking compared to EP and TCLP samples, and W1 relative to W2.

### 3.2.3b Particle Size

Elemental analysis of particulate incineration residues showed that finer particles contained more metals than coarser particles (Table 3.2). Analysis of various leachates from particulate residues shows that finer particles in general leached a greater concentration of metals than larger particle sizes in EP and TCLP leachates. The exception was Westchester composite ash (W1, W2) samples, where greater amount of metals including Pb, Zn, and Cd was extracted



from larger size particles (W2) than smaller particles (W1). This observation may be accounted for by the pH of the extraction fluid. In the case of the EP leachates of Westchester composite ash, the solution pH of W2 was 5.06, while that of W1 was 9.25 (Table 3.4), which may have resulted from the higher Ca content in smaller particle size fraction (Table 3.2). The difference in solution pH resulted in higher metal release from coarse particle sizes. For Huntington composite ash and New York City fly ash, however, pH differences between fine and large particles were very small but finer particles were found to contain more metals than coarser ones (Table 3.2). The higher metal release from finer particles is mainly due to the higher metal content of smaller particle sizes rather than pH differences. Results of Seawater Shaking leachate also showed higher metal release from smaller particles, where differences in pH between particle sizes were small (Table 3.4).

### 3.2.3c Comparison of Leaching Results with EPA Regulatory Limits for EP Toxicity

Metal concentrations in the EP, TCLP and Seawater Shaking leachates of incineration residues are compared to Hazardous Waste EP Toxic Criteria (Table 3.8). Seawater Shaking leachates did not exceed the EPA regulatory limit for toxicity, while Pb and Cd concentrations in EP and TCLP leachates of some particulate residues, particularly fly ash samples (C1, and C2) exceeded the regulatory limit.



Table 3.8 Comparison of EP, TCLP and Seawater Shaking leachate concentrations from particulate incineration residues with EPA regulatory limits for EP Toxicity.

		Fe <sup>a</sup>	Cu	Pb	Zn	Cd	Mn	Cr	As	Hg
Toxic Criteria <sup>b</sup>		--	--	5.0	--	1.0	--	5.0	5.0	0.2
EP:	W1	<0.001	0.20	<0.001	0.055	0.003	0.006	0.22	<0.001	<0.002
	W2	0.51	1.2	5.2	7.8	0.18	0.45	0.007	<0.001	0.007
	H1	0.10	1.4	0.054	32	0.31	15	0.002	0.004	<0.002
	H2	1.2	1.3	0.028	19	0.034	2.6	<0.001	<0.001	<0.002
	C1	0.24	7.7	12	1100	48	9.2	0.088	0.14	0.005
	C2	0.43	1.8	6.8	880	34	6.2	0.046	0.18	<0.002
TCLP:	W1	<0.001	0.30	0.016	1.9	0.011	0.52	0.22	0.001	<0.002
	W2	24	1.3	38	23	0.43	2.3	0.20	0.039	0.007
	H1	0.13	1.7	0.065	34	0.29	15	0.004	0.004	<0.002
	H2	27	1.7	7.0	31	0.11	9.0	0.052	0.010	<0.002
	C1	0.38	9.8	18	1300	47	9.6	0.11	0.014	0.004
	C2	5.3	0.39	10	1000	31	7.3	0.28	0.048	<0.002
Seawater:	W1	<0.001	0.46	<0.005	NA <sup>c</sup>	<0.001	<0.002	0.34	0.003	<0.002
	W2	<0.001	0.15	<0.005		0.020	0.066	0.003	<0.001	<0.002
	H1	0.011	0.84	0.025		0.22	1.4	0.002	0.003	<0.002
	H2	0.033	0.38	<0.005		0.38	1.1	<0.001	<0.001	<0.002
	C1	0.019	0.002	0.064		0.43	0.14	0.41	0.004	<0.002
	C2	0.031	0.026	0.41		0.35	1.5	<0.001	0.012	<0.002

<sup>a</sup> Unit of concentration is mg L<sup>-1</sup> and detection limits for each metal are listed in Table 3.5 through 3.7.

<sup>b</sup> Data from Federal Register (May, 1980).

<sup>c</sup> NA means not analyzed.

### 3.3 SEQUENTIAL EXTRACTION OF PARTICULATE INCINERATION ASH

#### 3.3.1 Introduction

Most leaching procedures involve single batch tests which yield information on the mass of contaminants which are leached from a waste under specific leach conditions. The EP, TCLP, and ASTM are batch tests designed to classify wastes as hazardous or non-hazardous based on contaminant concentrations in the leachate. Due to the high alkalinity associated with incineration ash, the alkalinity of the particle acts to neutralize the leachate solution. Therefore single extraction batch tests are of limited value when assessing the leachability of highly alkaline residues.

The sequential extraction procedure is designed to determine the association of metals with different fractions of incineration ash particles. Knowledge of the phase association of metals with the ash provides a basis for estimating the short-term and long-term leachability of metals from the ash. Five distinct fractions are identified with the sequential extraction procedure using increasingly more aggressive leaching solutions to recover metals associated with those specific fractions. Fraction A (exchangeable) is the ion exchangeable fraction and is considered easily available for leaching. Fraction B (carbonate) contains carbonate bound metals and is considered available for leaching under normal acidic landfill conditions. Fraction C (Fe and Mn oxides) consists of iron and manganese oxides which are excellent scavengers for metals and are considered leachable under more severe leaching conditions present in older landfills. Fraction D (organic) includes metals bound as sulfides or to organic matter and is not likely to be leached under normal conditions. Fraction E (matrix) contains the residual metal ions and is considered unavailable for leaching even under severe leaching conditions.

Samples of particulate incineration ash were subjected to a sequential extraction scheme to determine both the distribution and availability of metals in particulate incineration ash. Samples of particulate incineration ash were collected from Signal-RESCO facility in Westchester County, New York, in September 1985.

### 3.3.2 Methods

The particulate Westchester incineration ash was sieved to a particle size  $<250 \mu\text{m}$ . Samples were then oven dried at  $110^\circ\text{C}$  for 24 hours prior to analysis. Replicate samples  $1.0 \pm 0.1$  samples of incineration ash were weighed into 50 ml polyethylene centrifuge tubes. The extraction procedure partitions the elements into the following five fractions:

- Fraction A. Exchangeable Metals. The samples were extracted at room temperature for 1 hour with 10 ml of 1.0 M ammonium chloride with continuous agitation on a shaker table.
- Fraction B. Bound to Carbonates. The residue from A was extracted for 6 hours at room temperature with 10 ml of 1.0 M sodium acetate adjusted to pH 5 with acetic acid. Continuous agitation was maintained throughout the extraction.
- Fraction C. Bound to Fe and Mn Oxides. The residue from B was extracted for 6 hours at  $96 \pm 3^\circ\text{C}$  with 20 ml of 0.04 M hydroxylamine hydrochloride in 25% acetic acid, with occasional agitation.
- Fraction D. Bound to Organic Matter. The residue from C was extracted with 3 ml 0.02 M nitric acid and 5 ml of 30% hydrogen peroxide adjusted to pH 2 with nitric acid. The mixture was then heated to  $85 \pm 2^\circ\text{C}$  for 2 hours with periodic agitation. A second 3 ml aliquot of 30% hydrogen peroxide (pH 2 with nitric) was then added and the sample was again heated to  $85 \pm 2^\circ\text{C}$  for 3 hours with periodic agitation. After cooling, add 5 ml of 3.2 M ammonium acetate in 10% (v/v) nitric acid and the sample was diluted to 20 ml with distilled-deionized water and agitated on a shaker table for 30 minutes.
- Fraction E. Matrix Metals. The residue from D was digested in 5 ml of concentrated hydrofluoric acid for 24 hours on a shaker table. Forty milliliters of 3% boric acid was added and the samples were shaken for an additional 24 hours.

The extractions, A-E, were carried out in 50 ml polyethylene tubes to minimize the loss of solid material throughout the series of extractions. After each successive extraction separation was effected by centrifugation (International Clinical Centrifuge Model CL) at 5000 rpm for 30 minutes. The

supernatants were removed by pipet and filtered through 0.40  $\mu\text{m}$  Nuclepore<sup>®</sup> membrane filters. For Fractions A-D, the filtered supernatants were adjusted to 25 ml in volumetric flasks with distilled-deionized water and adjusted to pH 2 with nitric acid. Fraction E was adjusted to 50 ml in a volumetric flask with distilled-deionized water.

### 3.3.2a Acid Digestions

Approximately 0.5 g of dried particulate ash was weighed to 0.1 mg and placed into 125 ml linear polyethylene bottles followed by the addition of 10 ml of distilled-deionized water and 10 ml of concentrated hydrofluoric acid. The mixtures were then shaken for 24 hours. Seventy ml of 3% boric acid were then added to the samples and agitated for an additional 24 hours. The digests were filtered through 0.40  $\mu\text{m}$  Nuclepore<sup>®</sup> membrane filters and brought to volume in 100 ml volumetric flasks with 3% boric acid. The digest solutions were then stored in 125 ml linear polyethylene bottles prior to analysis.

### 3.3.2b Metal Analysis

Metal analyses for both extraction and total digest solutions were determined using a Perkin-Elmer model 5000 atomic absorption spectrophotometer (AAS). Iron, lead, copper, zinc, manganese, and calcium were determined using flame AAS with an air-acetylene flame. Calcium samples were diluted into the linear range with 1%  $\text{La}^{3+}$  added as  $\text{La}_2\text{O}_3$ . Cadmium analysis was performed with flameless AAS using a Perkin-Elmer 5000 equipped with an HGA 500 graphite furnace and an AS 40 autosampler. Due to high metal concentrations in the extraction solutions, it was necessary to further dilute the samples with distilled-deionized water (10-1000 X) prior to analysis. The metal concentrations were determined directly from calibration curves prepared with the components of the extraction fluids diluted by the same factor.

### 3.3.3 Results and Discussion

The distribution of the seven elements in the five fractions of particulate incineration ash is presented in Table 3.9. For each metal the sum of the five extraction fractions is compared to the total elemental composition

Table 3.9

## SEQUENTIAL EXTRACTION OF METALS FROM PARTICULATE INCINERATION ASH

FRACTION	CONCENTRATION	(%)	FRACTION	CONCENTRATION	(%)
<b>Fe</b>			<b>Pb</b>		
A	BDL	0.1	A	35 ± 9	0.5
B	79 ± 0.5	0.3	B	3826 ± 220	57.0
C	2370 ± 103	8.9	C	1590 ± 40	23.7
D	BDL	0.1	D	480 ± 90	7.2
E	23900 ± 890	90.6	E	790 ± 50	11.6
Σ	26350 ± 790	100.0	Σ	6710 ± 320	100.0
M <sub>T</sub>	27720 ± 280		M <sub>T</sub>	6630 ± 190	
<b>Mn</b>			<b>Ca</b>		
A	7 ± 0.3	0.8	A	22700 ± 880	35.5
B	160 ± 18	18.2	B	26032 ± 890	40.7
C	444 ± 7	50.6	C	12580 ± 1050	19.7
D	8 ± 1	0.9	D	2110 ± 260	3.3
E	260 ± 8	29.5	E	570 ± 170	0.8
Σ	877 ± 4	100.0	Σ	63990 ± 740	100.0
M <sub>T</sub>	913 ± 9		M <sub>T</sub>	66000 ± 350	
<b>Zn</b>			<b>Cd</b>		
A	3500 ± 390	16.5	A	76 ± 4	38.9
B	8360 ± 260	39.4	B	75 ± 18	38.5
C	4770 ± 310	22.5	C	17 ± 5	8.7
D	440 ± 8	2.1	D	4 ± 1	2.1
E	4160 ± 270	19.5	E	23 ± 4	11.8
Σ	21220 ± 270	100.0	Σ	194 ± 12	100.0
M <sub>T</sub>	24340 ± 1160		M <sub>T</sub>	195 ± 17	
<b>Cu</b>					
A	206 ± 17	17.8			
B	220 ± 37	18.9			
C	76 ± 8	6.6			
D	400 ± 28	34.5			
E	260 ± 6	22.2			
Σ	1160 ± 84	100.0			
M <sub>T</sub>	1270 ± 35				

of separate samples of the material as determined by the HF-H<sub>3</sub>BO<sub>3</sub> acid digest. With the exception of zinc, the comparison of the sum of the extracts and the total metal digests agree to within 5%. The zinc concentration in the ash was high and variable which may account for the differences.

### 3.3.3a Short-term and Long-term Leachability for Particulate Ash

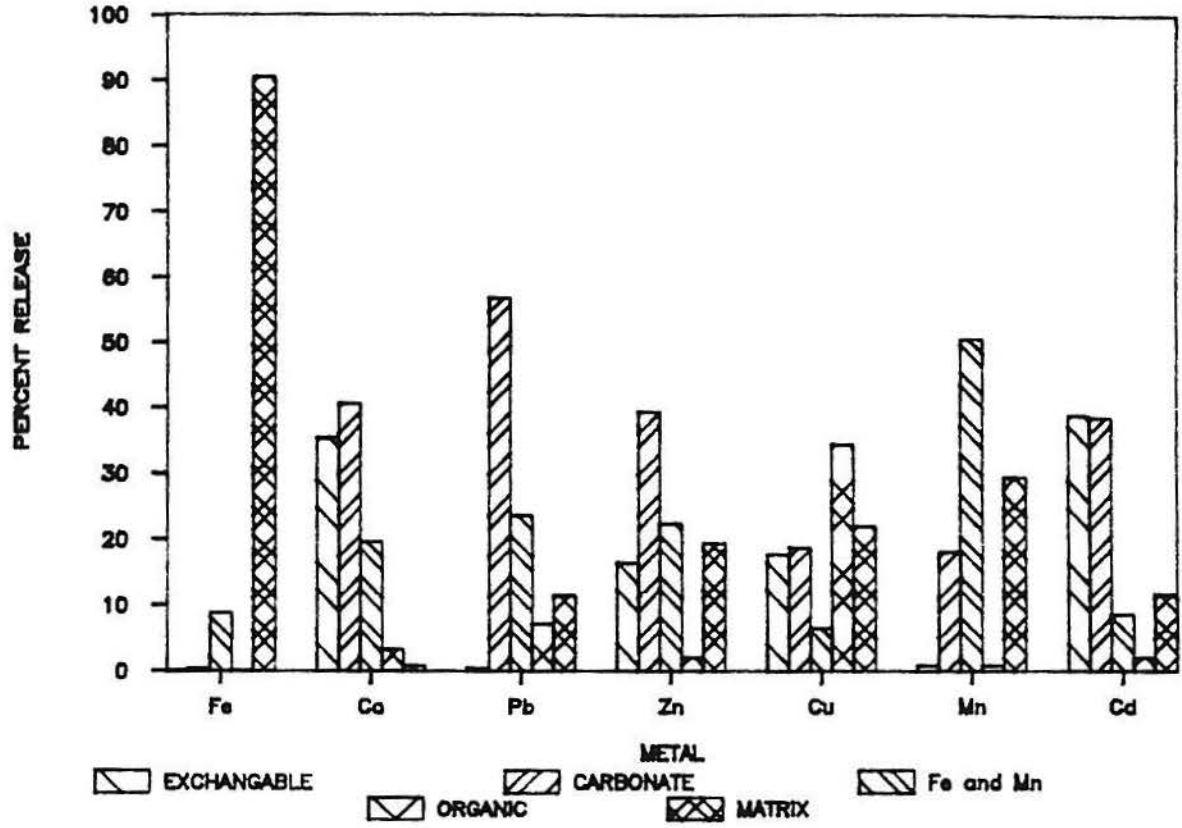
The distribution of metals in the five fractions of the incineration ash particle are shown in Table 3.9 and Figure 3.1. Results show that for Zn, Cd, Cu, and Ca, large percentages of these metals are associated with the exchangeable and carbonate fractions of the particle. In contrast, over 90% of the iron is associated with the matrix of the particle.

To assess potential environmental impacts of metal leaching, the results can be grouped into short-term and long-term leachable fractions. Short-term leachability estimates are based on the total metal extracted from the exchangeable and carbonate phases (Fractions A + B). Long-term leachability estimates are based on the total metal extracted from the exchangeable, carbonate, and Fe and Mn phases (Fractions A + B + C) (Figure 3.1).

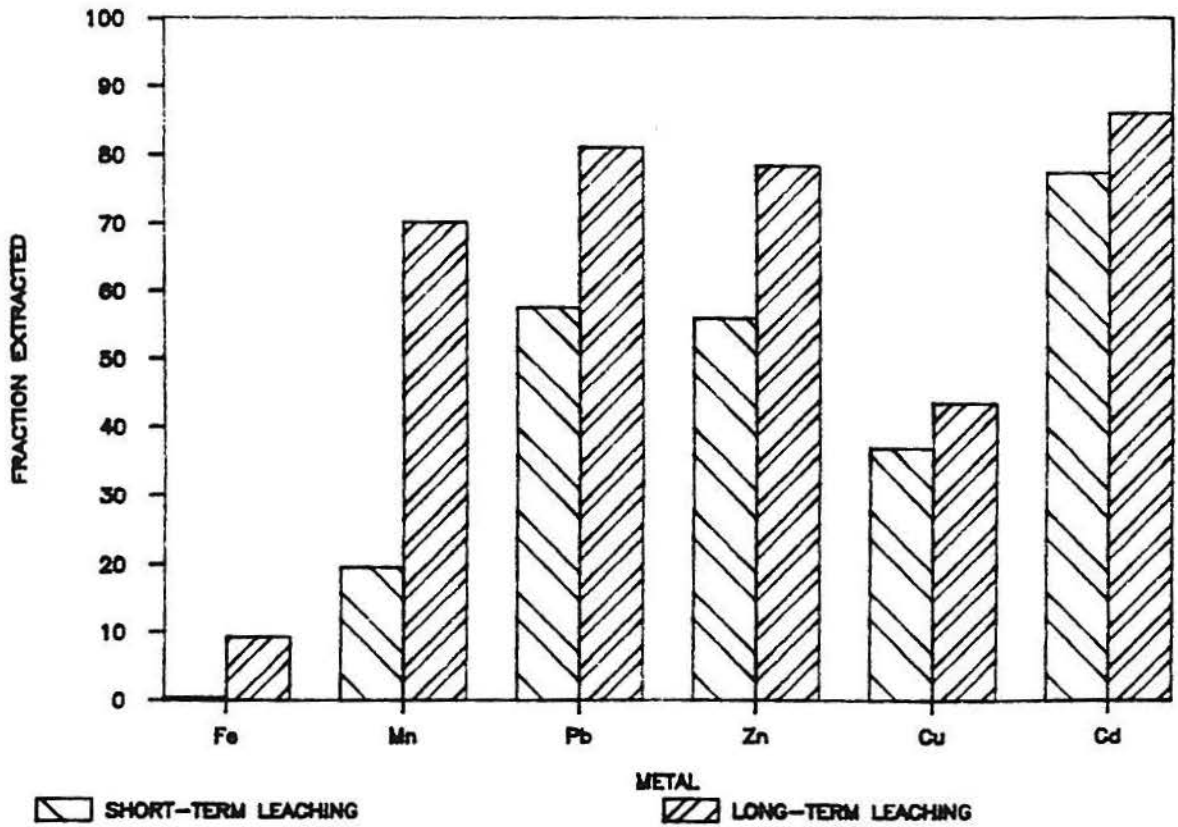
Results show that significant amounts of Cd (77.9%), Pb (57.5%), Zn (55.9%), and to a lesser extent Cu (36.7%) are available for leaching in the short-term from particulate incineration ash. Availability for long-term leaching increased for Cd (86.2%), Pb (81.2%), Zn (78.4%), and Cu (43.3%) for particulate incineration ash.

Figure 3.1 Sequential chemical extraction of particulate incineration residue.

SEQUENTIAL ASH EXTRACTION



ASH LEACHABLE FRACTIONS





## Section 4

### LARGE SCALE BLOCK PRODUCTION

#### 4.1 PROCESS FOR CONCRETE BLOCK FABRICATION

In a conventional concrete construction block factory the mix components of the blocks are typically fed in weighed amounts from hoppers into a mixer. Water may also be added to adjust the moisture content of the mix. The well mixed materials are then fed into the loader of a block making machine. A block machine uses vibration and pressure to mold materials into the blocks. The block mold rests on a steel pallet during the molding process and the material is fed into the mold box by vibration. Shoes then descend on top of the mold to exert pressure and a second cycle of vibration as the mold consolidates the contained material into blocks. As soon as the material is compacted and struck off, the mold box lifts, and the pallet holding the blocks emerges from the machine while a new pallet is being pushed in beneath the mold box for the next molding cycle. The pallets of blocks are loaded on racks and cured in steam kilns. Cured blocks are unracked, depalletized, and stacked by a cubing machine as cubes of interlocked blocks on carrying pallets. Block making is fast, a block machine can form more than 1,500 concrete blocks per hour. A simplified schematic of the block making process and pictures of equipment used for block making, are given in Figures 4.1-4.4.

#### 4.2 BENEFITS OF CONSTRUCTION SIZED BLOCK UNIT

- Construction size blocks [about 18 kg (40 lbs)] can be made at concrete factories, -- with fully developed engineering.
- Homogeneity is more easily accomplished, producing blocks of greater strength.
- Small blocks have more handling and transport options and are cheaper to move.
- If steam is used for accelerated curing, curing time might be reduced to one day, which would make direct ocean placement possible.
- Steam curing would provide independence from low winter temperatures (which normally slow the curing process).

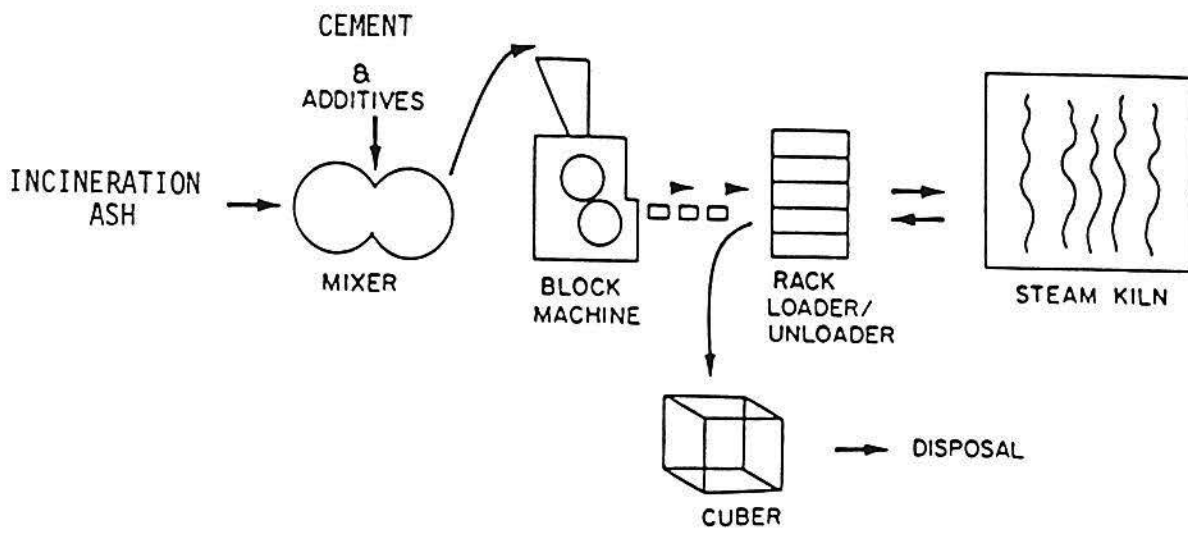


Figure 4.1. Simplified schematic of block processing.

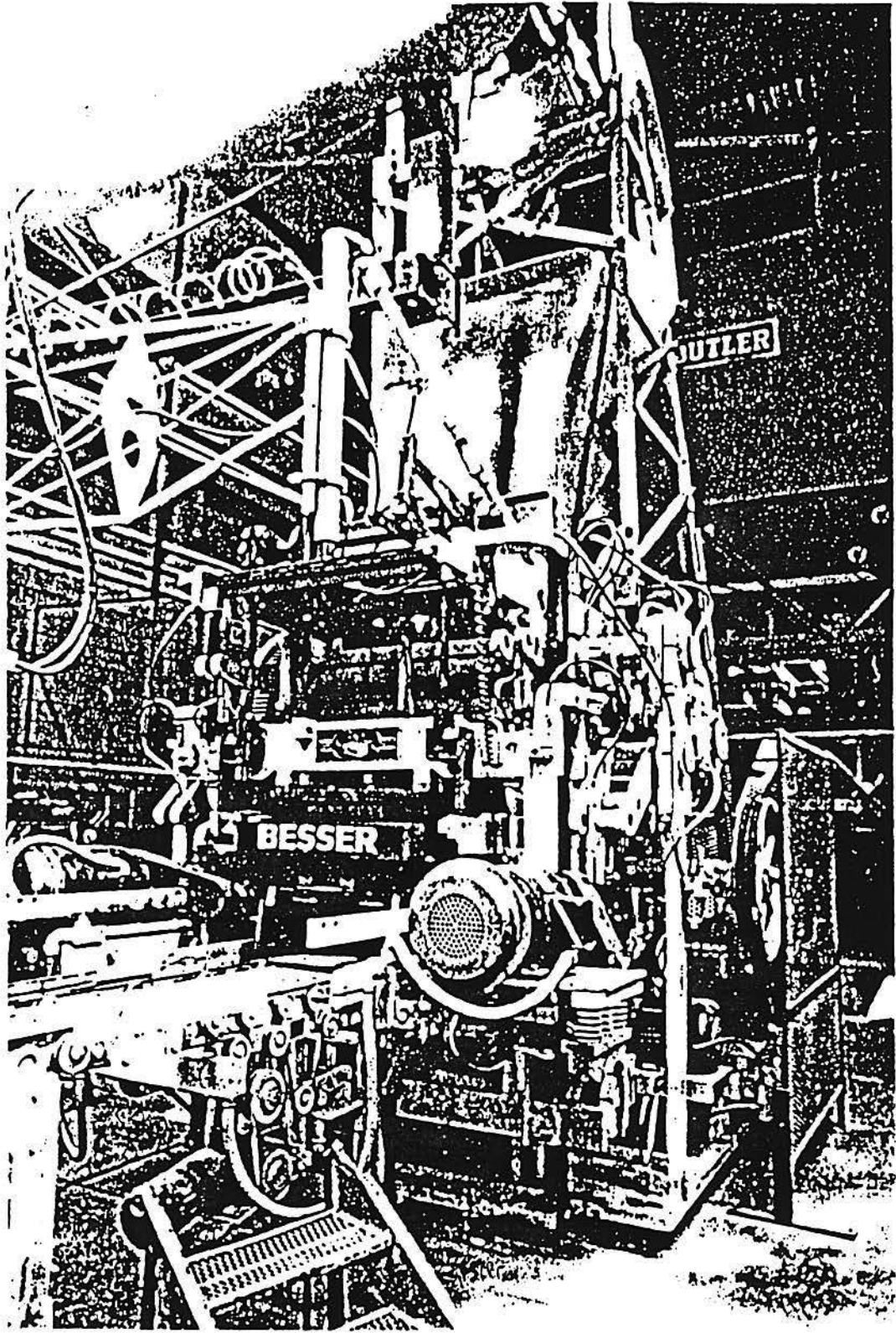


Figure 4.2. Besser Vibrapac block machine.

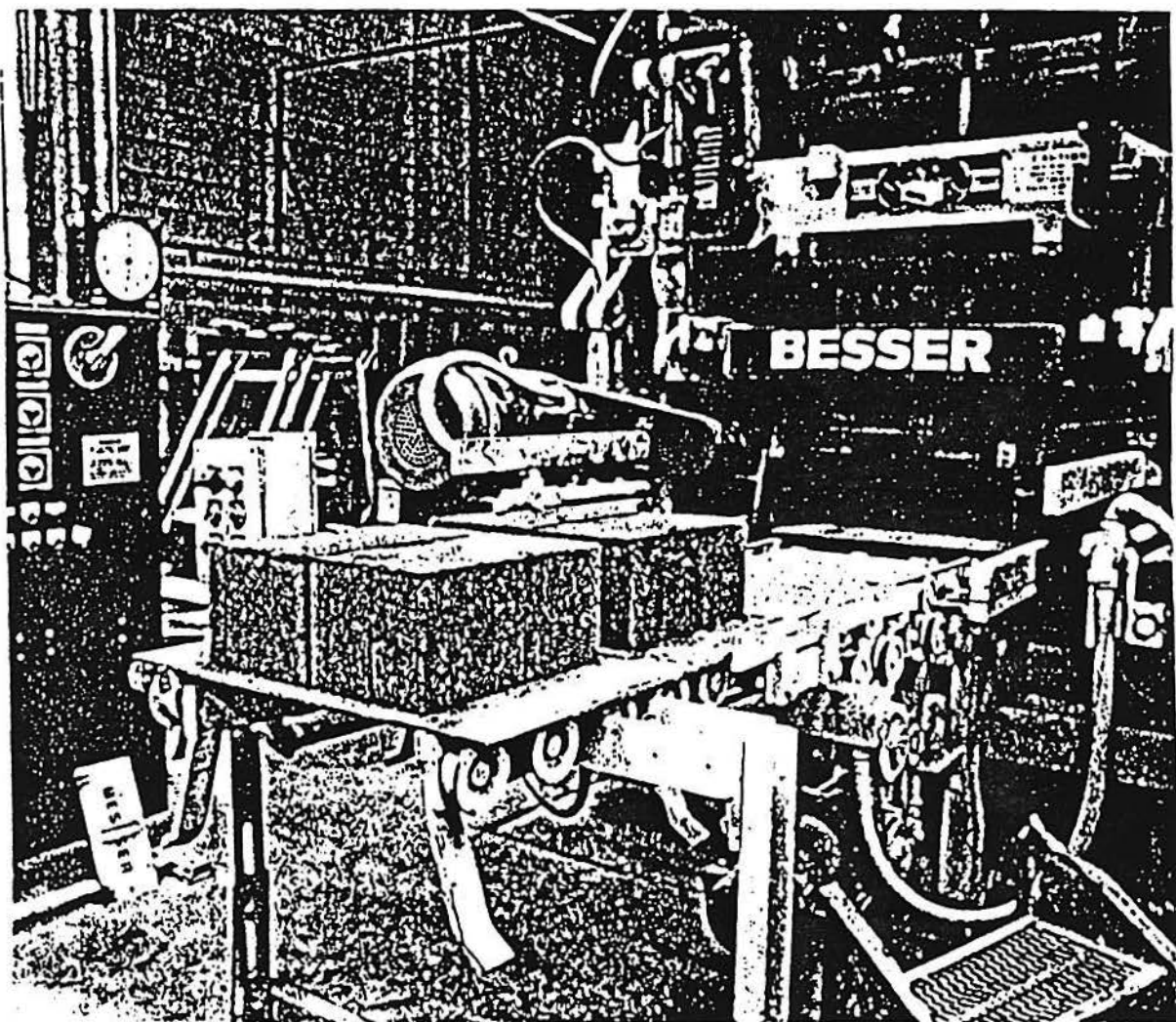


Figure 4.3. Experimental block produced at Alpena, Michigan.

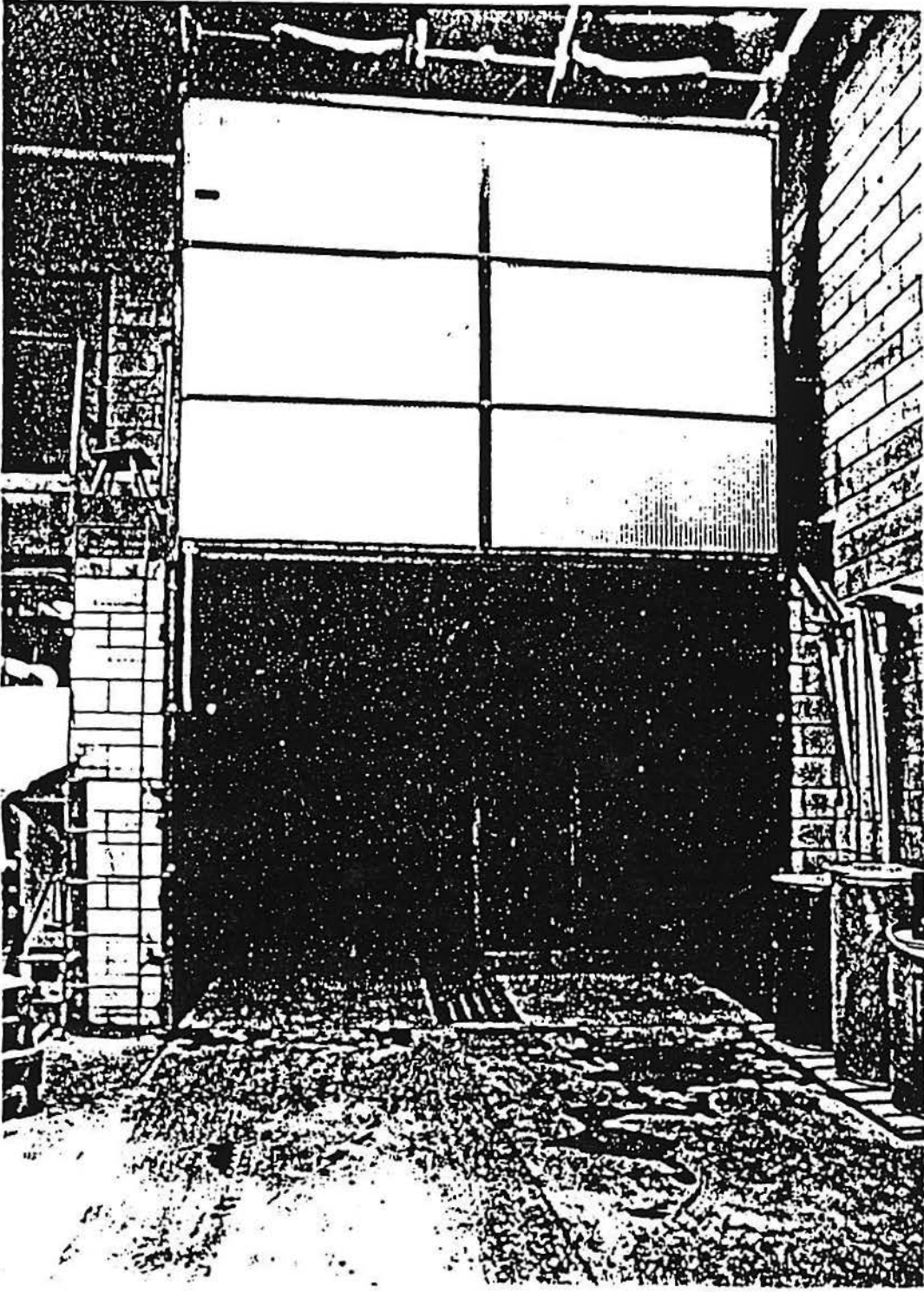


Figure 4.4. Steam kiln used to cure coal waste blocks, Alpena, Michigan.



### 4.3 BLOCK FABRICATION AT BARRASSO AND SONS, INC.

The facilities of Barrasso and Sons, Inc. at 160 Floral Park Road, Islip Terrace, New York were used for block fabrication on two occasions. The first visit in January 1986 utilized the Westchester ash sample also collected in January 1986. The second visit occurred in September 1986 using Westchester ash collected in September 1986.

The purpose of the first visit in January 1986 was to determine the feasibility of producing concrete hollow unit masonry blocks using incineration ash, Portland cement type III, and sand. These blocks were designed to meet strength and durability requirements for marine disposal and to determine if strengths sufficient for building purposes could be acquired. Also, any potential problems associated with substituting incineration ash for natural aggregate would hopefully be addressed and solved.

A Besser V3-12 Vibrapac block making machine (producing 3 blocks per pallet) was used for block fabrication. This machine was equipped with standard dimension mold and parts to produce two core 8" x 8" x 18" hollow masonry blocks.

Preprocessing of the ash consisted of sieving the material through a 3/4" flat mesh screen. This was necessary to ensure proper filling of the block molds, residue homogeneity, and to reduce the possibility of breakage of the machines internal parts. The material sieved out of the ash comprised approximately 1/6 the initial volume of the ash. This material proved to be mostly rocks, metal, masonry and ceramic products, and glass products formed during incineration.

Approximately 300 blocks were produced at Barrasso and Sons, Inc. in January 1986. Each mix design was color coded for ease of identification and cured for 18 hours at 134°F (Table 4.1). One difficulty during the block manufacturing process was the inability to use the mixers moisture probe to determine the moisture content of mix prior to compaction. This was due to the small sample size, and therefore only an estimate of the moisture content was established at the site. Subsamples of the mixes were placed in jars and

Table 4.1. Mix Designs and Color Coding of Barrasso Blocks (1/86).

MIX FORMULATION	RED		YELLOW		NATURAL	
	(%)	WEIGHT (lbs)	(%)	WEIGHT (lbs)	(%)	WEIGHT (lbs)
CEMENT TYPE 3	11.2	251	12.2	250	14.3	250
SAND	60.9	1368	43.9	900	0	0
COMPOSITE ASH	27.9	624	43.9	900	85.7	1500
MIX WEIGHT	100	2243	100	2050	100	1750

AVERAGE CURING TEMPERATURE - 134 F

AVERAGE CURING TIME - 18 HOURS

sealed and the moisture content of the mix was determined at MSRC. Barrasso personnel were impressed by the ease of handling the incineration ash and moving the mix throughout the facility by conveyor belts prior to compaction. Overall it was their impression that this material behaved similarly to the standard mixes they handle daily.

Following curing, the blocks were transported to MSRC where a number of blocks of each mix design were moistened and wrapped in plastic to determine whether additional moisture would result in a continuation of the curing process and therefore improve compressive strengths. Every seven days the structural integrity of the blocks was determined in replicate (n=3). Results of the strength development of these blocks are summarized in Section 5.

The purpose of the second visit to the Barrasso facility in September 1986 was to produce reef blocks for the construction of an artificial reef in Conscience Bay, Long Island Sound, New York. Also, experiments using different mix designs were conducted in an attempt to produce blocks of construction grade quality.

Twenty tons of composite ash were collected at the Westchester Resco-Signal incinerator, trucked to Port Jervis, New York and sieved through 1/2 inch sieves. The sieved ash was then reloaded into the truck and transported to Barrasso and Sons, Inc. At the Barrasso facility, the ash was further processed by removing ferrous metal using permanent magnets. Ferrous metal removal was labor intensive and time consuming. However, the benefits of removing this material before it is incorporated into the blocks were numerous. Ferrous metal corrodes, creating voids in the block that result in lower strengths. Of less concern is the fact that as this corrosion occurs, the block is discolored resulting in a cosmetically undesirable product. The incinerator at the Resco-Signal facility is equipped with electromagnets to remove ferrous metals from the ash. However, due to the poor market for scrap iron the incinerator must pay to have this material removed. Since electromagnets pull out substantial amounts of ash with attached iron, this process results in greater disposal expense to the incinerator and a less desirable iron product for the smelters. As a result, the electromagnets remain unused.



During block manufacture, the moisture probe in the mixer was again not used due to the relatively small batch sizes in comparison to normal production. Also, the higher iron and soluble salt content of the ash as compared to normally used aggregate results in the ash having a different conductivity than the natural aggregate. Thus, the moisture content of each batch was determined on subsamples collected for analysis at MSRC. As on the previous trip, different mix designs were color coded to aid in mix identification (Table 4.2). Two types of block molds were used on this occasion; 8" x 8" x 18", 2 core hollow masonry units for experimental construction blocks and 8" x 8" x 18", 3 core hollow masonry units for the artificial reef blocks. The 3 core hollow masonry units were chosen for use for reef blocks because they could be conventionally handled with forklifts without the added expense of using wooden pallets. The 3 core units are approximately 75% solid as compared to 52% solid for the 2 core blocks. Solid blocks (3 core) have the benefit of disposing more of the ash per block with a smaller surface area to volume ratio than 2 core hollow masonry units.

Block production proceeded without any unusual problems. Blocks were steam cured for 24 hours and moved on pallets by forklift to the yard where the curing process continued. The compressive strength of the blocks following initial steam curing were poor. Many blocks were broken simply by the normal handling procedure of moving them from the steam curing chamber to the yard. Results of unconfined compressive strength testing of these blocks are summarized in Section 5. The unfavorable results obtained with this ash sample illustrated the need to use a facility where smaller batch sizes and frequent changes in batch mix designs would not present major problems. This would provide a better idea of what additives would be successful when attempting to stabilize this material.

#### 4.4 BLOCK FABRICATION INVESTIGATIONS AT APLENA, DECEMBER 1986

During the period December 8-12 1986, experiments in incineration ash block fabrication were made at the research facilities of the Besser Company sited at the Alpena Community College, Alpena, Michigan. Principal aims of these investigations were to manufacture blocks of different cement and incineration ash mix designs employing conventional machines currently used by

Table 4.2. Mix designs and color coding of Barrasso blocks (9/86).

MIX FORMULATION	NATURAL		YELLOW	
	(%)	WEIGHT (lbs)	(%)	WEIGHT (lbs)
COMPOSITE ASH	61.6	3911	63.8	3911
SAND	24.7	1566	25.6	1566
CEMENT TYPE III	13.7	867	10.6	650
TOTAL MIX WEIGHT	100.0	6344	100.0	6127
TOTAL MOISTURE (MEASURED)	10.3		10.8	
MOISTURE STD. DEV.	0.1		0.7	
BLOCK TYPE	8 X 8 X 18 2 CORE		8 X 8 X 18 2 CORE	

MIX FORMULATION	RED		GREEN	
	(%)	WEIGHT (lbs)	(%)	WEIGHT (lbs)
COMPOSITE ASH	67.8	4260	66.4	4260
SAND	23.6	1480	23.1	1480
CEMENT TYPE III	8.6	543	10.5	679
TOTAL MIX WEIGHT	100.0	6283	100.0	6419
TOTAL MOISTURE (MEASURED)	10.4		9.6	
MOISTURE STD. DEV.	0.5		0.1	
BLOCK TYPE	8 X 8 X 18 2 CORE		8 X 8 X 18 2 CORE	

MIX FORMULATION	6/1 REEF		9/1 REEF	
	(%)	WEIGHT (lbs)	(%)	WEIGHT (lbs)
COMPOSITE ASH	86.5	5681	90.6	5681
CEMENT TYPE III	13.5	887	9.4	591
TOTAL MIX WEIGHT	100.0	6568	100.0	6272
TOTAL MOISTURE (MEASURED)	14.1		12.7	
MOISTURE STD. DEV.	0.5		0.3	
BLOCK TYPE	8 X 8 X 18 3 CORE		8 X 8 X 18 3 CORE	

AVERAGE CURING TEMPERATURE - 119°F

AVERAGE CURING TIME - 20 hours

commercial concrete block factories, and to investigate proper conditions for accelerated curing of incineration waste blocks in the steam kiln. These investigations were designed to produce both artificial reef quality blocks and construction grade blocks.

Two ash types were collected from the Westchester incinerator in November, 1986. These ash types were bottom ash only and the normal output of mixed bottom ash and fly ash (referred to as combined ash). The reason for this separation of the ash was to observe which ash type would be more easily stabilized. Processing of this ash at the Alpena facility prior to block fabrication involved screening the ash to obtain particle sizes less than 3/8". The material larger than this sieve size was crushed with a jaw-crusher and then resieved. It was noted that the material remaining on the sieve contained larger amounts of metal than previously sieved ash samples. The metal fragments were found after crushing large glass fragments. The glassious part of these chunks would shatter into fragments smaller than the sieve with the larger metal pieces retained on the sieve. Thus, using the jaw-crusher and screening has the beneficial effects of removing more of the metal present while increasing the amount of silica (from the crushed glass and rocks), thus improving the characteristics of the ash prior to block making.

Different additives were tested to observe their effects on block strength. Portland cement types I and II were used to observe whether the sulphate resistance of type II cement would increase strengths over type I and type III cement. (Type III cement was used at the Barrasso facility). Forrer's Mark V Plasticizer was tested to observe the effects of super plasticizer on the mechanical block making process and its effects on block strength before and after seawater submersion. Finally, the effects of blending in different proportions of common masonry sand were used in the attempt to produce construction quality blocks. Prior to large scale block manufacturing, small test bricks were tested to determine successful mix designs (Table 4.3). Mixes which yielded test bricks with high compressive strengths were used for large scale block production (Table 4.4).

Table 4.3. Mix designs for Alpena Bricks (12/86).

BOTTOM ASH MIXES														
MIX FORMULATION	1		2		3		4		5		6		7	
	%	WEIGHT(lbs)	%	WEIGHT(lbs)	%	WEIGHT(lbs)	%	WEIGHT(lbs)	%	WEIGHT(lbs)	%	WEIGHT(lbs)	%	WEIGHT(lbs)
SEIVED ASH	63.3	19.00	63.3	19.00	57.4	17.22	57.4	18.94	51.0	16.84	44.6	14.73	38.3	12.63
CRUSHED ASH	21.7	6.50	21.7	6.50	19.1	5.74	19.1	6.31	17.0	5.61	14.9	4.91	12.7	4.21
SAND					8.5	2.55	8.5	2.81	17.0	5.61	25.5	8.42	34.0	11.22
CEMENT (TYPE I) (TYPE II)	15.0	4.50	15.0	4.50	15.0	4.50	15.0	4.95	15.0	4.95	15.0	4.95	15.0	4.95
TOTAL MIX WEIGHT	100.0	30.00	100.0	30.00	100.0	30.01	100.0	33.01	100.0	33.01	100.0	33.01	100.0	33.01
WATER ADDED (ml)		1418		1418		1268		1395		1395		1350		1485
TOTAL MOISTURE MEASURED	13.7		13.3		13.2		13.0		11.0		12.2		11.8	

BOTTOM ASH MIXES														
MIX FORMULATION	8		18		19		20		21		22		23	
	%	WEIGHT(lbs)	%	WEIGHT(lbs)	%	WEIGHT(lbs)	%	WEIGHT(lbs)	%	WEIGHT(lbs)	%	WEIGHT(lbs)	%	WEIGHT(lbs)
SEIVED ASH	31.9	11.57	45.5	18.20	44.7	17.89	27.1	10.82	27.1	10.82	19.2	7.64	41.3	16.50
CRUSHED ASH	10.6	3.86	15.2	6.10	12.4	4.96	10.4	4.16	10.4	4.16	10.3	4.16	13.7	5.50
COAL FLY ASH							4.8	1.91	4.8	1.91	12.8	5.09		
SAND	42.5	15.43	20.3	8.10	19.9	7.95	42.6	16.97	42.6	16.97	42.6	16.97	30.0	12.00
LIME			4.0	1.60	8.0	3.20								
CEMENT (TYPE I) (TYPE II)	15.0	5.45	15.0	6.00	15.0	6.00	15.1	6.00	15.1	6.00	15.1	6.00	15.0	6.00
TOTAL MIX WEIGHT	100	36.31	100.0	40.00	100.0	40.00	100.0	39.86	100.0	39.86	100.0	39.86	100.0	40.00
WATER ADDED (ml)		1612		1700		1455		1410		1410		1380		1280
TOTAL MOISTURE MEASURED	12.3		12.8		13.5		10.0		11.0		10.8		11.1	

Table 4.3. Mix designs for Alpena bricks (12/86) continued.

COMBINED ASH MIXES													
MIX FORMULATION	9		10		11		12		13		14		
	%	WEIGHT(lbs)	%	WEIGHT(lbs)	%	WEIGHT(lbs)	%	WEIGHT(lbs)	%	WEIGHT(lbs)	%	WEIGHT(lbs)	
SEIVED ASH	57.4	17.22	44.6	14.73	31.9	12.73	71.8	26.25	68.7	26.10	65.5	24.90	
CRUSHED ASH	19.0	5.71	14.9	4.91	10.4	4.16	23.9	8.75	22.9	8.70	21.8	8.30	
SAND	8.6	2.55	25.5	8.42	42.6	16.97							
CEMENT (TYPE I)	15.0	4.50	15.0	4.95	15.1	6.00							
(TYPE II)							4.3	1.54	8.4	3.20	12.7	4.80	TOTAL MIX WEIGHT
100.0	29.98	100.0	33.01	100.0	39.86	100.0	36.54	100.0	38.00	100.0	38.00		
WATER ADDED (m1)		850		780		730		535		550		730	
TOTAL MOISTURE MEASURED	26.4		9.8		8.6		12.3		10.9		11.2		

COMBINED ASH MIXES													
MIX FORMULATION	15		16		17		24		25		26		
	%	WEIGHT(lbs)	%	WEIGHT(lbs)	%	WEIGHT(lbs)	%	WEIGHT(lbs)	%	WEIGHT(lbs)	%	WEIGHT(lbs)	
SEIVED ASH	44.7	19.73	31.9	12.73	31.9	12.73	63.8	25.50	45.0	18.00	45.0	18.00	
CRUSHED ASH	14.8	6.55	10.4	4.16	10.4	4.16	21.2	8.50	15.0	6.00	15.0	6.00	
SAND	25.5	11.23	42.6	16.97	42.6	16.97			25.0	10.00	25.0	10.00	
CEMENT (TYPE I)	15.0	6.60	15.1	6.00							15.0	6.00	
(TYPE II)					15.1	6.00	15.0	6.00	15.0	6.00			
TOTAL MIX WEIGHT	100.0	44.11	100.0	39.86	100.0	39.86	100.0	40.00	100.0	40.00	100.0	40.00	
WATER ADDED (m1)		11.52		854		780		730		730		720	
TOTAL MOISTURE MEASURED	10.8		8.2		8.4		10.0		8.7		8.3		

Table 4.4. Mix designs for Alpena blocks (12/86).

MIX FORMULATION	1		2		3		4		5		6		7	
	%	WEIGHT(lbs)	%	WEIGHT(lbs)	%	WEIGHT(lbs)	%	WEIGHT(lbs)	%	WEIGHT(lbs)	%	WEIGHT(lbs)	%	WEIGHT(lbs)
SEIVED ASH	63.8	255	45.0	270	32.0	192	32.0	128	32.0	192	48.0	192	63.8	255
CRUSHED ASH	21.2	85	15.0	90	10.5	63	10.5	42	10.5	63	15.8	63	21.2	85
SAND			25.0	150	42.5	255	42.5	170	42.5	255	21.2	85		
CEMENT (TYPE I)							15.0	60						
(TYPE II)	15.0	60	15.0	90	15.0	90			15.0	90	15.0	60	15.0	60
TOTAL MIX WEIGHT	100.0	400	100.0	600	100.0	600	100.0	400	100.0	600	100.0	400	100.0	400
WATER ADDED (gal)		2.5		1.3		1.1								
TOTAL MOISTURE MEASURED	11.4		9.7		8.7		8.5		7.8		9.7		10.2	
NUMBER OF BATCHES MADE		2		1		1		1		1		1		3

36 ml of Forrer's Mark V Plasticizer were added to the water for mix #1.

#### 4.4.1 Block Making Equipment

##### 4.4.1a Block machines

A Prestopac block machine was used to make small test bricks, 23 cm x 9.4 cm x 6.4 cm (9 in x 3.7 in x 2.5 in), to investigate handling and forming properties of the materials in block machines, and to conserve the material which was available. Based on results from the test bricks, larger blocks 20 cm x 20 cm x 40.6 cm (8" x 8" x 16") were made with a large Vibrapac block machine, the type of machine which was used to make incineration ash blocks at the Barrasso facility.

##### 4.4.1b Steam curing

Accelerated curing was carried out in a conventional concrete block steam kiln using saturated steam (wet curing) at a pressure of about one atmosphere. Wet steam curing assures adequate water for hydration while the increased temperature accelerates the hydration and bonding of block material. Control of the temperature cycle during steam curing is necessary to reduce the likelihood of fractures developing in the blocks due to internal stresses caused by differential thermal expansion.

In the first experiment, the kiln was heated rapidly to 165°F and held at that temperature for 1 hour, followed by cooling to room temperature over 12 hours. Blocks cured in this manner developed cracks. Subsequently, the optimal curing cycle for the incineration ash block program was increased to 24 hours. The temperature regime was: 6 hours at 70°F, 5 hour temperature increase to 165°F, hold temperature at 165°F for 1 hour, 1 hour 49°C (120°F), 1 hour 60°C (140°F), 12 hours 71°C (160°F) then decrease to room temperature over 12 hours.



## Section 5

### COMPRESSIVE STRENGTH TESTING OF INCINERATION ASH BLOCKS

#### 5.1 INTRODUCTION

#### 5.2 METHODS

##### 5.2.1 Compressive Strength Testing

Compressive strength was determined on stabilized incineration ash blocks using a Reihle Universal Testing apparatus following ASTM method C-39 (ASTM 1974). A compressive load was applied to the surface of the block and steadily increased until fracture of the block occurred. The total load at the time of the fracture divided by the cross-sectional area to which the pressure was applied yields the compressive strength. Compressive strengths are expressed in terms of both gross and net pounds per square inch (psi). Gross psi is calculated by dividing the total load applied to the block (lbs) by the total surface area of the block (sq in). Net psi is calculated by dividing the total load applied to the block by the area of the solid surface of the block.

##### 5.2.2 Resistance to Impact

Stabilized incineration ash blocks would be exposed to impact during handling and placement in the ocean. The resistance to impact test is the recommended test for the evaluation of the handling characteristics of the blocks. This test provides information on whether or not blocks can be safely handled by automatic depalleting and cubing equipment without chipping corners. Studies at the Besser Research and Training Center of the Besser Company, Alpena, Michigan, have resulted in a recommended minimum value of 70 deci-foot pounds per square inch (deci-ft.lb/sq in) for handling the blocks without damage.

Resistance to impact tests were conducted on blocks fabricated at the Besser Company after one day curing. The test consists of dropping a 0.2 lb weight on each corner of the block at increasing heights until the corner



cracks and finally fractures. The energy required to cause a fracture is recorded as the resistance to impact.

### 5.3 RESULTS AND DISCUSSION

#### 5.3.1 Compressive Strength of Barrasso January 1986 Blocks

Results of the net unconfined compressive strength testing of Barrasso blocks fabricated in January 1986 are shown in Table 5.1 and Figure 5.1. Seven day compressive strengths for the three block mixes varied from 748 psi for the Red mix to 923 psi for the Natural mix. Both the Red and Yellow mixes show a general increase in compressive strength with time. The compressive strengths for the Red and Yellow mixes increased from 748 psi to 901 psi and from 1016 psi to 1292 psi, respectively, after 28 day air-dry curing. The compressive strength of the Natural block remained the same over 28 days. These compressive strengths can be compared to values of 1710 psi and 2630 psi measured for Pumice and Standard concrete blocks obtained from Barrasso and Sons Inc.

The yellow mix contained intermediate amounts of cement and sand additives yet showed the highest 28 day compressive strengths of the three blocks studied (Table 5.1). This occurrence may be due to the moisture content of the mixes. High or low moisture contents can adversely effect the compressive strengths of cured mixes. Unfortunately, the moisture contents of these mixes were not determined.

#### 5.3.2 Compressive Strength of Barrasso September 1986 Blocks

Results of the net unconfined compressive strengths of the six mixes fabricated at Barrasso and Sons, Inc. in September 1986 are shown in Table 5.2 and Figure 5.2. Initial compressive strengths for these mixes ranged from 99 psi to 247 psi for the 9/1 Reef block and the Yellow block, respectively. All of these mixes showed continuous gains in compressive strength with time. After 41 days, the compressive strengths of the Yellow and 9/1 Reef block increased to 1209 psi and 627 psi, respectively.

The Yellow, Red, Green, and Natural mixes were formulated using ash,

Table 5.1. Compressive strengths of Barrasso January 1986 hollow masonry blocks.

Curing Time		<u>Compressive Strength (total load) in pounds</u>				
Time (day)		<u>RED MIX</u>	<u>YELLOW MIX</u>	<u>NATURAL</u>	<u>PUMICE</u>	<u>STANDARD</u>
7	Net psi std. <sup>a</sup>	748 108	901 23	993 162	1710 374	2630 25
14	Net psi std.	739 74	1261 183	1013 245		
21	Net psi std.	827 88	1330 338	992 22		
28	Net psi std.	1016 156	1292 209	892 302		

<sup>a</sup> std. Standard deviation (n=3)

Figure 5.1 Compressive strength of Barrasso January 1986 blocks versus time.

# COMPRESSIVE STRENGTH OF BARRASSO BLOCKS

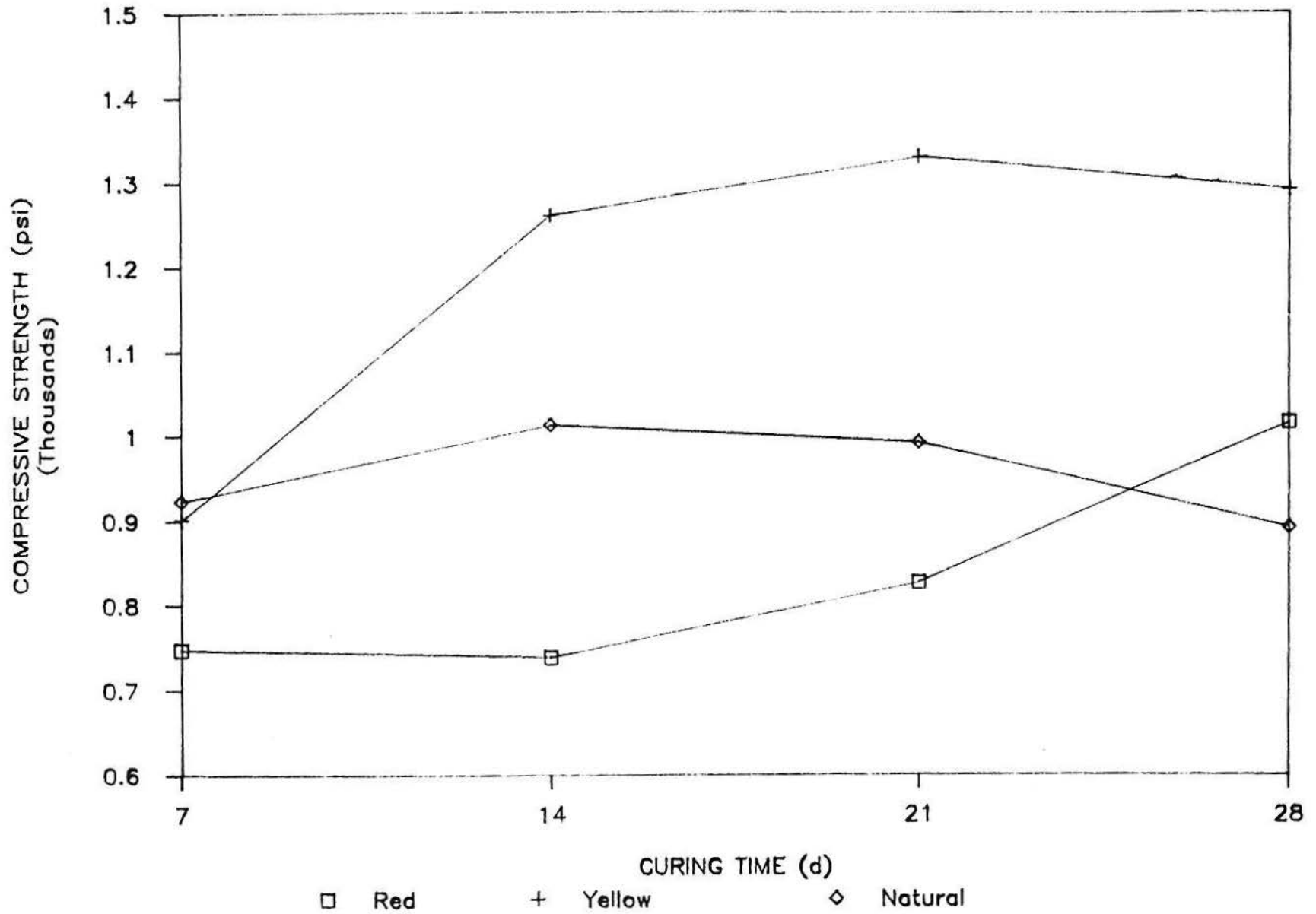
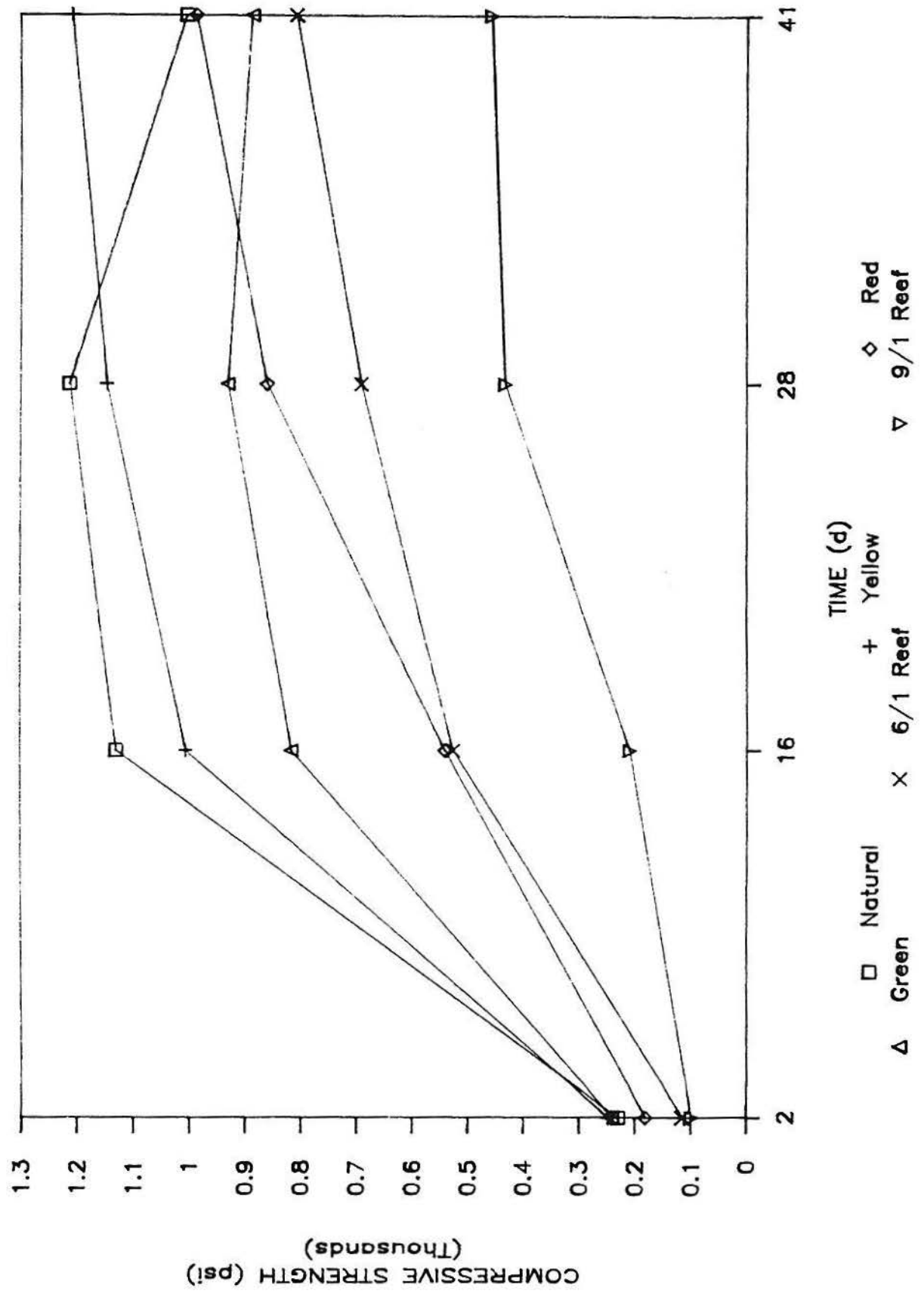


Table 5.2. Compressive strengths of Barrasso September 1986 blocks.

	NATURAL BLOCK	YELLOW BLOCK	RED BLOCK	GREEN BLOCK	6/1 REEF BLOCK	9/1 REEF BLOCK
CURE TIME 2 d						
Avg. GROSS psi	120	128	94	125	84	73
STD.	18	38	37	6	34	6
Avg. NET psi	230	247	181	241	115	99
STD.	35	74	72	11	66	15
CURE TIME 16 d						
Avg. GROSS psi	587	523	281	424	383	153
STD.	46		18		5	
Avg. NET psi	1129	1005	540	816	525	209
STD.	88		35		10	
CURE TIME 28 d						
Avg. GROSS psi	631	596	446	484	504	315
STD.	24	12	26	26	39	1
Avg. NET psi	1213	1147	859	930	691	432
STD.	46	23	51	51	76	3
CURE TIME 41 d						
Avg. GROSS psi	522	629	513	461	590	458
STD.	192	53	79	42	39	58
Avg. NET psi	1004	1209	987	887	808	627
STD.	369	101	152	81	76	111

Figure 5.2 Compressive strength of Barrasso September 1986 blocks versus time.

# Compressive Strength of Barrasso Blocks



Portland type III cement, and sand to determine an optimum block mix design for use in construction. A minimum compressive strength of 1000 psi is required for use in construction (ASTM). The Natural and Yellow mixes exceeded this minimum criteria after a 16 day air-cure. The higher strengths observed for the Yellow and Natural blocks may be a result of the high cement content of these mixes (Table 4.2).

The 6/1 and 9/1 blocks were fabricated using only incineration ash and cement for use in artificial reef construction. A minimum compressive strength of 300 psi is required for ash blocks used for artificial reef construction. The 6/1 Reef block exceeded this minimum criteria after a 16 day cure reaching a compressive strength of 525 psi. The 9/1 Reef block exceeded the 300 psi criteria after 28 days with a compressive strength of 432 psi. The higher strengths observed for the 6/1 Reef block may be a result of the higher cement content of this mix (Table 4.2).

### 5.3.3 Compressive Strength of Alpena Test Bricks

#### 5.3.3a Bottom Ash

Results of the net unconfined compressive strength testing of the bricks fabricated at the Besser Company, Alpena, Michigan, are shown in Table 5.3. Bricks were made using both bottom ash and composite ash. Initial compressive strengths of bricks made with bottom ash (#1-#8, #18-#23) were too low to measure. Twenty eight day strengths of brick samples #1-#7 were also too low to measure. The bottom ash used in these mixes, when present as a major additive, resulted in poor quality bricks.

The twenty eight day strengths of bricks #20, #21, and #22 exceeded 1000 psi. These mixes contained bottom ash, sand, cement, and coal fly ash (Table 4.3). The sand and coal fly ash additives lowered the overall percentage of bottom ash in the mixes resulting in the higher strengths observed.

#### 5.3.3b Composite Ash

Bricks produced using composite ash resulted in bricks with high



Table 5.3. Compressive strengths of Alpena 12/86 bricks.

BOTTOM ASH MIXES							
BATCH NUMBER	1	2	3	4	5	6	7
1 DAY CURE TOTAL LOAD (lbs) AVG PSI ± (STD.DEV.)	TOO LOW	TOO LOW	TOO LOW	TOO LOW	TOO LOW	TOO LOW	TOO LOW
28 DAY CURE TOTAL LOAD (lbs) AVG PSI ± (STD.DEV.)	ND <sup>a</sup>	ND	ND	ND	ND	ND	45000 39000 1050 (106)
BATCH NUMBER	8	18	19	20	21	22	23
1 DAY CURE TOTAL LOAD (lbs) AVG PSI ± (STD.DEV.)	TOO LOW	TOO LOW	TOO LOW	TOO LOW	TOO LOW	TOO LOW	TOO LOW
28 DAY CURE TOTAL LOAD (lbs) AVG PSI ± (STD.DEV.)	43000 46000 1113 (53)	ND	ND	38500 48000 1081 (168)	71000 78000 1863 (124)	53000 42000 1188 (194)	22000 25000 588 (53)

<sup>a</sup> These values were not determined.

Table 5.3. Compressive strengths of Alpena 12/86 bricks, continued.

COMBINED ASH MIXES						
BATCH NUMBER	9	10	11	12	13	14
1 DAY CURE						
TOTAL LOAD (lbs)	17200	22300	32400	6900	10800	27400
	16700	21500	35300	5300	10400	28000
AVG PSI ± (STD.DEV.)	424 (9)	548 (14)	846 (51)	153 (28)	265 (7)	693 (11)
28 DAY CURE		ND <sup>a</sup>		ND		
TOTAL LOAD (lbs)	40000		101500		40500	60500
	35000		78500		36000	66000
AVG PSI ± (STD.DEV.)	938 (88)		2250 (407)		956 (80)	1581 (97)
BATCH NUMBER	15	16	17	24	25	26
1 DAY CURE						
TOTAL LOAD (lbs)	33200	35200	60000	17100	38500	9300
	31300	31400	73000	14600	42000	9300
AVG PSI ± (STD.DEV.)	806 (34)	833 (67)	1663 (230)	396 (44)	1006 (62)	233 (0)
28 DAY CURE						
TOTAL LOAD (lbs)	100500	69500	140500	52500	71000	53000
	99000	88000	124500	55000	64500	54000
AVG PSI ± (STD.DEV.)	2494 (27)	1969 (327)	3313 (283)	1344 (44)	1694 (115)	1338 (18)

<sup>a</sup> These values were not determined.

compressive strengths (Table 5.3). One day compressive strengths of these bricks ranged from 153 psi to 1663 psi for mixes #12 and #17, respectively. The strengths of the bricks increased with time, with 28 day strengths ranging from 938 psi to 3313 psi for mixes #9 and #17, respectively.

#### 5.3.4 Effects of Additives on Brick Strength

Additives including Portland cement type I, Portland cement type II, and sand were varied to determine the effects of these additives on the compressive strengths of the bricks.

##### 5.3.4a Sand

Various amounts of sand (8.5%, 25.5%, 42.6%) were added to mixes #9, #10, and #11 while keeping a constant 3:1 ratio of composite ash to crushed ash and a 15% cement content (Table 4.3). Results show that increasing the sand content of the mix increases the 1 day and 28 day compressive strengths of the mix. One day compressive strength of the mixes ranged from 424 psi for mix #9 to 846 psi for mix #11 (Table 5.3).

##### 5.3.4b Portland Type II Cement

The effect on brick strength of varying the amount of Portland type II cement (4.2%, 8.4%, 12.6%) in mixes #12, #13, and #14 was investigated while maintaining a 3:1 composite ash to crushed ash ratio (Table 4.3). Results show that the compressive strength of these mixes increases with increasing cement content. One day compressive strengths increased from 153 psi for mix #12 to 693 psi for mix #14 (Table 5.3).

Differences in the compressive strengths of the mixes were observed when using Portland type II cement in place of Portland type I cement. Mix pairs #16 and #17, and #25 and #26 are duplicate mixes with the exception of cement type. Both mixes #17 and #25, containing Portland type II cement, showed higher compressive strengths at 1 day and 28 days than their respective duplicate mixes using Portland type I cement (Table 5.3).

### 5.3.5 Compressive Strength of Alpena Blocks

Seven mix designs using composite ash were used for large scale block production at the Besser Company. Mix designs for the large scale production were based on the results of the one day compressive strength testing of the bricks. Based on these result, a constant 3:1 ratio of composite ash to crushed ash was used in the mixes. Portland cement type I, Portland cement type II, and sand were the main additives. Mixes #1 and #7 were designed for artificial reef construction while mixes #2, #3, #4, #5, and #6 were designed to produce an optimum block for construction purposes.

Mixes #1 and #7 easily exceeded the minimum strength criteria for artificial reef construction of 300 psi at both 1 day and 28 days. The 28 day compressive strengths for mix #1 and mix #7 were 1926 psi and 2185 psi, respectively.

Mixes #2, #3, #4, #5, and #6 were designed to produce 8" x 8" x 16" blocks acceptable by the construction industry. Results show that four of these mixes exceeded the 1000 gross psi minimum strength criteria set by the building industry (Table 5.4). After 28 days of curing, these strengths ranged from 1118 psi for mix #7 to 1592 psi for mix #6.

Portland cement type II contributed to higher strength development than Portland cement type I in these mixes. Mixes #3 and #4 were identical with the exception of the cement type. Mix #3, with Portland type II cement, had a 28 day net compressive strength of 2743 psi while mix #4, containing Portland cement type I, had a 28 day compressive strength of 1408 psi (Table 5.4).

### 5.3.6 Resistance to Impact

Fabricated incineration ash blocks must have sufficient resistance to impact loading so they would not break during handling and transportation. Results of the resistance to impact test for Alpena blocks are shown in Table 5.5. Five of the seven Alpena blocks tested exceeded the minimum resistance to impact value of 70 deci-ft lb/sq in after one day of curing. Impact resistance values ranged from 52 deci-ft lb/sq in for block mix #3

Table 5.4. Compressive strengths of Alpena (8 X 8 X 16 inch) 12/86 blocks.

	MIX NUMBER						
	1	2	3	4	5	6	7
<b>1 DAY CURE</b>							
TOTAL LOAD(1bs)	51000 69000	62000 59000	79000 81000	49500 52000	136000 128000	113000 130000	76000 90000
GROSS PSI ± (Std.Dev)	504 (107)	508 (18)	672 (12)	426 (15)	1109 (48)	1021 (101)	697 (83)
NET PSI ± (Std.Dev)	986 (209)	994 (35)	1314 (23)	834 (29)	2168 (93)	1996 (197)	1363 (163)
<b>28 DAY CURE</b>							
TOTAL LOAD(1bs)	117000 117500	99000 134000	160000 174000	76400 95000	161000 192000	190000 189000	156000 110000
GROSS PSI ± (Std.Dev)	985 (3)	979 (208)	1403 (83)	720 (111)	1483 (184)	1592 (6)	1118 (273)
NET PSI ± (Std.Dev)	1926 (6)	1914 (407)	2743 (163)	1408 (216)	2899 (360)	3113 (12)	2185 (534)

Table 5.5. Alpena Block (12/86) Weights, Densities, and Impact Resistance After 1 Day Cure.

Mix Design #	1	2	3	4	5	6	7
Block Weight (lbs)	35.27 35.69	36.95 36.70	38.41 38.45	38.92 39.13	37.20 37.65	37.70 37.50	34.40 35.10
Average Weight	35.48 (0.30)	36.83 (0.18)	38.43 (0.03)	39.03 (0.15)	37.43 (0.32)	37.60 (0.14)	37.45 (0.49)
Block Density (lbs/ft <sup>3</sup> ) (g/cc)	132 2.11	137 2.19	143 2.29	145 2.32	139 2.23	140 2.24	129 2.07
Avg. Impact Resistance after 1 day curing (deci ft.lb/in <sup>2</sup> )							
Crack	77 (24)	64 (78)	36 (20)	36 (10)	186 (90)	124 (46)	166 (72)
Fracture	115 (37)	104 (108)	52 (24)	61 (19)	205 (108)	174 (67)	202 (75)

Note: Values in parentheses denote the standard deviation.

to 205 deci-ft lb/sq in for block mix #5.

The impact resistance is plotted versus the compressive strength for the Alpena blocks and is shown in Figure 5.3. In general, the resistance to impact increases with increasing compressive strength.

### 5.3.7 Effects of Seawater Exposure on Block Strength

Samples of stabilized incineration ash mixes were placed on a seatable at the MSRC Flax Pond facility. Filtered seawater was continuously circulated through the seatable to provide an environment similar to the environment the blocks must endure once placed in the sea. Periodically, two blocks were retrieved from the seatable and tested to determine their compressive strength.

#### 5.3.7a Westchester Proctors

Effects of the long-term seawater exposure on the compressive strengths of proctors fabricated in December 1985 using Westchester ash sampled during August 1985 are shown in Table 5.6 and Figure 5.4. Details of the proctor fabrication are given in Roethel *et al.* (1986). Results show a slight increase in the compressive strength of the proctors after 360 days of seawater exposure. Compressive strengths increased from an initial value of 1231 psi to 1287 psi, an increase of 4.5%.

#### 5.3.7b Barrasso Blocks

Samples of the Natural block and the 6/1 Reef block, fabricated during September 1986, were placed in seatables to determine the effects of seawater exposure on the compressive strengths of the blocks. The Natural blocks showed an increase in net compressive strength of 1004 psi to 1424 psi after 120 days of seawater exposure. In contrast, the compressive strength of the 6/1 Reef block decreased from 808 psi to 757 psi after 120 days, a loss of 6.4% (Table 5.7, Figure 5.5).

#### 5.3.7c Alpena Blocks

The net compressive strength of Alpena reef block, mix #7, was 2102 psi after 90 days of seawater exposure (Table 5.8).

Figure 5.3 Impact resistance versus compressive strength for Alpena blocks.



# ALPENA BLOCKS

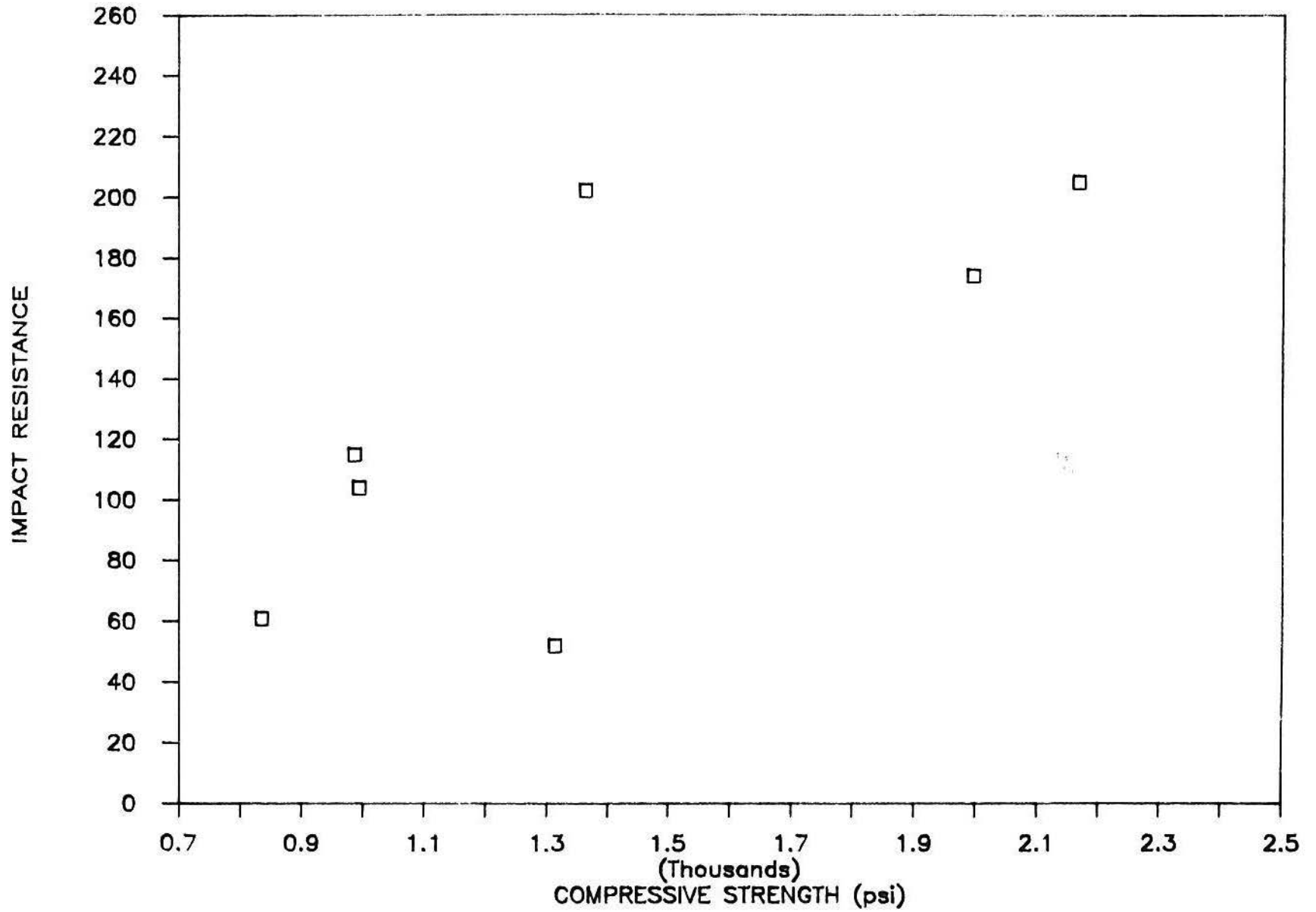


Table 5.6. Seawater Submersion Test of Westchester Proctors.<sup>a</sup>

Total submersion time (days)	0	60	122	185	241	306	360
Removal Date		2/18/86	4/21/86	6/23/86	8/18/86	10/22/86	12/15/86
Compressive Strength (psi)		1468 1456	1110 1385	1170 1206	1301 1353	1353 1233	1350 1223
Ave. Strength Std. Dev.	1231 54	1462 6	1248 138	1188 18	1327 26	1293 60	1287 64

<sup>a</sup> Westchester ash, 15% cement, 17% moisture, cured at 49°C for 24 hours.

Figure 5.4 Compressive strength versus seawater submersion time for Westchester proctors.

# WESTCHESTER PROCTORS

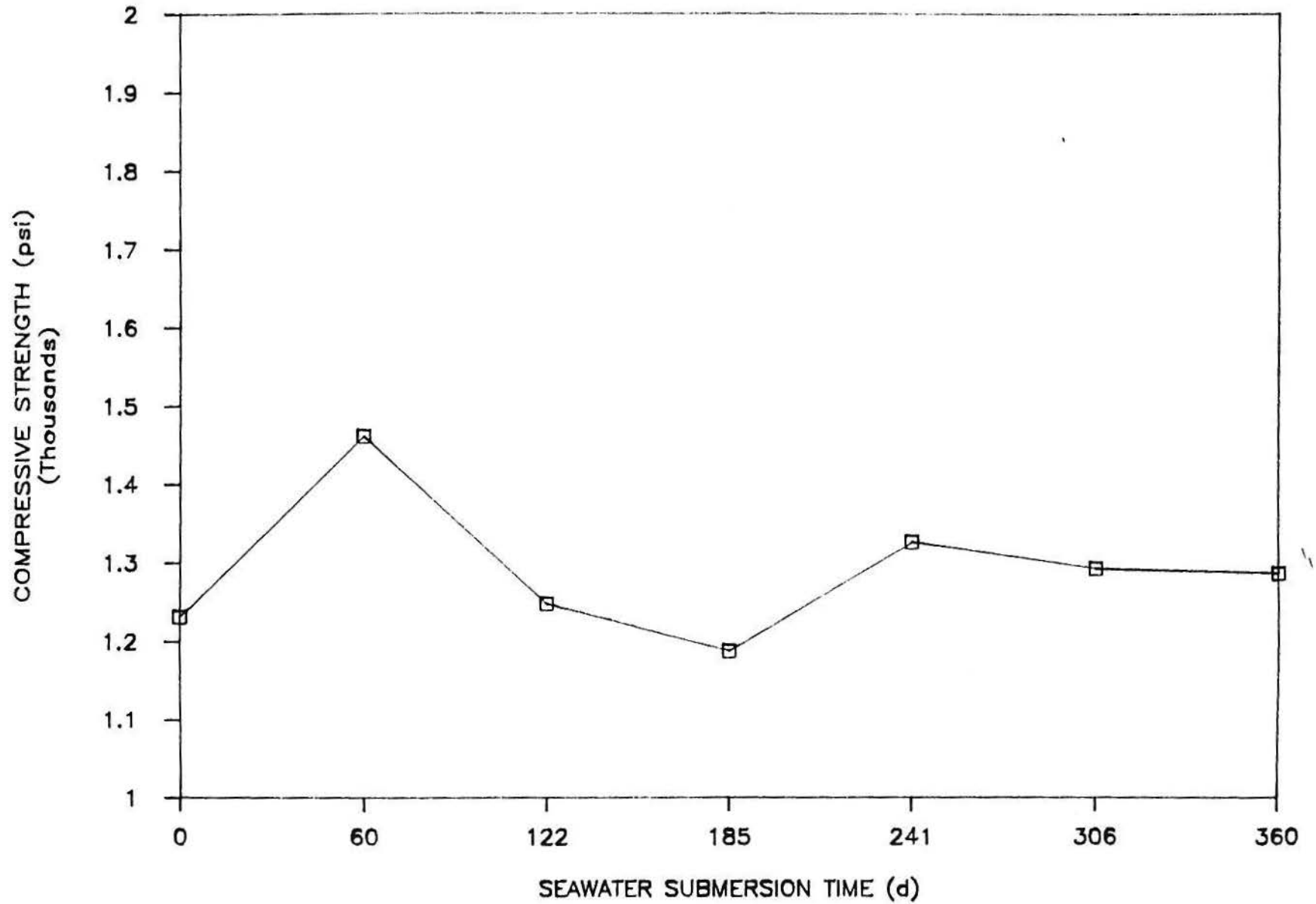


Table 5.7. Compressive strength of seawater submerged Barrasso (9/86) blocks.<sup>a</sup>


---

Total submersion time (days):	0	28	66	120
Removal Date:		12/1/86	1/8/87	3/3/87
NATURAL BLOCK: <sup>b</sup>				
Avg.Gross psi	522	517	547	740
Std.Dev.	192	5	5	205
Avg.Net psi	1004	995	1052	1424
Std.Dev.	369	10	10	395
REEF BLOCK: <sup>c</sup>				
Avg.Gross psi	590	584	595	552
Std.Dev.	39	132	11	82
Avg.Net psi	808	800	816	757
Std.Dev.	76	180	14	112

---

<sup>a</sup> Blocks cured at 119°C for 20 hours; yard curing time 41 days.

<sup>b</sup> Natural block; 61.6% ash, 24.7% sand, 13.7% cement, 10.5% moisture.

<sup>c</sup> 6/1 Reef block; 86.5% ash, 13.5% cement, 13.2% moisture.

Figure 5.5 Compressive strength versus seawater submersion time for Barrasso blocks.

# BARRASSO BLOCKS

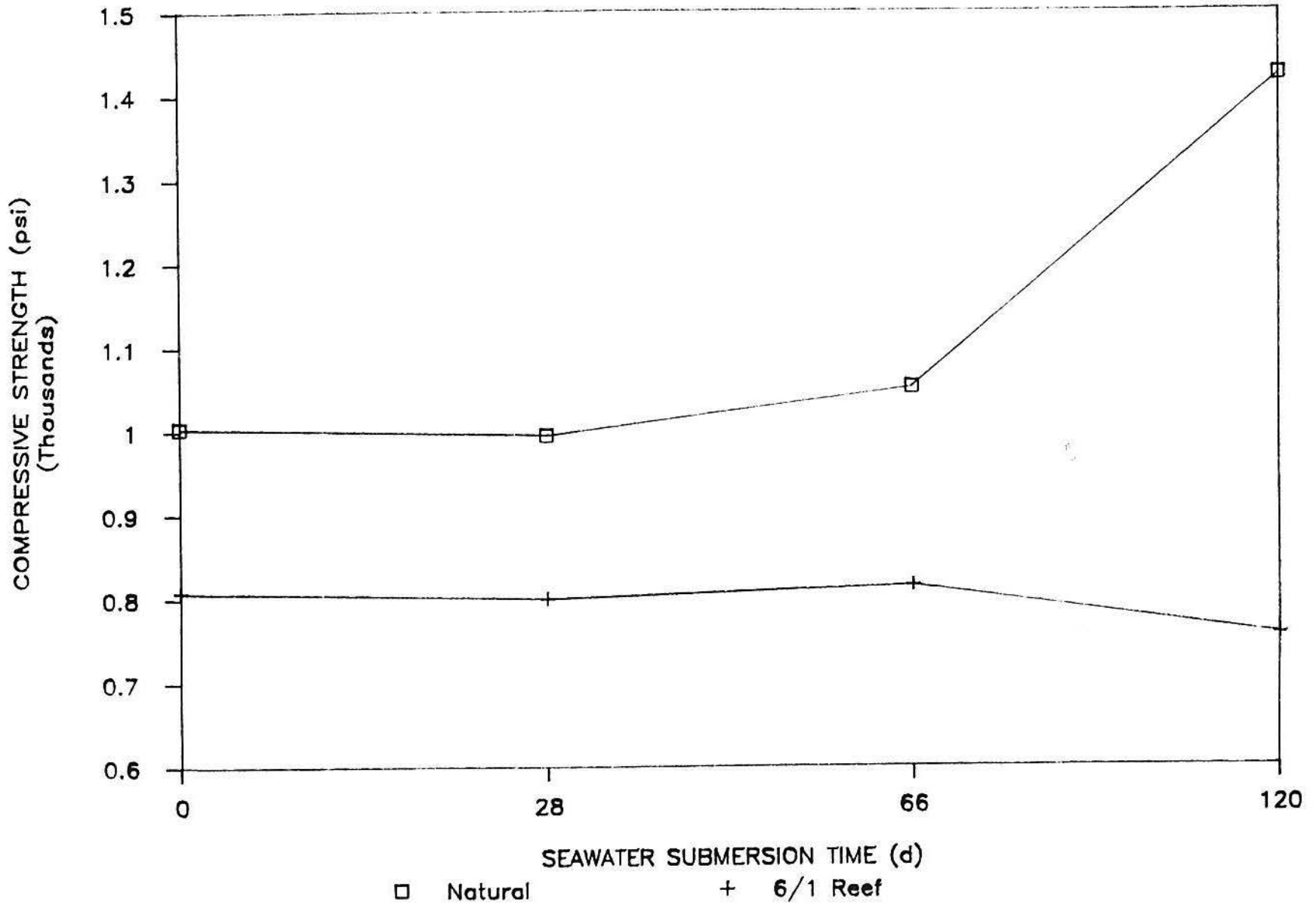


Table 5.8. Seawater submersion test for Alpena Reef block<sup>a</sup>.

---

Mix #7		
BLOCK TYPE	8 X 8 X 16	2 CORE
REMOVAL DATE :	1/14/87	4/14/87
SUBMERSION TIME (d) :	0 <sup>b</sup>	90
AVG. GROSS PSI	1118	1076
STD.DEV.	273	178
AVG.NET PSI	2185	2102
STD.DEV.	534	348
% CHANGE		9.2

---

<sup>a</sup> 63.8% composite ash, 21.3% crushed ash, 15% cement, 11.4% moisture

<sup>b</sup> After 28 day air cure



## 5.4 NONDESTRUCTIVE TESTING OF INCINERATOR WASTE BLOCKS

### 5.4.1 Introduction

The field of quantitative nondestructive testing (NDE) using ultrasonic wave propagation has recently taken on great importance in science and industry as a means of diagnostically testing materials and structures without the need of destroying or altering the samples. The value of NDE methods is therefore obvious and advances have recently been made in characterizing internal microstructure, prediction of strength, measurement of bulk and surface properties, detection of flaws, inspection of welds and bonds, and the investigation of fundamental physical processes, all over characteristic lengths not accessible to x-rays but visible to ultrasound (Thompson and Thompson, 1985).

As shown in a previous preliminary study on backscattering in commercial concrete (Carleton and Muratore, 1986) and a number of related works (Muratore and Carleton, 1981; Muratore and Carleton, 1982; Carleton and Muratore, 1985), such techniques are valuable for lossy, highly inhomogeneous media, such as the incinerator ash material being studied here, in order to develop methods of testing the material for its strength and the change in strength over time. This has much bearing on its potential as a structural material. Such an investigation was undertaken to assess the changes undergone by the material during its initial curing period immediately after manufacture and to attempt a correlation between its strength, as measured by destructive compressive strength data, and the nondestructive measurements of density, ultrasonic velocity of propagation, and elastic modulus.

In an isotropic material, or an inhomogeneous material whose inhomogeneities are on a small scale compared to the ultrasonic wavelength and are randomly distributed throughout the material, a macroscopic elastic modulus  $M$  can be defined by noting the classical one-dimensional wave equation for elastic wave propagation (Auld, 1973):

$$M \nabla^2 u = \rho \frac{\partial^2 u}{\partial t^2} \quad 5.1$$

where  $M$  is the elastic modulus,  $\rho$  is the density, and  $u$  is a suitable acoustic field quantity such as the particle displacement. Assuming simple harmonic wave functions of the form:

$$u(x,t) = u_0 \exp[j(\omega t - kx)] \quad 5.2$$

where  $\omega$  is the frequency and  $k$  is the wavenumber, it is straightforward to show, by substitution of eq. 5.2 in eq. 5.1, that eq. 5.1 gives the dispersion formula:

$$k^2 M = \rho \omega^2 \quad 5.3$$

The velocity of propagation is defined as:

$$v = \omega/k \quad 5.4$$

so that, using eq. 5.3, we can get the velocity in terms of the two material parameters, elastic modulus and density:

$$v = (M/\rho)^{1/2} \quad 5.5$$

and an expression for the elastic modulus in terms of the measurable parameters, density and velocity:

$$M = \rho v^2 \quad 5.6$$

The elastic modulus, under the assumptions of an isotropic and nondispersive material, can be calculated from the measured ultrasonic velocity and the density using eq. 5.6, and is a parameter that indicates the compressive or tensile strength of the material in the direction of wave propagation. It is one of the goals of this investigation to measure the elastic modulus for the incinerator ash material and find a possible correlation with the compressive strength, as determined by the conventional destructive tests. The other goal is to show how these properties change with time during their initial curing period.

#### 5.4.2 Methods

In order to obtain  $M$  using eq. 5.6,  $v$  and  $\rho$  must be measured. The velocity  $v$  is measured by a time-of-flight technique (Muratore and Carleton, 1981; Carleton and Muratore, 1985) using short ultrasonic pulses; and the density is

measured by a mass displacement method. Both techniques were employed successfully in the investigations of the properties of stabilized coal waste material and other porous, fluid-filled materials (Muratore and Carleton, 1981; Carleton and Muratore, 1985).

The measurements here are made on a group of thirty cylindrically-shaped samples of the incinerator ash material which were all fabricated within as short a time as possible (6 hours) and left to air cure for 24 hours before being immersed in water for two days prior to the start of the ultrasonic testing schedule. In this way the material properties are being measured for changes in the early stages of curing soon after manufacture. The proctors were prepared using a 3:1 ash:sand mix ratio. The ash component consisted of a 1:1 mix of Westchester August 1985 ash to Westchester November 1986 crushed ash. Fifteen percent of the total mix weight was added as Portland type II cement. The moisture content of the proctor mixes ranged from 12.5% to 13.8%, with an average moisture content of 13.4%.

Thirty samples were made as identically as possible but showed small but significant variations in length, diameter, and shape. This required the measurement of length and diameter for each sample to preserve accuracy in the velocity and compressive strength calculations, respectively. The differences in shape and the irregularity and lack of parallelism of the end faces could not be compensated for and will cause significant error in the compressive strength tests, which is another disadvantage of compressive testing improved upon by the NDE measurements, as seen in the variation in the data for each parameter. The mean length of all the samples was 11.79 cm with a maximum range of variation of 0.455 cm, and the mean width was 10.41 cm with variation of 0.25 cm.

The testing schedule is as shown in Fig. 5.6. The testing started on day 1 and progressed with increasing intervals in time to allow for the changes in properties due to hydration and cementation in the fluid-filled pores of the material, similar to the process that takes place in concrete and has been shown to occur in the stabilized coal waste material (Carleton and Muratore, 1985). On each test day, after density and ultrasonic velocity measurements were made, a group of three samples was removed for compressive tests, and in this way the number of samples was reduced by three on each test day until only three samples remained on the last day (day 35). This allowed a progressive

Figure 5.6 Testing schedule.

Test day	1	2	3	5	7	10	14	21	28	35
# Samples for Compressive Test	3	3	3	3	3	3	3	3	3	3
# Samples for NDE	30	27	24	21	18	15	12	9	6	3

chronological series of compressive strength measurements for the whole set of samples in conjunction with the velocity, density, and modulus measurements for each group, terminated on that test day due to the destructive nature of the compression test. The compressive strength tests therefore comprise a time series with respect to individual groups, but this could not be done for each individual sample during its testing cycle, for obvious reasons. This means that the compressive test time series results and their correlation with the results of the other parameters, such as the modulus, are dependent on the uniformity of the samples for their accuracy, since this was necessarily done for a different group each time in the testing schedule. The testing schedule thus described also allowed a full 35 day time series of density, velocity, and elastic modulus measurements to be done on only the last 3 samples that remained by day 35.

With the data resulting from the testing procedures described above, plots of density, ultrasonic propagation velocity, and elastic modulus versus time are done for the last three samples during the 35 day period and also for the three samples before those for the first 28 days of the testing schedule. These are done to show the growth of these properties as the material cured. Plots of the compressive strength and the elastic modulus are also made for the groups of three as time progressions, with the qualifications of uniformity kept in mind, as mentioned above. This is done to show changes in strength with curing time. Finally, a plot of compressive strength against elastic modulus for the groups is made to determine if there is a correlation between the destructive measurement and the NDE modulus measurement.

The density measurements are made with the same displacement technique used in the previous work. The actual mass  $m$  of the sample and its submerged mass  $m_s$ , while immersed in water, are measured on a precision digital electronic balance (Sartorius Model 1213MP) and, knowing the density  $\rho_w$  of the water, the density  $\rho$  of the sample is given by

$$\rho = \frac{\rho_w m}{m - m_s} \quad 5.7$$

since the change in mass is equal to the mass of the water displaced.

The velocity of sound propagation  $v$  for each sample was obtained by using the time-of-flight technique employed successfully in previous investigations (Muratore and Carleton, 1981; Carleton and Muratore, 1985). This was accomplished using the ultrasonic immersion, through-transmission testing system shown schematically in Fig. 5.7. A Panametrics 5052PR pulser-receiver is triggered by pulses from an HP214B pulse generator to put out 1.6 nsec exponential pulses at a rate of 33 Hz. These electrical pulses excite a 500kHz broadband piezoelectric immersion transducer (Panametrics Model V-391) to produce ultrasonic pulses which propagate through the water of the test tank, and through any sample material mounted in the acoustic beam path, to another V-391 transducer acting as a receiver, which converts the ultrasonic pulse back to an electrical signal. The signal is then input into a 40 dB pre-amplifier inside the 5052PR and the output is then filtered using a bandpass filter before entering the vertical amplifier module of a Tektronix 7854 digital storage oscilloscope. The bandpass filter was necessary to eliminate both 60 Hz and high frequency noise and thus increase the signal-to-noise ratio (SNR) enough to make accurate time delay measurements. The sample material is very lossy and, even with the amplification and filtering described above, the peak-to-peak amplitude of the sample pulses were initially as low as 25 mv. As material integrity and strength increased with time during the testing period, the signal strength also increased, giving an improved SNR. The signal waveforms were then digitized at a sampling frequency of  $f_s = 20.48$  MHz, each with a total record length of 1024 points per waveform. The signals are also averaged on acquisition to further increase the SNR. The resulting digital waveforms, now discrete data sets, are then stored in the scope memories for further processing.

Each sample is inserted in the acoustic beam path and the resulting signal is acquired and stored digitally, as described above. A reference signal through the water coupling medium without any sample is also acquired and stored. Since the reference signal is about 200 times as strong as the sample signal, 44 dB of attenuation has to be switched in to prevent overdriving the preamplifier and distorting the signal. The digitized reference and sample signals for a typical sample are shown in Fig. 5.8. It can immediately be seen that the sample signal appears sooner in time than the reference. Since the velocity of sound is much higher in the more dense medium of the sample, the

Figure 5.7 Block diagram of ultrasonic testing system.



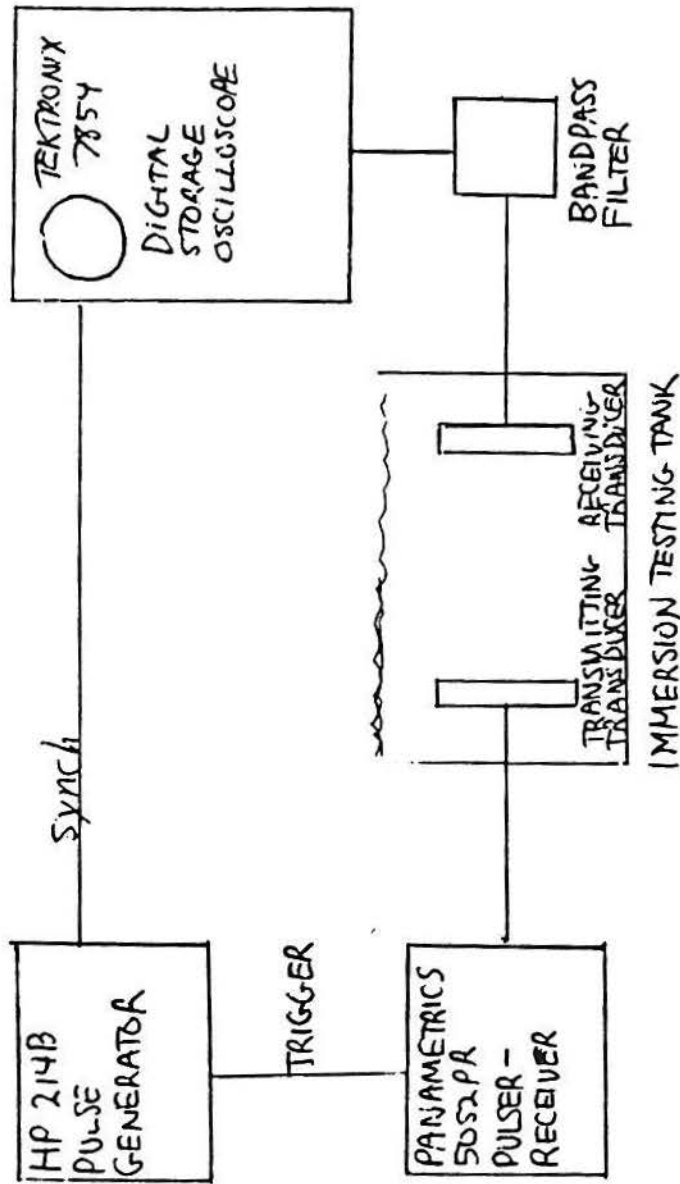
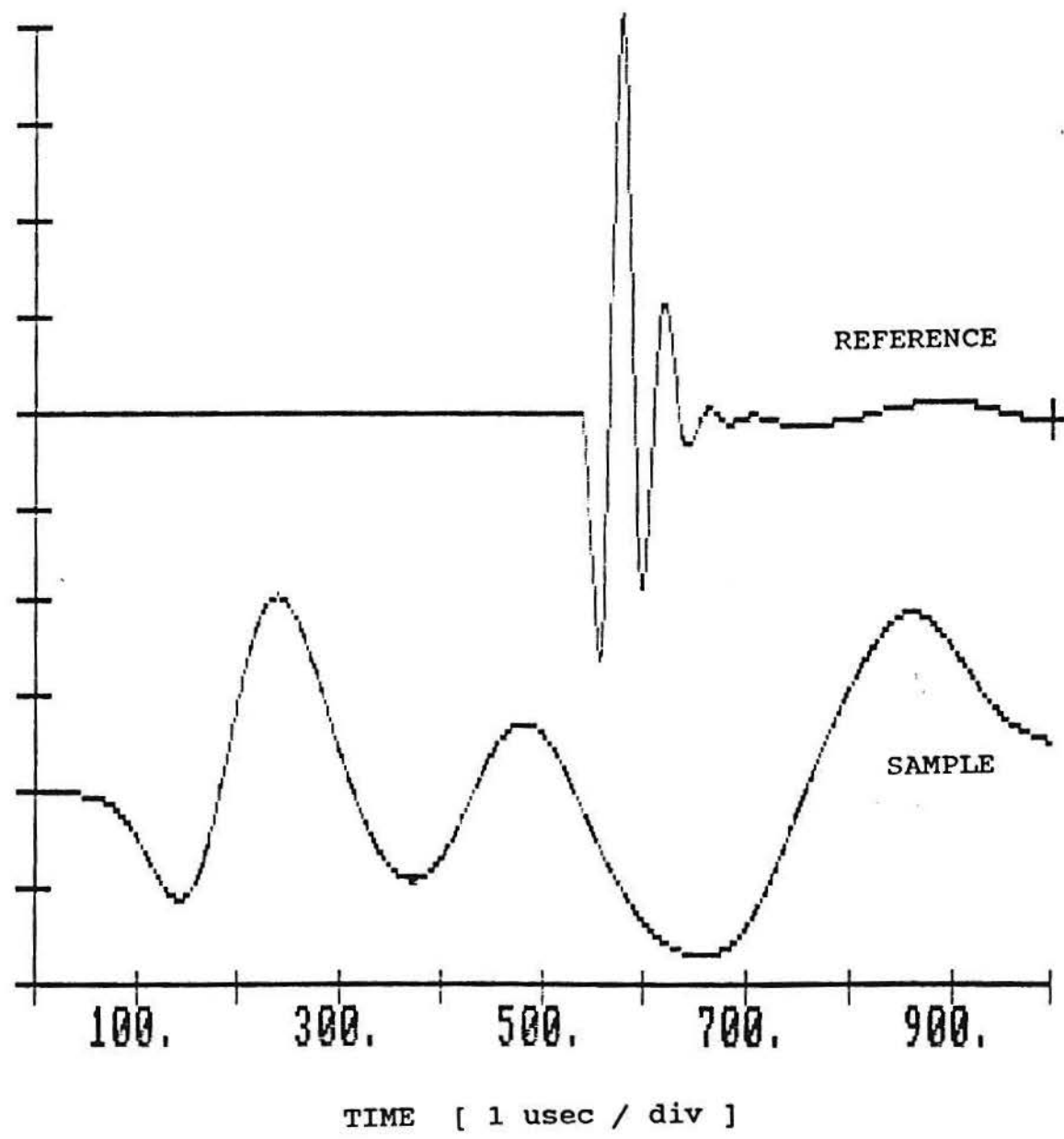


Figure 5.8 Digitized reference and sample signals.



pulse that went through the sample will arrive earlier in time than the reference pulse, which goes through water in the place where the sample had been; the sample signal pulse has a smaller time delay than the reference pulse (Fig. 5.8). By measuring the difference  $\Delta t$  in time delay between the first zero crossings of the two pulses, the velocity can be calculated as:

$$v = \frac{L}{\frac{L}{v_w} - \Delta t} \quad 5.8$$

where  $v_w$  is the velocity of sound in water and  $L$  is the length of the sample. Though the material is highly dispersive, as seen by the difference in shape, and therefore frequency content, of the reference and sample pulses in Fig. 5.8, respectively, the time delay difference  $\Delta t$  gives a good zeroth order approximation of the group velocity of the sample material (Carleton and Muratore, 1985).

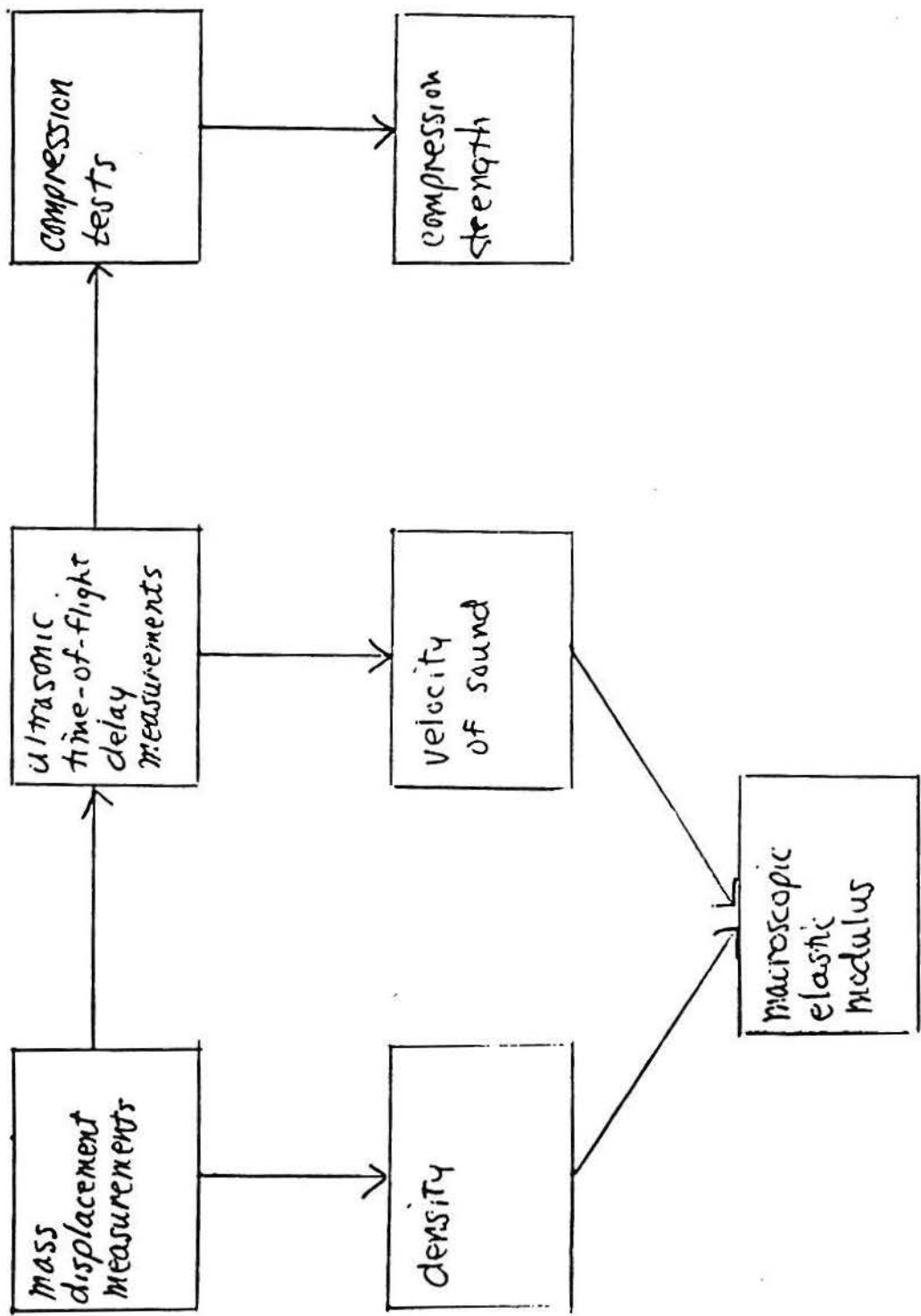
Using the values of density and velocity calculated from the data in eq. 5.7 and eq. 5.8, respectively, eq. 5.6 will then give the elastic modulus  $M$ . Though 5.4 is strictly valid for phase velocity in a dispersive material, the use of eq. 5.8 is still a good approximation.

On each testing day, after the density and velocity measurements are made, three samples are tested for compressive strength on a Forney compression testing machine, with a loading rate of 0.036 mm/sec. These samples were therefore destroyed and could not be used for any further testing. This was done for each test on the schedule in order to have compressive strength data concurrent with the nondestructive parameters of density, velocity, and elastic modulus. The entire testing procedure is summarized in the block diagram of Fig. 5.9.

#### 5.4.3 Results and Discussion

Using the above procedure, density, velocity, and elastic modulus were determined for each sample on each test day, except for those samples that were destroyed in compression strength tests on previous days. Thus,

Figure 5.9 Block diagram of testing procedure.



each day there were three less samples. Only the last three samples have nondestructive parameter data for the entire 35 day period during which tests were performed. Table 5.9 gives the density, velocity, and elastic modulus for the last group of three samples for the 35 day time period and also gives the means for the group. Table 5.10 gives the same data for the group of three before these for a 28 day period.

These data are plotted in Figs. 5.10, 5.11 and 5.12 for density, velocity, and elastic modulus, respectively. As can be seen, the values of these parameters all show the same logarithmic-type increase over time and are still growing by the end of the 35 day testing period. Ultimately, these growth curves will approach an asymptotic value at which most changes have peaked out. It is seen from this that it takes at least 100 days to reach within experimental error of this value. It is also seen that there is much individual variation among the different samples, since the growth curves, though of similar shape, are shifted significantly with respect to each other. These show consistency in the measurement technique and in the growth processes in the material but also show the inconsistency in the initial parameters of the different samples due to differences in the material for the different samples at the fabrication stage prior to testing. Maximum deviations of the density, velocity, and elastic modulus are 1.4 %, 6.6 %, and 13.9 % of the mean values, respectively, for all 30 samples on the initial day of testing. Note in Tables 5.9 and 5.10 and in Fig. 5.10 that the first density value seems to be consistently too high in all six samples. This anomaly also occurred in many of the other samples. We must therefore conclude that this first density measurement is in error for reasons as yet undiscovered and it is therefore treated suspiciously in the analysis and not included in any curve approximations in the time series plots.

Results from the group measurements are also interesting but less enlightening. Table 5.11 gives the values of the compressive strength, density, velocity, and elastic modulus for the individual samples in the the ten groups of three tested destructively each test day. Table 5.12 gives the means and standard deviations for all four parameters for each group, showing the variation in properties for the individual members of each group listed in Table 5.11. Table 5.13 gives the initial values on Day 1 for the groups. It is

Table 5.9. Chronological NDE data for individual samples 28, 29, and 30, and their group mean.

28				29			
t [day]	P [g/cm <sup>3</sup> ]	v [m/sec]	M [10 <sup>10</sup> Pa]	t [day]	P [g/cm <sup>3</sup> ]	v [m/sec]	M [10 <sup>10</sup> Pa]
1	2.096	2620	1.439	1	2.122	2770	1.628
2	2.096	2659	1.482	2	2.120	2800	1.662
3	2.097	2676	1.502	3	2.122	2826	1.695
5	2.097	2723	1.555	5	2.124	2863	1.741
7	2.100	2752	1.590	7	2.125	2898	1.785
10	2.103	2814	1.665	10	2.128	2942	1.842
14	2.105	2872	1.736	14	2.131	2994	1.910
21	2.110	2959	1.847	21	2.136	3045	1.984
28	2.112	3004	1.906	28	2.137	3105	2.060
35	2.115	3048	1.965	35	2.141	3139	2.110

30				MEAN			
t [day]	P [g/cm <sup>3</sup> ]	v [m/sec]	M [10 <sup>10</sup> Pa]	t [day]	P [g/cm <sup>3</sup> ]	v [m/sec]	M [10 <sup>10</sup> Pa]
1	2.117	2737	1.586	1	2.112	2709	1.550
2	2.115	2770	1.623	2	2.110	2743	1.588
3	2.116	2788	1.645	3	2.112	2763	1.612
5	2.118	2828	1.694	5	2.113	2805	1.663
7	2.119	2859	1.732	7	2.115	2836	1.701
10	2.121	2908	1.794	10	2.117	2888	1.766
14	2.125	2962	1.864	14	2.120	2943	1.836
21	2.129	3016	1.937	21	2.125	3007	1.921
28	2.131	3078	2.019	28	2.127	3062	1.994
35	2.135	3115	2.072	35	2.130	3101	2.048



Table 5.10. Chronological NDE data for individual samples 25, 26, and 27, and their group mean.

25				26			
t [day]	P [g/cm <sup>3</sup> ]	v [m/sec]	M [10 <sup>10</sup> Pa]	t [day]	P [g/cm <sup>3</sup> ]	v [m/sec]	M [10 <sup>10</sup> Pa]
1	2.087	2534	1.340	1	2.100	2662	1.488
2	2.087	2554	1.361	2	2.096	2696	1.523
3	2.088	2582	1.392	3	2.097	2717	1.548
5	2.088	2622	1.435	5	2.100	2765	1.605
7	2.091	2663	1.483	7	2.100	2801	1.658
10	2.094	2711	1.539	10	2.103	2855	1.714
14	2.097	2765	1.603	14	2.105	2915	1.789
21	2.100	2838	1.691	21	2.110	2981	1.875
28	2.103	2894	1.761	28	2.112	3035	1.945

27				MEAN			
t [day]	P [g/cm <sup>3</sup> ]	v [m/sec]	M [10 <sup>10</sup> Pa]	t [day]	P [g/cm <sup>3</sup> ]	v [m/sec]	M [10 <sup>10</sup> Pa]
1	2.093	2570	1.382	1	2.093	2589	1.403
2	2.091	2620	1.416	2	2.091	2617	1.432
3	2.093	2619	1.436	3	2.093	2639	1.458
5	2.093	2663	1.484	5	2.094	2683	1.507
7	2.095	2690	1.516	7	2.095	2716	1.548
10	2.098	2737	1.572	10	2.098	2768	1.607
14	2.101	2794	1.640	14	2.101	2825	1.677
21	2.105	2867	1.730	21	2.105	2895	1.764
28	2.107	2914	1.789	28	2.107	2948	1.831

Figure 5.10a Density time series for individual time series and means.  
(□) 25; (+) 26; (◇) 27; (△) mean.

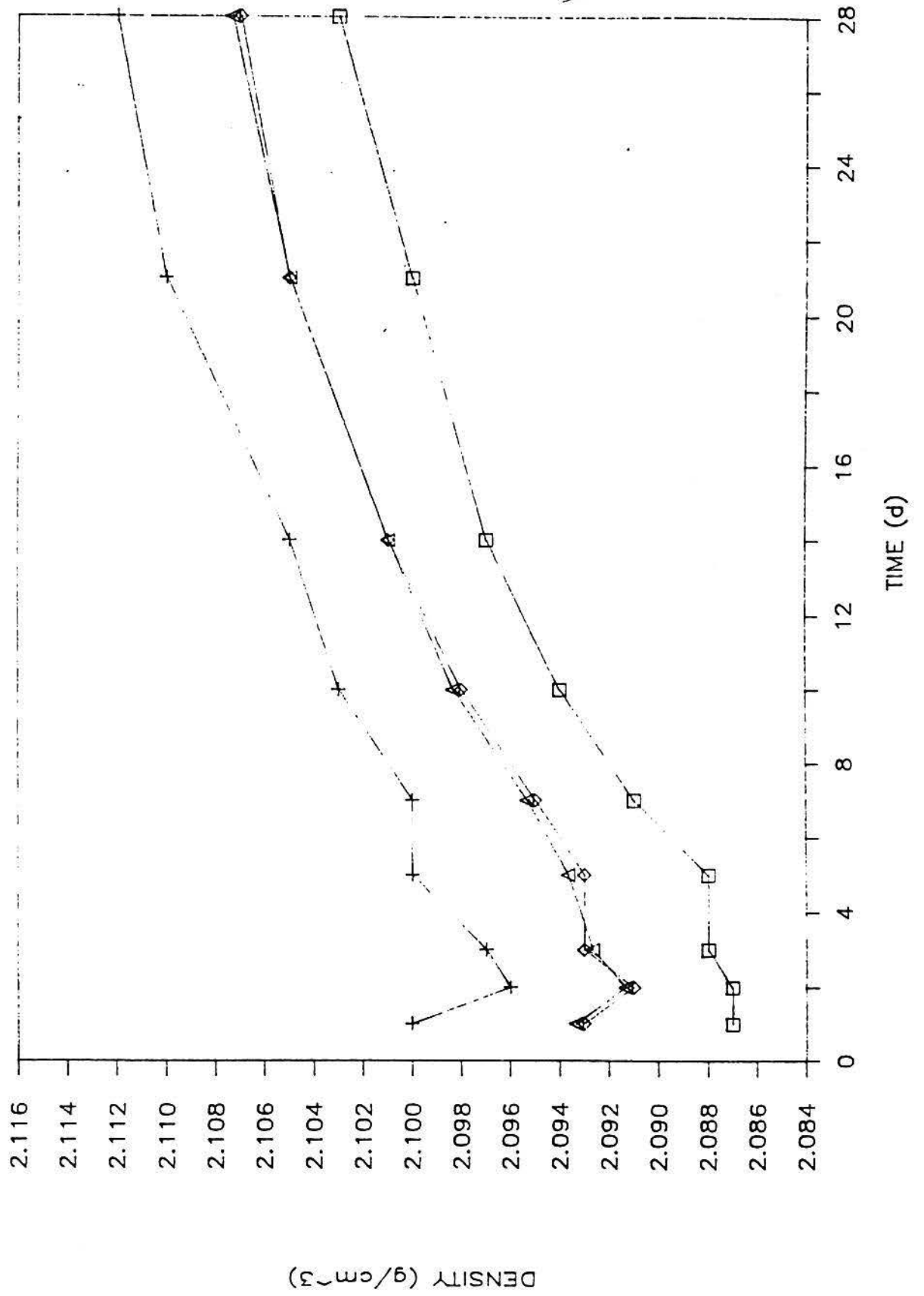


Figure 5.10b Density time series for individual samples and means.  
(□) 28; (+) 29; (◇) 30; (△) mean.

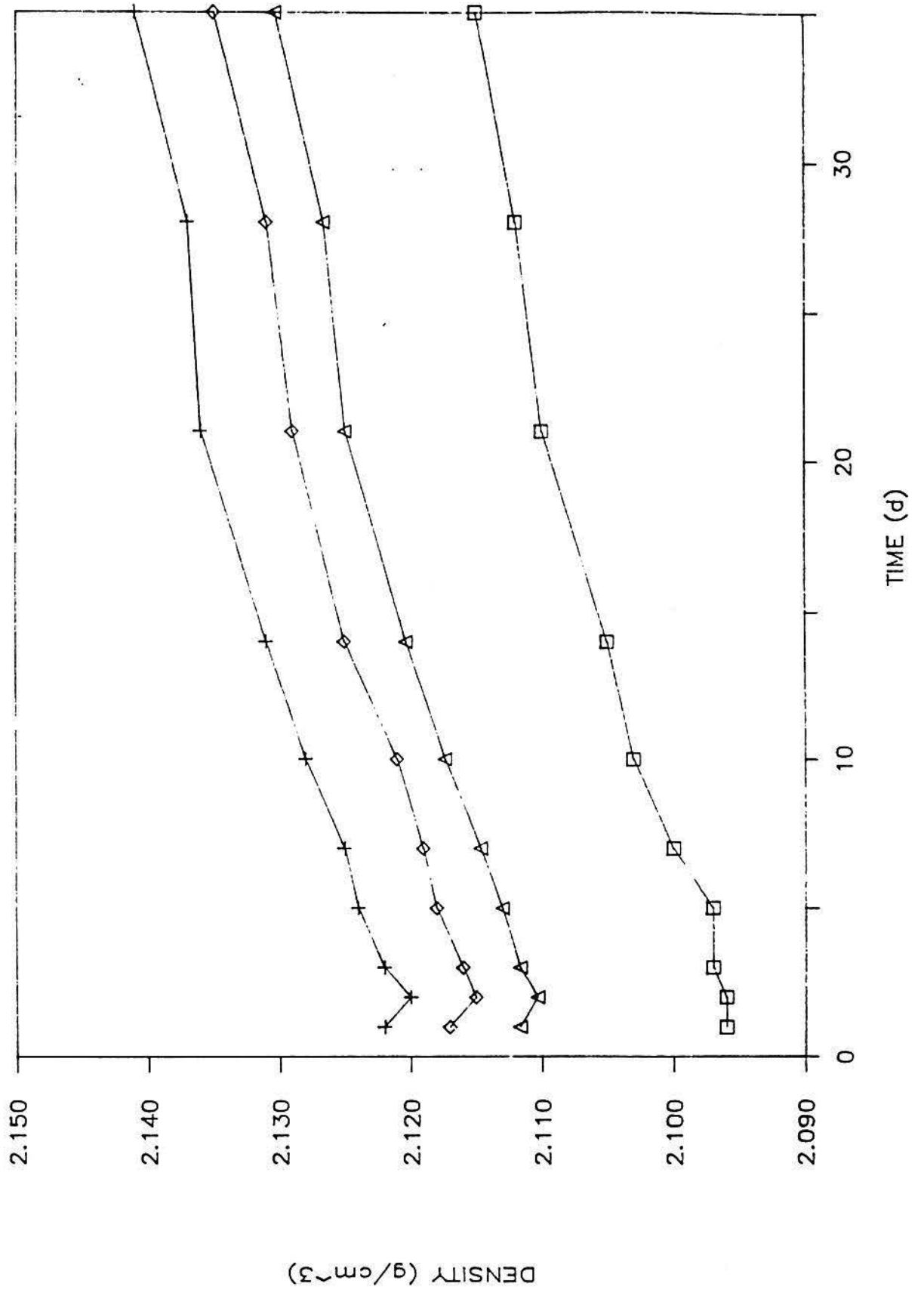


Figure 5.11a Velocity time series for individual samples and means.  
(□) 25; (+) 26; (◇) 27; (△) mean.

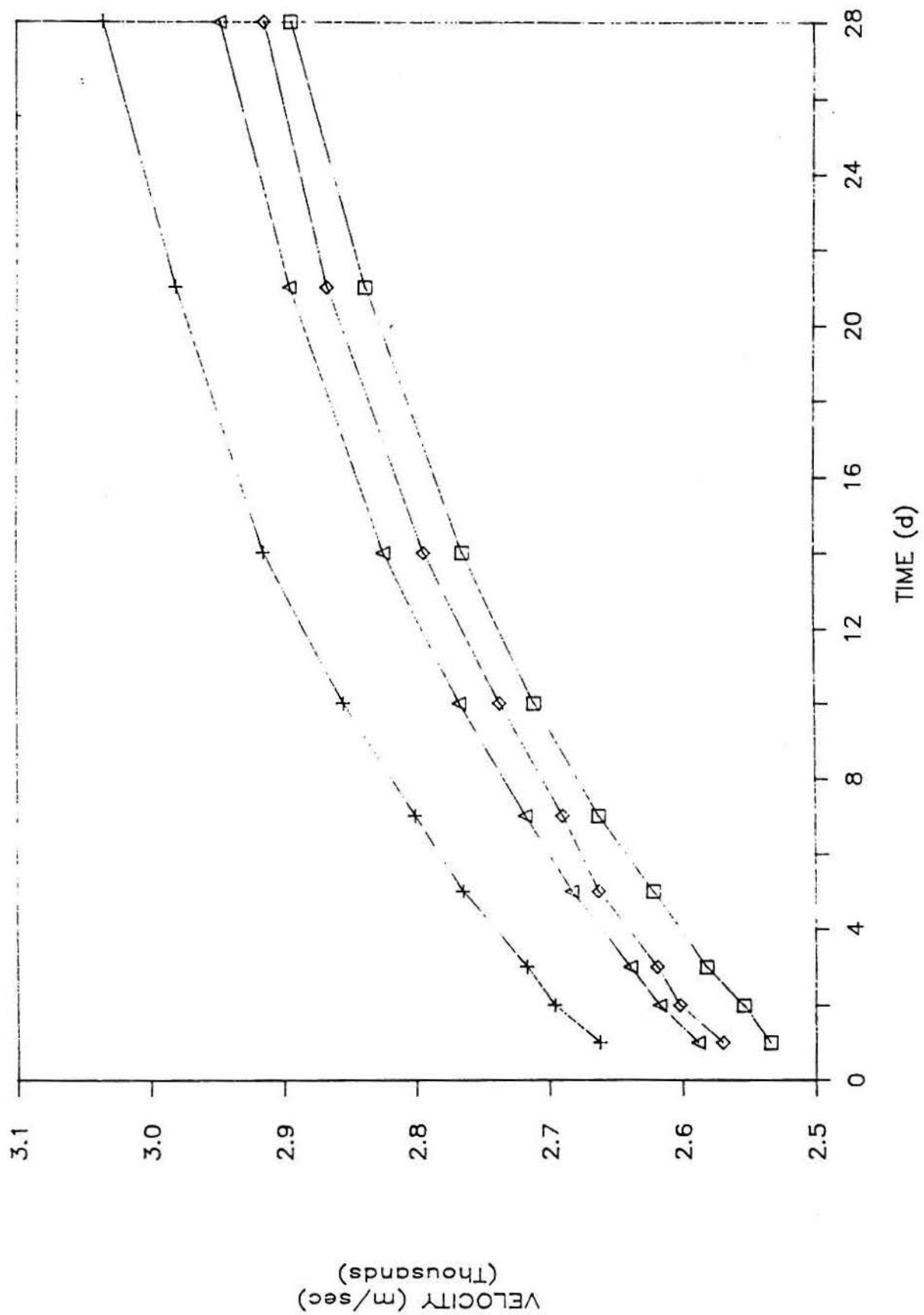


Figure 5.11b Velocity time series for individual samples and means.  
(□) 28; (+) 29; (◇) 30; (△) mean.



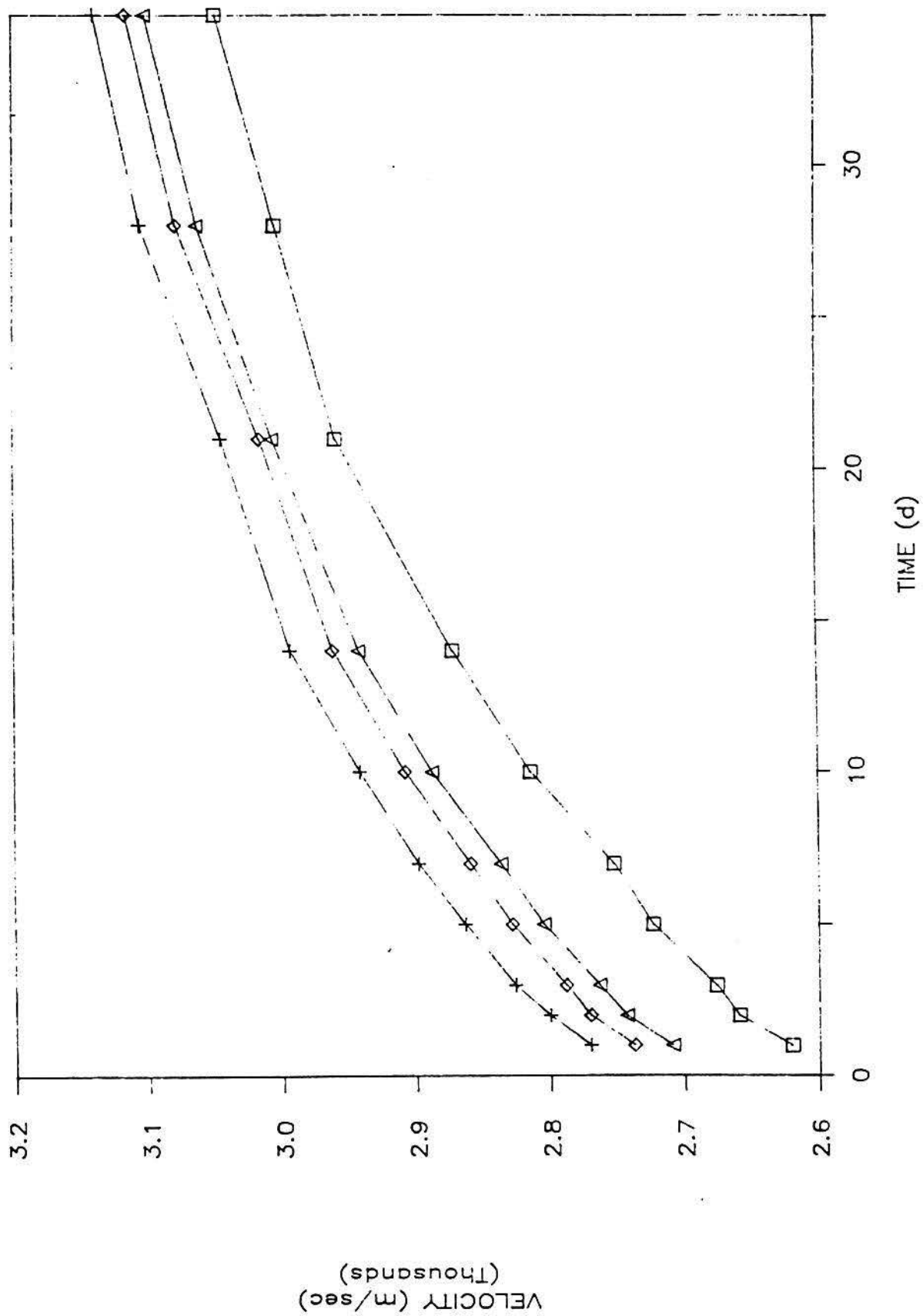


Figure 5.12a Elastic modulus time series for individual samples and means.  
(□) 25; (+)26; (◇) 27; (△) mean.

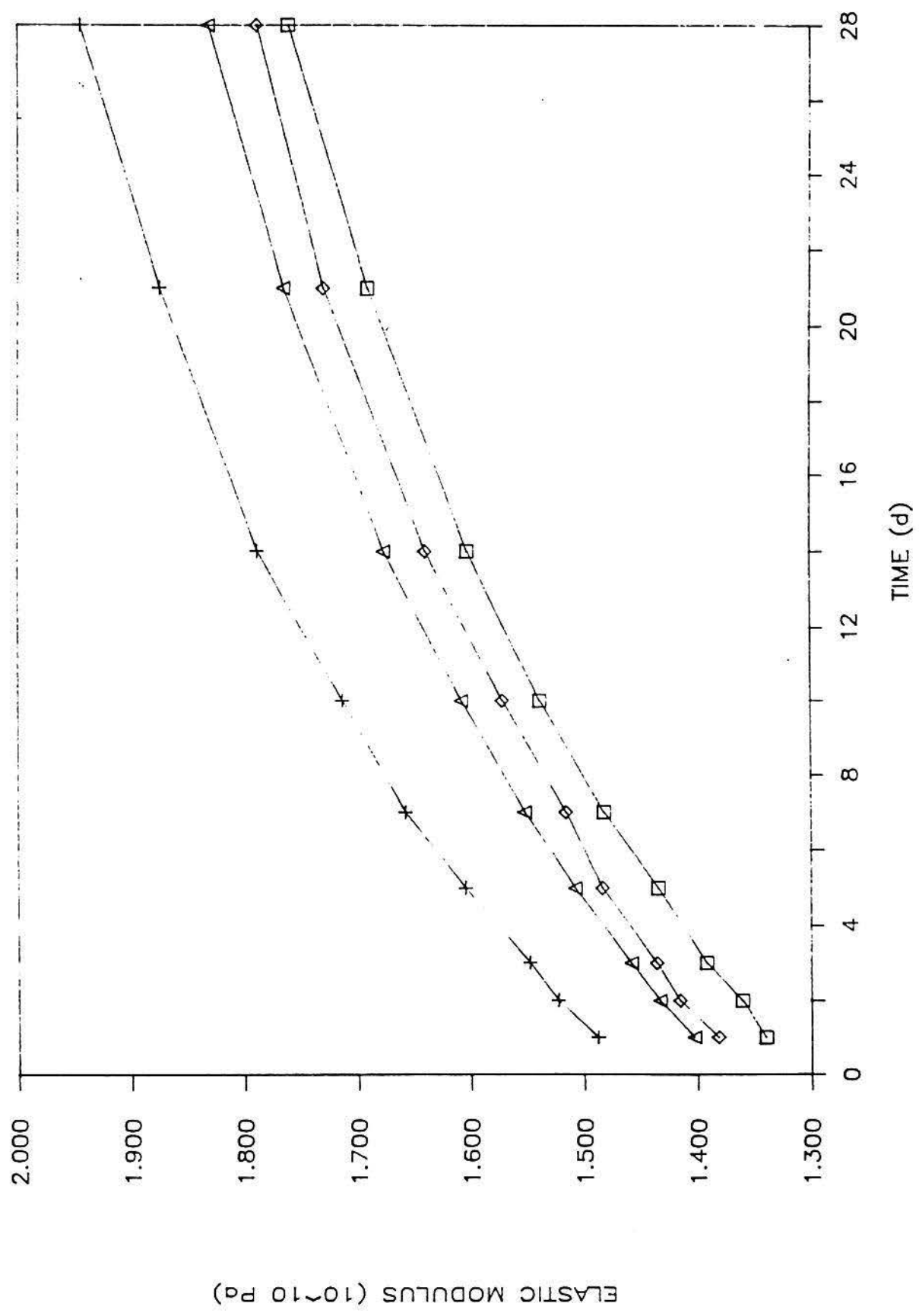


Figure 5.12b Elastic modulus time series for individual samples and means.  
(□) 28; (+) 29; (◇) 30; (△) mean.

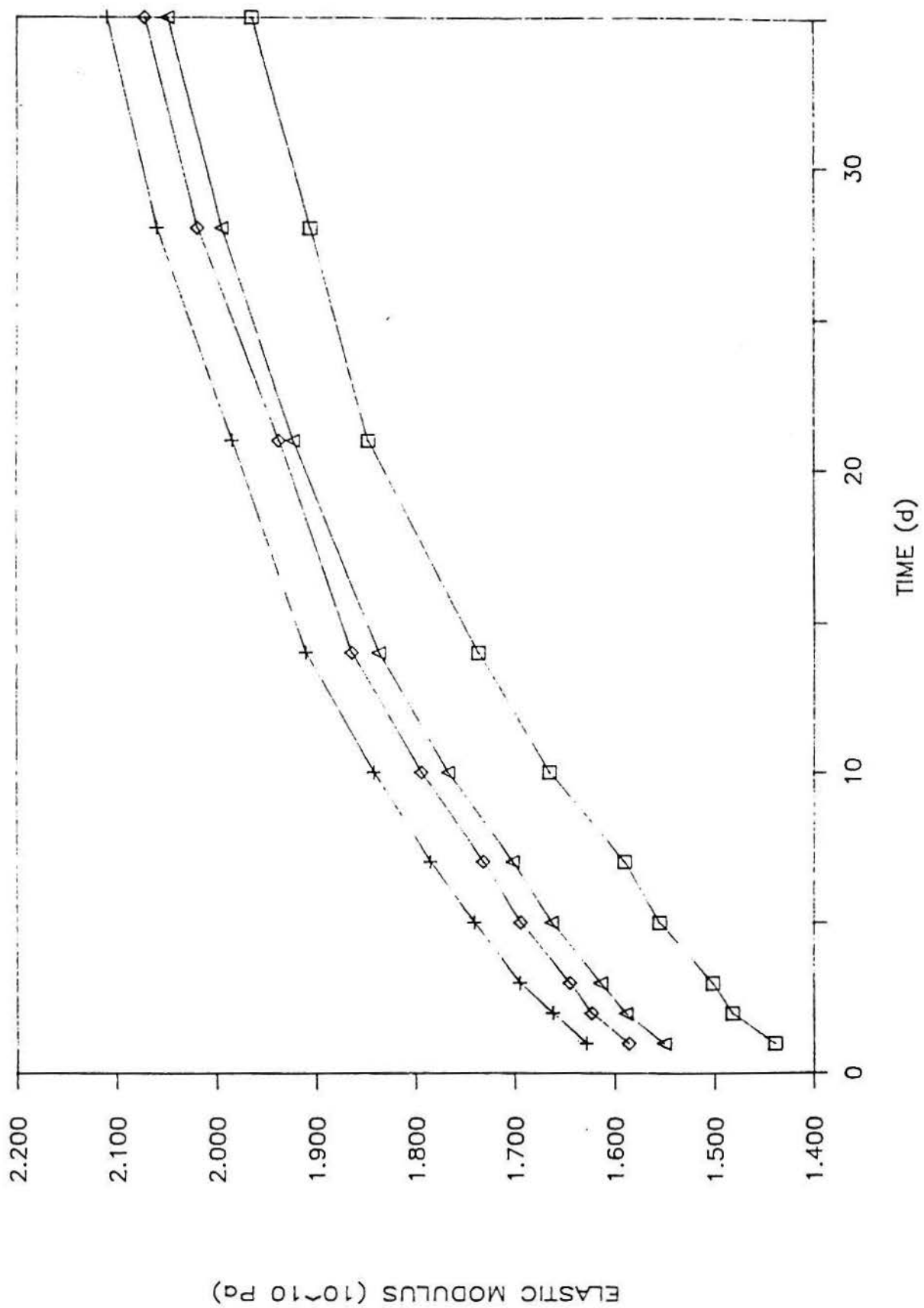


Table 5.11. Initial parameter values for chronological test groups: values on days of compressive tests.

Group [day]	#	S [10 <sup>6</sup> Pa]	P [g/cm <sup>3</sup> ]	v [m/sec]	M [10 <sup>10</sup> Pa]
1	1	6.729	2.130	2720	1.576
	2	5.592	2.131	2811	1.684
	3	3.647	2.118	2868	1.742
2	4	6.164	2.117	2753	1.604
	5	7.453	2.142	2870	1.764
	6	6.247	2.125	2808	1.676
3	7	7.619	2.106	2701	1.536
	8	6.233	2.100	2753	1.592
	9	6.550	2.098	2639	1.461
5	10	5.792	2.111	2742	1.587
	11	5.392	2.104	2814	1.666
	12	5.943	2.112	2786	1.639
7	13	5.888	2.124	2841	1.714
	14	5.895	2.108	2821	1.678
	15	6.219	2.119	2868	1.743
10	16	6.474	2.141	2907	1.809
	17	7.046	2.127	2825	1.697
	18	6.902	2.121	2874	1.752
14	19	7.012	2.123	2985	1.892
	20	6.116	2.118	2940	1.831
	21	6.888	2.112	2936	1.821
21	22	5.971	2.110	3030	1.937
	23	7.205	2.112	3019	1.925
	24	6.191	2.113	2915	1.795
28	25	8.225	2.103	2894	1.761
	26	6.771	2.112	3035	1.945
	27	6.605	2.107	2914	1.789
35	28	6.212	2.115	3048	1.965
	29	8.467	2.141	3139	2.110
	30	7.812	2.135	3115	2.072

Table 5.12. Mean parameter values and standard deviations for chronological test groups: values on days of compressive tests.

Group [day]	S [ $10^6$ Pa]	P [g/cm <sup>3</sup> ]	v [m/sec]	M [ $10^{10}$ Pa]
1	5.323 1.559	2.126 0.00723	2800 74.6	1.667 0.0842
2	6.621 0.721	2.128 0.0128	2810 58.5	1.681 0.0801
3	6.801 0.726	2.101 0.00416	2698 57.1	1.530 0.0657
5	5.709 0.285	2.109 0.00436	2781 36.3	1.631 0.0402
7	6.001 0.189	2.117 0.00819	2843 23.6	1.712 0.0326
10	6.807 0.296	2.130 0.0103	2869 41.3	1.753 0.0560
14	6.672 0.485	2.118 0.00551	2954 27.2	1.848 0.0384
21	6.456 0.658	2.112 0.00153	2988 63.5	1.886 0.0787
28	7.200 0.891	2.107 0.00451	2948 76.3	1.832 0.0991
35	7.497 1.160	2.130 0.0136	3101 47.2	2.049 0.0752

Table 5.13. Initial mean NDE parameter values for chronological test groups on day 1.

---

Group [day]	P [g/cm <sup>3</sup> ]	v [m/sec]	M [10 <sup>10</sup> Pa]
1	2.126	2800	1.667
2	2.127	2802	1.671
3	2.100	2657	1.483
5	2.107	2708	1.545
7	2.113	2735	1.581
10	2.123	2714	1.564
14	2.108	2740	1.583
21	2.099	2688	1.518
28	2.093	2589	1.403
35	2.112	2709	1.551

---



clear that, as expected, the variation in the compressive tests is significantly higher than in the nondestructive parameters, by about an order of magnitude: the mean variation for the compressive strength is 8.45 %, compared to 1.8 % for the velocity and 0.34 % for the density. In addition, each value of a parameter in this case is from a different group of three samples, subject to the variation seen in the sample population of thirty. Time series plots of the group data, even the nondestructive parameters, will reflect these deviations in the samples. Each point in the plot is from a different set of samples.

This is seen in the plot of compressive strength with time of the groups, shown in Fig. 5.13. Here, a definite increasing trend is seen, but the significant variation in compressive strength values, as discussed above, results in a plot of indeterminate shape. Qualitatively, it is clear that the strength of the material is increasing with curing time, as expected; but the lack of consistency in sample shape for the compressive tests introduces large errors which result in a variation 2.3 times larger than that for the nondestructive elastic modulus parameter.

The elastic modulus for the groups is plotted in Fig. 5.14, and like that for the individual samples measured to the end, shows an increase consistent with that of the compressive strength in Fig. 5.13, but also with some variation, making quantitative interpretation difficult. From Table 5.10, it is clear that the fluctuations in the time plot for the groups can be traced to initial group variations, inherent in the samples from fabrication. Unfortunately, there is no such initial data available for compressive strengths, but the data in Table 5.12 shows it to be an order of magnitude more variable than the NDE parameters, as expected. Not surprisingly, then, a plot of compressive strength against elastic modulus in Fig. 5.15 shows no apparent correlation, though an argument can be made for an approximately linear increase of compressive strength with elastic modulus in the plot. Similar plots of compressive strength with density and velocity are also inconclusive.

The plot of velocity against density in Fig. 5.16 also does not exhibit any apparent correlation. The lack of correlation between these two NDE parameters is at first surprising since they are so well-behaved in the

Figure 5.13 Compressive strength versus time.

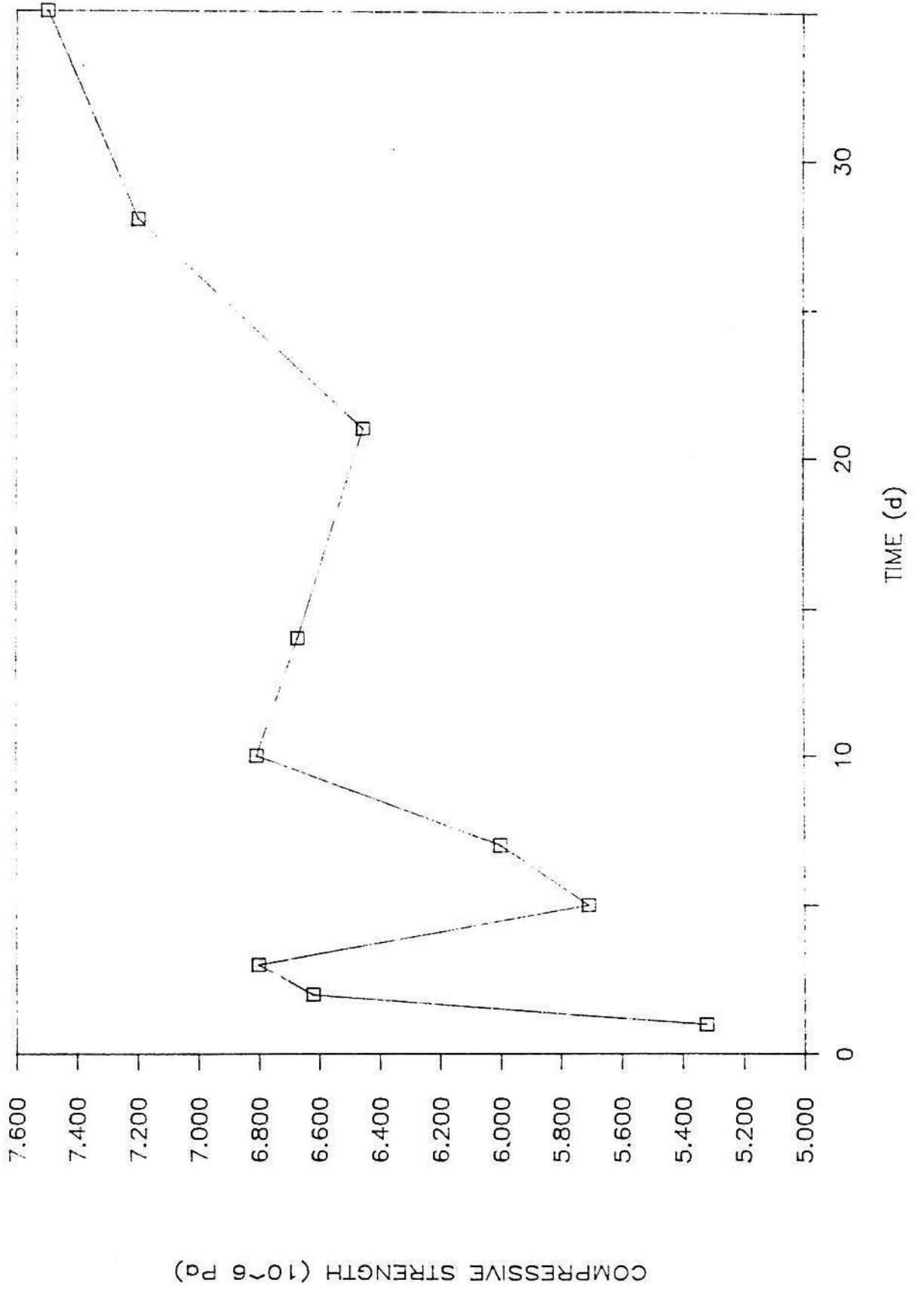


Figure 5.14 Elastic modulus versus time.

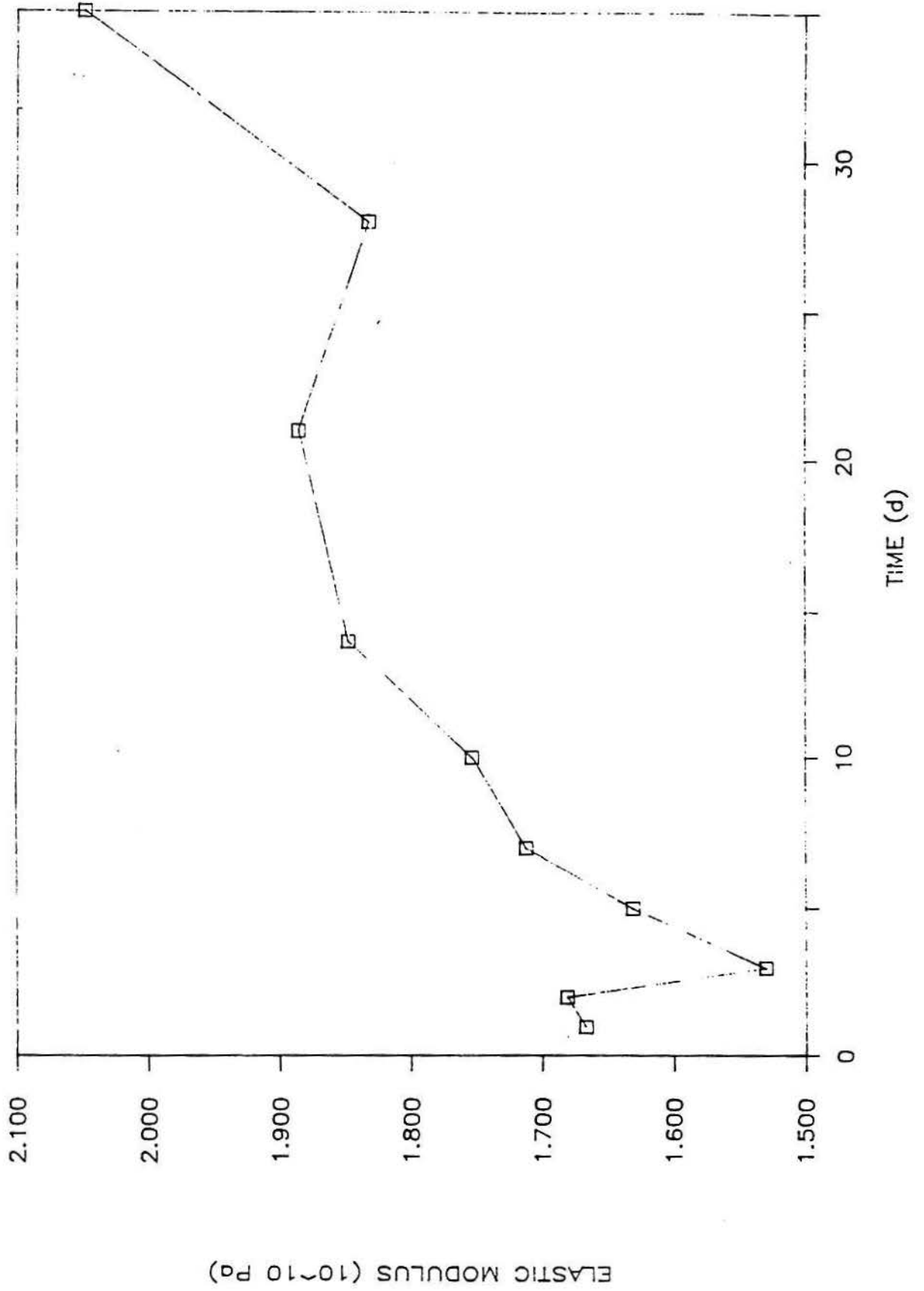


Figure 5.15 Compressive strength versus elastic modulus.

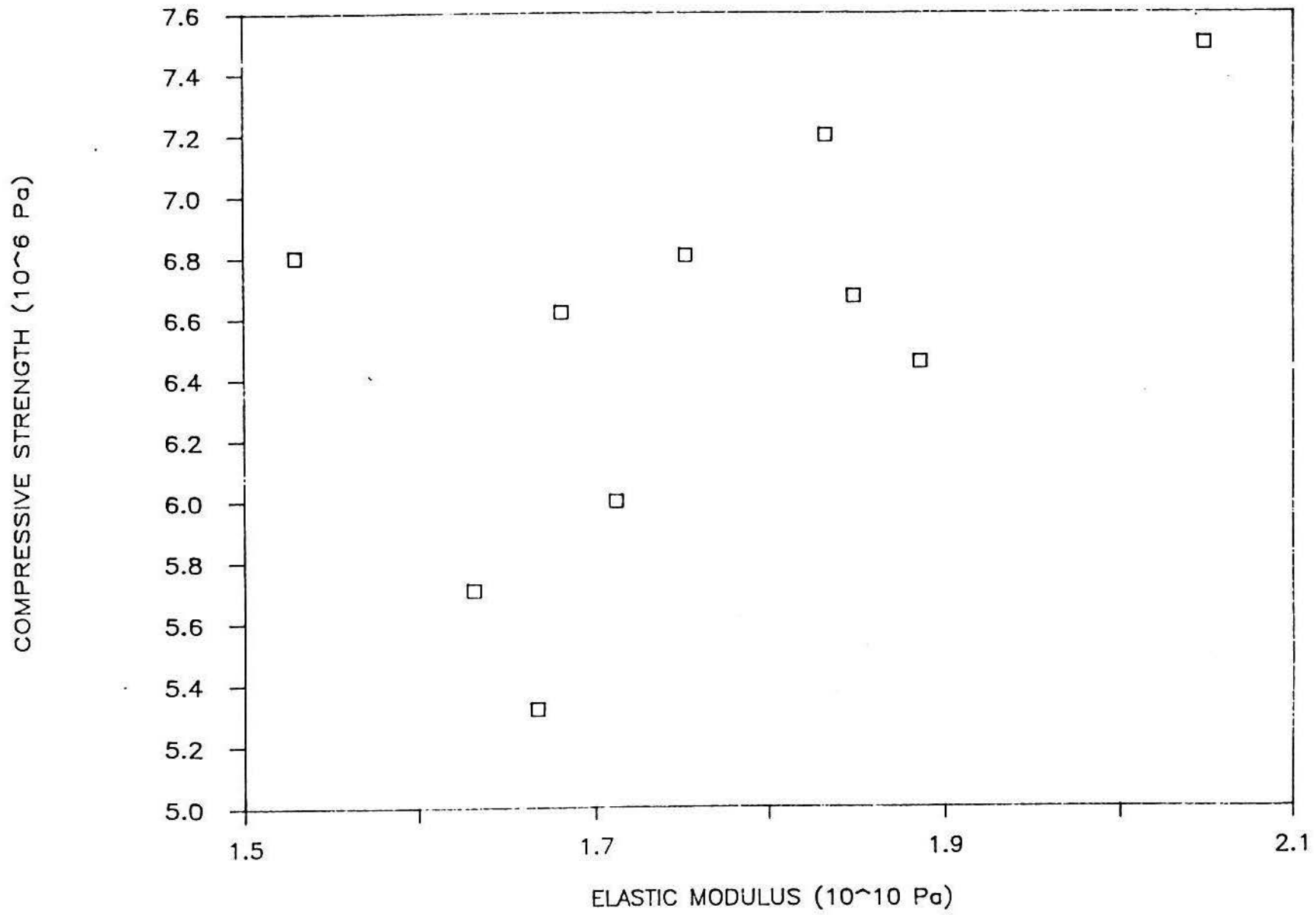
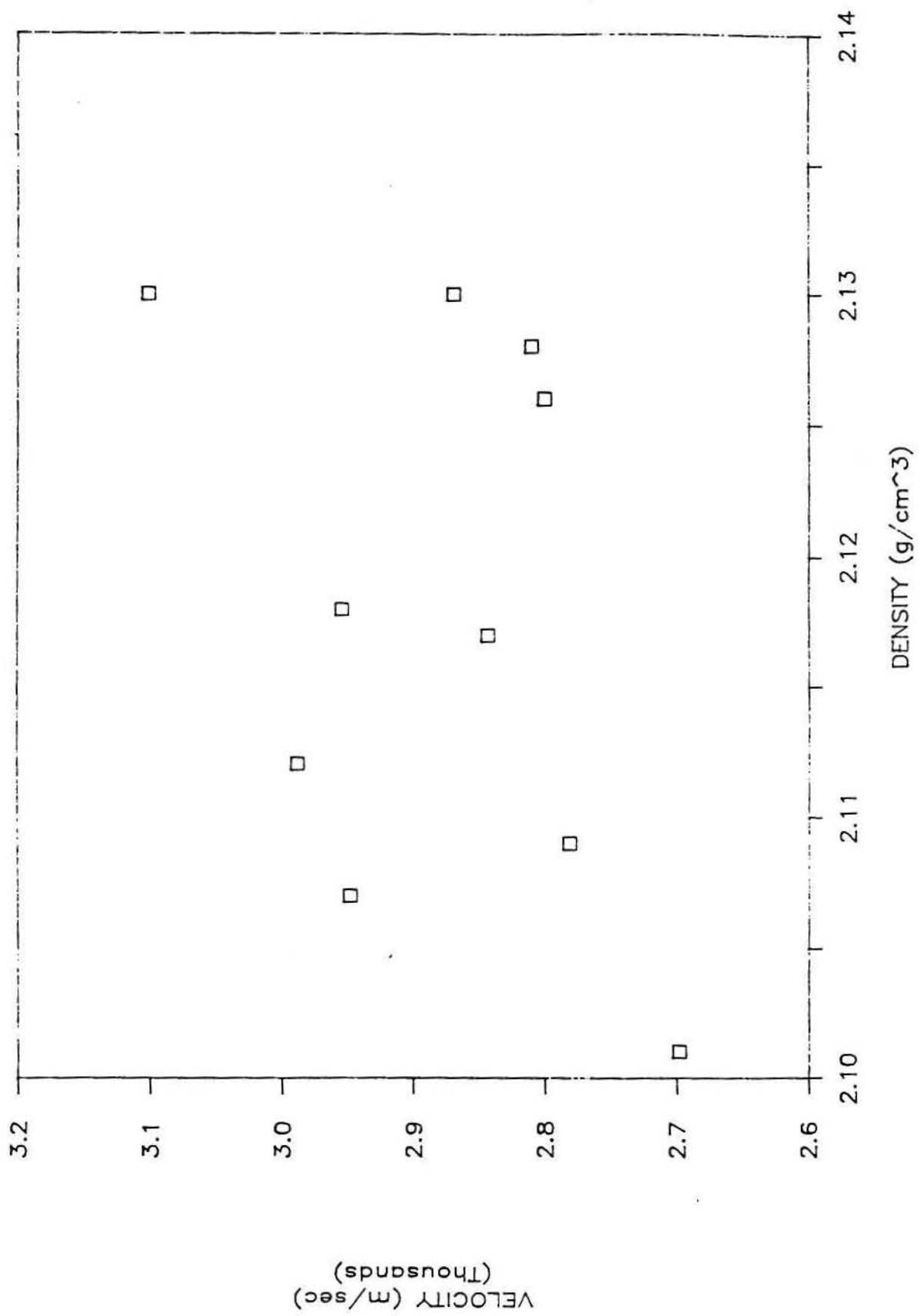


Figure 5.16 Velocity versus density.

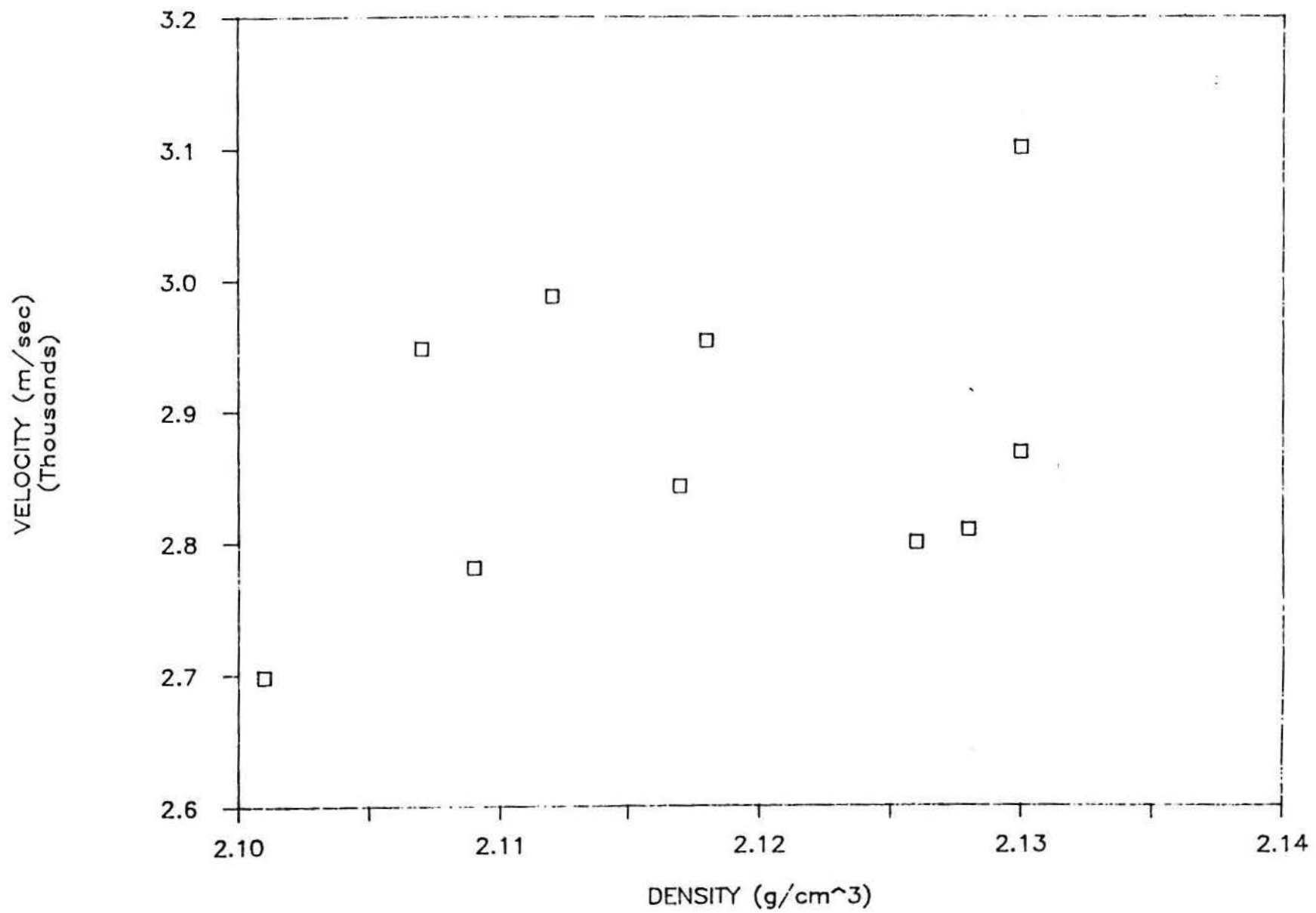




individual time series of Figs. 5.10 and 5.11 and are related by the dispersion eq. 5.5. It must be remembered, however, that eq. 5.5 is strictly true only for a homogeneous isotropic material or a single crystal along one direction. Inspection of the incinerator ash material of the samples shows it to be highly inhomogeneous, and there is a great variation in the size and shape of the component particulates, with particle sizes ranging from a few micrometers to the order of a centimeter, for over four orders of magnitude. With a nominal sound velocity of 3000 m/sec and the transducer center frequency  $f = 500$  kHz, the nominal acoustic wavelength is on the order of 6 mm. There are therefore many inclusions larger in size than the wavelength of the incident ultrasonic waves. Each sample is randomly different in its distribution of these particulates, so it is reasonable to assume that, for each sample, local variations in density and modulus, with a wide range of characteristic lengths, will result in little or no correlation from sample to sample. This is because local variations of density and modulus are different from sample to sample. A plot of velocity against density for the individual sample # 30, as shown in Fig. 5.17, however, does show a definite correlation as expected of these two parameters in the case of an individual material, where all parameters are well-behaved. And, for individual samples, unfortunately, compressive strength data is only available on the final day of testing, for obvious reasons.

The behavior in the time series plots in Figs. 5-10-5.12 brings up some important differences between this and the coal waste investigation (Carleton and Muratore, 1985), though the materials are similar in degree of heterogeneity and the experimental procedures are similar. In contrast to the coal waste study, the measurement of the density, velocity, and elastic modulus for the incinerator waste material was from the start of the curing period, and the data reflects the early rapid changes before these parameters level off to asymptotic values. With the coal wastes, most of the growth in parameters had taken place by the time the tests were started, so the time series plots showed no change, since the parameters had already leveled off. Correlations between the compressive strength and the NDE parameters were therefore indicated in the coal waste data, as expected for the success of the technique as a diagnostic tool. Here, the compressive strength tests were more consistent since samples were all prepared according to standard ASTM testing size and shape.

Figure 5.17 Velocity versus density for sample #30.



In the present case of the incinerator ash material, however, samples are not of consistent standard size and shape, so the compressive tests are subject to this inconsistency and produce large variations in values, as already shown in the data tables. Also, the samples are all undergoing their initial growth stage long before leveling off to their asymptotic value. So here the correlations are inconclusive and show no apparent trends, but the time series plots are of interest and do contain information about the increase in the nondestructively measured parameters of density, velocity, and elastic modulus, and they allow the prediction of the long term asymptotic values of these parameters from a knowledge of the initial curing period values. In addition, knowledge of the elastic modulus growth curve indicates the increase of bulk material strength as hydration and cementation occurs in the water-filled pores. The plot of compressive strength over time for the groups in Fig. 5.13 does show this behavior qualitatively.

In conclusion, the results of this study, though not conclusive in showing correlations between destructive and nondestructive parameters, give much information about the internal processes and macroscopic properties of a complicated inhomogeneous cementitious material during its curing stage and provide a measure of predictive capabilities for its future properties. The potential for the quantitative NDE method is therefore indicated and more research along this line needs to be done to develop the method to a more advanced stage. In particular, the relationship between compressive strength and the NDE parameters can be better studied by performing the tests on carefully prepared standard shapes of the material and over a larger sample population to get the needed consistency in the compressive tests.

In addition, it has been shown that ultrasonic spectroscopy techniques provide an even more accurate and complete analysis of material properties, in particular, of highly dispersive and lossy materials. Such methods, described elsewhere (Muratore and Carleton, 1985; Muratore, 1987), can be of great value in characterizing the microstructure and evaluating the parameters of materials such as the incinerator ash mixes (Muratore and Carleton, 1985; Muratore, 1987). Therefore, from the standpoint of quantitative NDE, it would be useful to apply this technique here, and, for

this purpose, such work has been initiated and awaits further development for future publication.

## Section 6

## MINERALOGY: COMPOSITION AND ALTERATIONS

X-ray diffraction (XRD) analysis was used to identify mineral phases in incineration ashes and stabilized incineration ash products. Optimum strength blocks and seawater submerged blocks were examined using XRD to determine alterations in mineralogy after block fabrication and subsequent seawater exposure.

## 6.1 APPARATUS AND PROCEDURES

## 6.1.1 X-ray Diffraction Analysis

Mineralogical composition of the specimen was determined by x-ray diffraction analysis of unoriented mounts of powdered samples. The powdered samples were prepared by grinding a freeze-dried sample and passing it through a No. 200 sieve (mesh size 75  $\mu\text{m}$ ). A portion of the sample was spread in a thin layer on a glass slide and analyzed on a Picker (New Hyde Park, New York) x-ray diffractometer using Cu-K $\alpha$  radiation at 35 Kv and 23 mA and a 70° to 5° 2 $\theta$  scan.

The diffractograms were examined for the presence of minerals using the alphabetical index for inorganic materials compiled by the Joint Committee on Powder Diffraction Standards, (JCPDS, 1979) for peak identification. Classification of major or minor mineral phases was based upon the number of diffraction peaks identified and peak intensities. This classification scheme is qualitative since the intensity of x-ray diffraction by a given mineral phase is a function of the degree of mineral crystallinity as well as crystal size. For example, an authigenetically precipitated phase, such as ettringite, may yield a weak diffraction pattern even though present in large quantity since it may be poorly crystallized in incineration residues.

## 6.2 RESULTS

### 6.2.1 Incineration Residues

Mineralogies of the five Westchester ash samples are similar (Table 6.1) Calcite, quartz, anhydrite, and NaCl are generally present as the major mineral phases in the ash samples. Gypsum is present in both the bottom ash and composite ash fractions of the Westchester ash. Portlandite and ettringite were identified as minor constituents in Westchester composite ash. Illmenite is tentatively identified as a minor component in Westchester composite ash.

### 6.2.2 Barrasso Fabricated Blocks

Mineralogical data for blocks fabricated at Barrasso Bros., Islip Terrace, N.Y. in September 1986 using ash collected during that month, is summarized in Table 6.2. Calcite, quartz and ettringite are the major mineral phases present in the 1 week cured block and the 100 day cured block. Minor amounts of sodium chloride, anhydrite and gypsum are present after one week of curing but do not appear in the 100 day cured block. White crystals observed on the surface of the blocks during yard curing consist mainly of sodium chloride, calcite, and quartz.

### 6.2.3 Effects of Seawater Submersion on Barrasso Blocks

Calcite, quartz and ettringite are also major mineral phases in seawater submerged blocks. Blocks submerged for 60 days in seawater also contain brucite (Table 6.2). White crystals were found growing on the seawater submerged blocks. XRD analysis of these crystals show brucite was present as a major component, while aragonite and sodium chloride are present in minor components.

### 6.2.4 Alpena Fabricated Blocks

Calcite, quartz, ettringite and portlandite are major mineral components in all Alpena block mix designs (Table 6.3). No observable differences were found in the diffraction patterns of mix designs using Portland type I cement and Portland type II cement.



Table 6.1. Mineral composition of Westchester incineration ash samples.

8/85 Composite Ash			1/86 Composite Ash			9/86 Composite Ash			11/86 Bottom Ash			11/86 Composite Ash			Mineral
2θ	d	class*	2θ	d	class*	2θ	d	class*	2θ	d	class*	2θ	d	class*	
29.5	3.03		29.5	3.03		29.5	3.03		29.5	3.03		29.5	3.03		Calcite [CaCO <sub>3</sub> ]
39.5	2.28	M	39.4	2.29	M	39.4	2.29	M	39.4	2.29	M	39.4	2.29	M	
43.1	2.10		43.1	2.10		43.1	2.10		43.1	2.10		43.1	2.10		
23.1	3.86		47.6	1.91											
25.6	3.48		25.6	3.48		25.5	3.49		25.5	3.49		25.5	3.49		Anhydrite [CaSO <sub>4</sub> ]
31.5	2.84	M	31.5	2.84	m	31.4	2.85	M	31.4	2.85	M	31.4	2.85	m	
38.8	2.32		43.5	2.08		38.6	2.33		40.9	2.21		40.9	2.21		
41.0	2.20		48.8	1.87		40.8	2.21								
26.8	3.31		26.8	3.33		26.7	3.34		26.7	3.34		26.7	3.34		Quartz [SiO <sub>2</sub> ]
20.9	4.25	M	20.9	4.25	m	20.9	4.26	M	20.9	4.26	M	20.9	4.26	M	
50.2	1.82		50.4	1.81		50.2	1.82								Halite [NaCl]
			31.9	2.81		31.7	2.82		31.7	2.82		31.7	2.82		
			45.7	1.99	M	45.6	1.99	M	45.6	1.99	M	45.6	1.99	m	
			56.4	1.63		56.5	1.63		56.5	1.63		56.5	1.63		
						31.3	2.86					31.3	2.86		Gypsum [CaSO <sub>4</sub> •2H <sub>2</sub> O]
						20.8	4.27	m				20.8	4.27	m	
						33.5	2.68					33.5	2.68		
34.2	2.62														Portlandite [Ca(OH) <sub>2</sub> ]
18.2	4.87	m													
47.2	1.93														
50.9	1.79														
9.2	9.61														Ettringite [Ca <sub>6</sub> A <sub>1</sub> <sub>2</sub> (SO <sub>4</sub> ) <sub>3</sub> (OH) <sub>12</sub> •25H <sub>2</sub> O]
15.8	5.61	m													
22.9	3.88														
32.3	2.77														
						32.7	2.74								Ilmenite [FeTiO <sub>3</sub> ]
						53.3	1.72	m							
						35.3	2.54								

\* Class = Mineral classification based on peak height, M = major, m = minor

Table 6.2. Mineral composition of seawater submerged and air cured hollow masonry units fabricated by Barrasso & Sons, Inc.

Block (after 1 week curing)			White Crystals (after 2 weeks curing)			Block (after 100 days curing)			Submerged Block (after 60 days submersion)			White Crystals (after 60 days submersion)			Identity
2θ	d	class*	2θ	d	class*	2θ	d	class*	2θ	d	class*	2θ	d	class*	
29.5	3.03		29.5	3.03		29.5	3.03		29.5	3.03					Calcite [CaCO <sub>3</sub> ]
39.5	2.28	M	39.4	2.29	M	39.5	2.28	M	39.5	2.28	M				
43.1	2.10		43.1	2.10		43.1	2.10		43.1	2.10					
26.8	3.31		26.8	3.31		26.8	3.31		26.8	3.31					Quartz [SiO <sub>2</sub> ]
20.9	4.25	M	20.9	4.25	M	20.9	4.25	M	20.9	4.25	M				
50.2	1.82					50.2	1.82		50.2	1.82					
9.2	9.61					9.2	9.61		9.2	9.61					Ettringite [Ca <sub>6</sub> A1 <sub>2</sub> (SO <sub>4</sub> ) <sub>3</sub> (OH) <sub>12</sub> •25H <sub>2</sub> O]
15.8	5.61	M				15.8	5.61	M	15.8	5.61	M				
22.9	3.88					22.9	3.88		22.9	3.88					
31.9	2.81	m	31.7	2.82								31.7	2.82		Halite [NaCl]
			45.6	1.99	M							45.6	1.99	M	
			56.5	1.63								56.5	1.63		
									38.1	2.37		38.1	2.37		Brucite [Mg(OH) <sub>2</sub> ]
									18.6	4.77	m	18.6	4.77	M	
									50.9	1.79		50.9	1.79		
												26.2	3.40		Aragonite [CaCO <sub>3</sub> ]
												45.8	1.98	m	
												27.3	3.27		
25.6	3.48														Anhydrite [CaSO <sub>4</sub> ]
31.5	2.84	m													
31.1	2.87														Gypsum [CaSO <sub>4</sub> •2H <sub>2</sub> O]
20.8	4.28	m													
33.4	2.68														
									11.2	7.90	m	11.0	8.04	m	(Unidentified)

\* Class = Mineral classification based on peak height, M = major, m = minor

Table 6.3. Mineral composition of Alpena fabricated hollow masonry blocks.

2θ	Reef Block		25% Sand & Type II Cement			50% Sand & Type I Cement			50% Sand & Type II Cement			Mineral
	d	class*	2θ	d	class*	2θ	d	class*	2θ	d	class*	
29.4	3.04		29.4	3.04		29.4	3.04		29.4	3.04		Calcite [CaCO <sub>3</sub> ]
39.3	2.29	M	39.3	2.29	M	39.3	2.29	M	39.4	2.29	M	
43.1	2.10		43.1	2.10		43.1	2.10		43.1	2.10		
26.7	3.34		26.7	3.34		26.7	3.34		26.7	3.34		Quartz [SiO <sub>2</sub> ]
20.9	4.26	M	20.9	4.26	M	20.9	4.26	M	20.9	4.26	M	
50.2	1.82		50.2	1.82		50.2	1.82		50.2	1.82		
9.1	9.73		9.1	9.73		9.1	9.73		9.1	9.73		Ettringite [Ca <sub>6</sub> A1 <sub>2</sub> (SO <sub>4</sub> ) <sub>3</sub> (OH) <sub>12</sub> •25H <sub>2</sub> O]
15.8	5.61	M	15.8	5.61	M	15.8	5.61	M	15.8	5.61	M	
22.9	3.88		22.9	3.88		22.9	3.88		22.9	3.88		
32.3	2.77		32.3	2.77		32.3	2.77		32.3	2.77		
34.1	2.63		34.1	2.63		34.1	2.63		34.1	2.63		Portlandite [Ca(OH) <sub>2</sub> ]
18.1	4.85	M	18.1	4.85	M	18.1	4.85	M	18.1	4.85	M	
47.4	1.92		47.4	1.92		47.4	1.92		47.4	1.92		

\* Class = Mineral classification based on peak height, M = major, m = minor

### 6.3 DISCUSSION

Mechanisms responsible for the development of strength in stabilized incineration ash blocks have their origin in the mineralogy of the reactant end members. The property that makes incineration ash a viable material in the stabilization process is its pozzolanic nature. A pozzolan is a siliceous material or alumino-siliceous material which is not cementitious in itself, but which, in finely divided form and in the presence of moisture, reacts with alkali and alkaline-earth constituents producing cementitious products (ASTM, 1975). Pozzolanic reactions between the incineration waste and the stabilization additive can be greatly influenced by the mineralogy of each of the residues. The reactivity, defined as the bonding capability of ash, is a function of several factors (Barber, 1970; Thorn and Walt, 1965; Vincent *et al.*, 1961) including:

- a. the total amount of quartz and alumina associated with the ash,
- b. the amount of free lime present in the ash,
- c. the presence of carbon in the ash,
- d. the fineness of the ash, and
- e. the particle morphology of the ash.

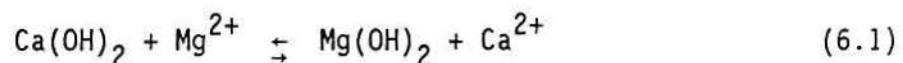
For items a, b, and d, the greater the quantity, value or degree of, the greater the pozzolanic reactivity. For item c, excess carbon will inhibit the pozzolanic reactivity of the ash (Vincent *et al.*, 1961).

Knowledge of alterations in the mineralogy of the reactants subsequent to stabilization provides information on the structure of bonding components. Crystal development increased following fabrication leading to a strong block. X-ray diffraction patterns clearly identify quartz and a variety of calcium compounds in each of the residues. These compounds are necessary for the development of structurally important reaction products such as ettringite and calcium silicates.

Westchester incineration ash samples differed markedly in their pozzolanic properties as was observed in the resultant block compressive strengths

(Section 5). The mineralogy of the block samples provides an insight into the possible causes of the observed variability in compressive strengths. The role and significance of each mineral found in the fabricated blocks is summarized as follows:

1. Quartz. This mineral reacts with the available calcium to produce the bonding crystals involved in the cementation process. The increased pozzolanic reactivity of the ash favors the formation of minerals such as calcium silicates and calcium aluminosilicates which enhance the structural integrity of the blocks.
2. Calcite, Portlandite, Anhydrite and Gypsum. All of these minerals present in the mix components supply calcium for the precipitation of cementitious products in the blocks. Sulphate present in anhydrite and gypsum is also incorporated into cementitious minerals (ettringite). However, excess sulfate attacks the concrete by reacting with tricalcium aluminate  $3\text{CaO}\cdot\text{Al}_2\text{O}_3$  in Portland cement resulting in the formation of undesirable expansion products (Criswell and Vanderbilt, 1983). Furthermore, the increase in molar volume that results from the hydration of anhydrite to form gypsum can cause the loss of structural integrity of the block if there is insufficient pore space available in the block to accommodate the formation of these crystals (Roethel *et al.*, 1983)
3. Halite. The presence of halite in the ash provides an indication of the amount of chloride present. Chlorides retard both setting speed and strength development in concrete. Blocks fabricated with high chloride incineration ash may possess low compressive strengths.
4. Ettringite. This mineral is one of the important cementing agents which helps to knit together the ash particles into a solid block.
5. Aragonite and Brucite. These minerals were present as crystals growing on seawater submerged blocks. The precipitation of brucite occurs due to highly alkaline conditions in the pore spaces of the block which results from the dissolution of calcium compounds in the block. Brucite can form under high pH conditions (Garrels and Chis, 1965) with its precipitation represented by the following reaction:



Aragonite, an alternate form of calcium carbonate, precipitates with brucite in the white crystalline stalagmites present on the block.

#### 6.3.1 Barrasso Blocks

The effects of the various minerals on block strength and their presence or absence in different ash samples and blocks helps explain the variability of properties between the blocks fabricated. Barrasso blocks fabricated from the September 1986 Westchester composite ash had initially low compressive strengths (Section 5.3.2). Both ash samples contained major amounts of anhydrite and halite which may account for the very slow gain in compressive strength for these blocks.

Halite was present as a minor component in the blocks fabricated at the Barrasso facility from the Westchester ash sampled in September 1986. White crystals growing on the curing blocks were found to contain halite as a major mineral phase. X-ray diffractograms of submerged Barrasso blocks and the white precipitate found on the blocks consistently showed a peak at 11.2 which is as yet unidentified. The progressive reduction of anhydrite and gypsum in the ash when compared to cured blocks, from 1 week curing to 100 days curing, was observed. Anhydrite and gypsum may have reacted with cement components in the blocks to form ettringite, thus increasing cementation between particles within the block resulting in strength gains (Table 6.2).

The precipitation of brucite and aragonite during seawater submersion of Barrasso blocks does not appear to alter the strength of these blocks after 60 days (Section 5.3.7b).

#### 6.3.2 Alpena Blocks

No significant differences in the mineralogy of the four Alpena blocks were observed. These blocks were fabricated using Westchester composite ash sampled in November 1986. It can be noted that the minor mineral phases of the Westchester ash, anhydrite, gypsum and halite are absent from the block diffraction patterns indicating that anhydrite and gypsum are converted to ettringite while portlandite is formed as a by-product of cementitious reactions.

## Section 7

### LEACHING PROPERTIES OF STABILIZED INCINERATION ASH BLOCKS

#### 7.1 BLOCK DIGESTIONS FOR ELEMENTAL ANALYSIS

##### 7.1.1 Sample Preparation

Analysis of hydrofluoric-boric acid ( $\text{HF-H}_3\text{BO}_3$ ) digests by atomic absorption spectroscopy was used to determine the elemental composition of stabilized incineration ash (SIA) blocks (Section 3.1.1). Block materials including SIA blocks and a cement block, were ground using mortar and pestle to achieve a size of less than 9.5 mm (Table 7.1). Samples were prepared using the same procedure explained in Section 3.1.1.

##### 7.1.2 Digest Analysis by Atomic Absorption Spectroscopy

Replicate samples ( $n=3$ ) of each SIA block and cement block were analyzed for calcium, magnesium, aluminum, iron, copper, lead, zinc, cadmium, nickel, manganese, chromium, cobalt, arsenic and mercury by atomic absorption spectrophotometry.

Analysis of Ca, Mg, Fe, Cu, Zn, Mn, Ni and Al were performed with flame Atomic Absorption Spectrophotometer [AAS] (Section 3.1.2). Concentration of Pb, Cd, Cr, Co and As was determined using flameless AAS (Section 3.1.2). Mercury was determined using the MHS-10 hydride generator attached to the Perkin Elmer Model 5000 AAS (Section 3.1.2).

##### 7.1.3 Results and Discussion

Major elements (defined at Section 3.1.3) in all three SIA blocks include Ca, Mg, Al, Fe, Pb and Zn (Table 7.1). Copper was a major element in Westchester optimum block (WOB) and Huntington optimum block (HOB) and a minor element in New York City optimum block (COB). Manganese was a major element in COB and a minor element in WOB and HOB. Chromium was a minor element in the trace blocks whereas Ni, Co, As and Hg were trace elements. Cadmium was a minor element in COB and a trace element in WOB and HOB.



Table 7.1 Metal concentrations in stabilized incineration ash blocks.

	Ca (%)	Mg (%)	Al (%)	Fe (%)	Cu (%)	Pb (%)	Zn (%)	Cd ( $\mu\text{g/g}$ )	Mn (%)	Ni ( $\mu\text{g/g}$ )	Cr ( $\mu\text{g/g}$ )	Co ( $\mu\text{g/g}$ )	As ( $\mu\text{g/g}$ )	Hg ( $\mu\text{g/g}$ )
CB <sup>a</sup>	6.6	1.9	5.4	4.5	0.0013	0.0004	0.0053	0.26	0.092	47	31	25	33	BDL <sup>d</sup>
SD <sup>b</sup>	0.8	0.3	0.2	0.9	0.00001	0.0002	0.0003	0.10	0.015	3	7	5	5	
WOB <sup>c</sup>	14	1.4	5.8	4.9	0.47	0.51	0.45	44	0.083	110	150	20	4.8	11
	0.5	0.1	0.6	0.4	0.26	0.21	0.03	5	0.001	10	4	2	0.8	6
HOB	13	0.96	4.0	7.3	0.14	0.10	0.23	13	0.081	55	140	12	16	BDL
	0.3	0.10	0.2	0.2	0.04	0.03	0.06	2	0.008	6	10	1	2	
COB	13	1.3	7.0	1.6	0.061	0.73	1.86	730	0.11	78	190	20	73	1.3
	0.4	0.0	0.1	0.1	0.001	0.03	0.01	30	0.0003	13	3	1	2	0.9

<sup>a</sup> Particle size used: < 9.5 mm for CB, WOB, HOB and COB.

<sup>b</sup> Values denote the standard deviation of replicate samples (n=3).

<sup>c</sup> Optimum mix designs are shown in Table 7.7.

<sup>d</sup> BDL means below detection limit; 1 ( $\mu\text{g L}^{-1}$ ) for Hg.



Metal concentrations in Table 7.1 indicate that stabilized blocks contained lower metal concentrations than the corresponding ashes (Table 3.2). Two factors may account for this observation:

1) Ash particles >4.75 mm were used when fabricating the optimum mix blocks while only particle sizes <4.75 mm were digested for elemental analysis of ashes. Metals are enriched in smaller particle sizes (Table 3.2). The abundance of small particle sizes in ash samples resulted in higher metal concentrations in the ash digest solutions.

2) The addition of Portland cement (15%) when stabilizing incineration ashes diluted the ash content of the blocks resulting in lower metal concentrations. Calcium was the only exception; higher concentrations of calcium in the blocks is due to the addition of Portland cement. Major compounds found in the Portland cement are dicalcium silicate ( $2\text{CaO}\cdot\text{SiO}_2$ ), tricalcium silicate ( $3\text{CaO}\cdot\text{SiO}_2$ ) and tricalcium aluminate ( $3\text{CaO}\cdot\text{Al}_2\text{O}_3$ ) [Roethel et al., 1986].

## 7.2 EP, TCLP AND MODIFIED ASTM (SEAWATER SHAKING) LEACHING TESTS

### 7.2.1 Sample Preparation

The EPA Toxicant Extraction Procedure (EP), EPA Toxicant Characteristic Leaching Procedure (TCLP) and Seawater Shaking Extraction Procedure were performed on stabilized incineration ash (SIA) blocks to evaluate their leaching behavior in seawater and in acid solutions.

Leaching procedures used for particulate incineration residues were used for stabilized blocks and a cement block (Section 3.2.1). Particle sizes used for leaching tests are listed in Table 7.2. Block materials, stabilized blocks and cement block, were ground to a particle size less than 9.5 mm for ASTM test and 1.0 mm for EP, TCLP and Seawater Shaking leaching tests. Measured pH values are also shown in Table 7.2.

### 7.2.2 Leachate Analysis

Calcium and magnesium in the leachates obtained using the EP, TCLP and Seawater Shaking leaching tests were analyzed using flame Atomic Absorption Spectrophotometry [AAS] (Section 3.1.2). Zinc and copper in EP and TCLP

Table 7.2 Measured pH values for stabilized incineration ash blocks in EP, TCLP and Seawater Shaking leaching tests and amount of acetic acid added in EP test.

Block <sup>a</sup>	Particle Size	EP		TCLP	Seawater
		pH	Acid <sup>b</sup>	pH	pH
Westchester Block (WOB)	< 1.0 mm	9.69	160	8.92	11.2
Huntington Block (HOB)	< 1.0 mm	10.1	160	9.05	11.2
New York City Block (COB)	< 1.0 mm	9.56	160	8.61	11.6
Cement Block (CB)	< 1.0 mm	5.20	110	6.09	10.6

<sup>a</sup> Optimum mix designs are listed in Table 7.7.

<sup>b</sup> Total amount of acetic acid (0.5 N, ACS Reagent grade) added in 40 grams of samples (mls).

leachates were also determined with an air-acetylene flame on the Perkin Elmer Model 5000 AAS without background correction. Copper in EP and TCLP leachates of CB and COB were analyzed using the AAS equipped with a HGA-500 graphite atomizer and AS-40 Autosampler with background correction. Manganese in EP and TCLP leachates of CB were also analyzed using flame AAS without background correction. Analysis of Al, Fe, Pb, Cd, Ni, Cr, Co, and As in EP and TCLP leachates were performed using flameless AAS. All standards for the analysis of EP and TCLP leachates were dilutions of Fisher Certified atomic absorption standards that were made up in the same matrix present in the samples to be analyzed. For Cd analysis, samples and standards were prepared in 1%  $(\text{NH}_4)_2\text{HPO}_4$  (w/v) and for As analysis, 0.1% Ni (w/v) as  $\text{Ni}(\text{NO}_3)_2$  (1:1) was used to allow the use of higher charring temperatures (Ediger, 1975).

For analysis of Seawater Shaking leachates, Fe, Cu, Pb, Cd, Mn, Ni, Cr, and Co were determined using flameless AAS using a  $\text{NH}_4\text{NO}_3$  (Section 3.2.2). Serial dilutions of Fisher Certified atomic absorption standards were prepared with reagent concentrations equivalent to those in the samples to be analyzed. Copper and Cr standards were made up in the (1+100) diluted seawater with 0.2% Ultrex<sup>®</sup>  $\text{HNO}_3$  while (1+10) diluted seawater was used to prepare standard solutions for analysis of Fe, Pb, Cd, Mn, Ni, and Co. Cadmium samples and standards were diluted with 1% (w/v)  $(\text{NH}_4)_2\text{HPO}_4$  solution to allow for the use of higher charring temperatures.

Analyses of Hg in EP, TCLP and Seawater Shaking leachates were performed with the use of the MHS-10 hydride generator attached to the Perkin-Elmer Model 5000 AAS (Section 3.1.2). Arsenic in Seawater Shaking leachate was determined using the MHS-10 hydride generator attached to the Perkin-Elmer Model 5000 AAS with an air-acetylene flame.

### 7.2.3 Results and Discussion

Metal concentrations in EP, TCLP, and Seawater Shaking leachates from SIA blocks are shown in Tables 7.3 through 7.5. Leaching behavior of ions in solution may be accounted for by the pH values of the extraction fluid; low pH value (acidic condition) favors the leaching of heavy metals.

Table 7.3 Metal concentrations in EP leachate of stabilized incineration ash blocks.

	Ca (g/L)	Mg (mg/L)	Al (mg/L)	Fe ( $\mu\text{g/L}$ )	Cu (mg/L)	Pb ( $\mu\text{g/L}$ )	Zn (mg/L)	Cd ( $\mu\text{g/L}$ )	Mn ( $\mu\text{g/L}$ )	Ni ( $\mu\text{g/L}$ )	Cr ( $\mu\text{g/L}$ )	Co ( $\mu\text{g/L}$ )	As ( $\mu\text{g/L}$ )	Hg ( $\mu\text{g/L}$ )
CB <sup>a</sup>	1.3	31	0.60	110	0.061	6.5	6.2	29	320	15	58	6.7	BDL	BDL
SD <sup>b</sup>	0.05	1	0.14	20	0.006	0.7	0.2	3	10	1	3	0.2		
WOB <sup>c</sup>	2.2	69	0.47	3.6	0.14	BDL <sup>d</sup>	0.047	BDL	1.5	3.0	170	BDL	BDL	BDL
	0.03	2	0.05	0.6	0.01		0.004		0.1	0.2	4			
HOB	2.2	32	0.22	19	0.92	BDL	0.044	BDL	1.4	12	110	1.2	5.0	BDL
	0.06	2	0.002	2	0.01		0.003		0.2	1	3	0.1	1.0	
COB	1.9	46	0.63	2.1	BDL	3.1	0.054	110	3.6	1.5	160	BDL	2.5	BDL
	0.04	9	0.06	0.2		1.6	0.007	30	0.5	0.2	7		0.2	

<sup>a</sup> Particle size ranges and pH values are listed in Table 7.2.

<sup>b</sup> Values denote the standard deviation of replicate samples (n=3).

<sup>c</sup> Optimum mix designs are listed in Table 7.7.

<sup>d</sup> BDL means below detection limit.

: 0.05 ( $\mu\text{g L}^{-1}$ ) for Cd and As,

0.5 ( $\mu\text{g L}^{-1}$ ) for Cu, Pb and Co, and

2 ( $\mu\text{g L}^{-1}$ ) for Hg.

Table 7.4 Metal concentrations in TCLP leachate of stabilized incineration ash blocks.

	Ca (g/L)	Mg (mg/L)	Al (mg/L)	Fe (ug/L)	Cu (mg/L)	Pb (ug/L)	Zn (mg/L)	Cd (ug/L)	Mn (ug/L)	Ni (ug/L)	Cr (ug/L)	Co (ug/L)	As (ug/L)	Hg (ug/L)
CB <sup>a</sup>	2.1	43	0.48	330	0.069	BDL <sup>d</sup>	0.84	54	900	40	4.9	17	BDL	BDL
SD <sup>b</sup>	0.03	1	0.06	20	0.006		0.04	7	30	3	0.3	2		
WOB <sup>c</sup>	2.2	110	1.3	3	0.13	BDL	0.038	2	28	8.8	170	BDL	BDL	BDL
	0.01	1	0.1	1	0.01		0.002	1	1	0.3	5			
HOB	2.0	76	0.46	38	0.85	BDL	0.029	BDL	37	22	98	1.2	4.9	BDL
	0.05	4	0.04	16	0.02		0.002		2	1	4	0.1	0.4	
COB	1.8	99	1.4	BDL	BDL	22	0.24	350	63	3.2	160	BDL	1.8	BDL
	0.01	6	0.1			2	0.05	10	2	0.3	4		0.4	

<sup>a</sup> Particle size ranges and pH values are listed in Table 7.2.

<sup>b</sup> Values denote the standard deviation of replicate samples (n=3).

<sup>c</sup> Optimum mix designs are listed in Table 7.7.

<sup>d</sup> BDL means below detection limit.

0.05 ( $\mu\text{g L}^{-1}$ ) for Cd and As,

0.5 ( $\mu\text{g L}^{-1}$ ) for Fe, Cu, Pb and Co, and

2 ( $\mu\text{g L}^{-1}$ ) for Hg.

Table 7.5 Metal concentrations in Seawater Shaking leachate of stabilized incineration ash blocks.

	CB (g/L)	Mg (g/L)	Fe ( $\mu\text{g/L}$ )	Cu (mg/L)	Pb ( $\mu\text{g/L}$ )	Cd ( $\mu\text{g/L}$ )	Mn ( $\mu\text{g/L}$ )	Ni ( $\mu\text{g/L}$ )	Cr ( $\mu\text{g/L}$ )	Co ( $\mu\text{g/L}$ )	As ( $\mu\text{g/L}$ )	Hg ( $\mu\text{g/L}$ )
CB <sup>a</sup>	1.6	-1.0 <sup>d</sup>	BDL <sup>e</sup>	0.003	BDL	BDL	BDL	BDL	370	BDL	BDL	BDL
SD <sup>b</sup>	0.06	0.01		0.001					10			
WOB <sup>c</sup>	1.4	-1.0	BDL	0.21	BDL	BDL	BDL	BDL	330	BDL	BDL	BDL
	0.03	0.0004		0.002					6			
HOB	1.4	-1.0	2.8	2.7	BDL	BDL	BDL	54	390	BDL	2.2	BDL
	0.02	0.0002	2.3	0.04				3	10		0.6	
COB	0.78	-1.0	BDL	0.005	9.5	4.9	27	8.2	580	BDL	6.3	BDL
	0.03	0.001		0.001	2.1	0.1	8	1.9	30		0.4	

<sup>a</sup> Particle size ranges and pH values are listed in Table 7.2.

<sup>b</sup> Values denote the standard deviation of replicate samples (n=3).

<sup>c</sup> Optimum mix designs are listed in Table 7.7.

<sup>d</sup> Negative sign means the Mg concentration in the leachate was lower than that of seawater (0.45  $\mu\text{m}$ ) blank.

<sup>e</sup> BDL means below detection limit.

- : 0.5 ( $\mu\text{g L}^{-1}$ ) for Cd,
- 1 ( $\mu\text{g L}^{-1}$ ) for Fe, Co and As,
- 2 ( $\mu\text{g L}^{-1}$ ) for Mn, Ni and Hg, and
- 5 ( $\mu\text{g L}^{-1}$ ) for Pb.

### 7.2.3a pH

Metal concentrations in EP, TCLP, and Seawater Shaking leachates from SIA blocks are shown in Tables 7.3 and 7.4. Like particulate incineration ashes, pH's of TCLP solutions were generally lower than those of EP. The higher metal concentrations in TCLP relative to EP leachate is attributable to the lower pH of TCLP leachates. The percent of total metal release from SIA blocks was higher in EP and TCLP leachates, than in ASTM leachate (Section 3.2.3).

Additional maximum amount of acetic acid ( $4 \text{ ml g}^{-1}$ ) could not lower the solution pH to 5.0 ( $\pm 0.2$ ) for SIA block materials. This high buffering capacity for SIA blocks may be due to the dissolution of mineral phases such as calcite ( $\text{CaCO}_3$ ) and anhydrite ( $\text{CaSO}_4$ ) present in the incineration residues, and calcium silicates ( $2\text{CaO}\cdot\text{SiO}_2$ ) and  $3\text{CaO}\cdot\text{SiO}_2$ ) present in Portland cement (Section 3.2.3).

### 7.2.3b Effect of Stabilization of Incineration Residues on Metal Leaching

Elemental analysis (Table 3.2 and 7.1) showed that SIA blocks as well as particulate residues were enriched with metals including Pb, Cu and Zn. SIA blocks however generally showed far lower leachability than incineration residues in the EP, TCLP and Seawater Shaking leachates. The leaching of heavy metals in both the acidic and alkaline solutions was substantially reduced by the chemical fixation of the incineration residues with Portland Type I cement. Chemical fixation may be defined as a process to limit or minimize the movement of contaminants from the disposal site and to improve the physical characteristics of the waste (Landreth and Mahloch, 1977). It has been demonstrated that chemically fixated wastes can effectively retain heavy metals within stabilized blocks (Poon *et al.*, 1985; Shively *et al.*, 1986). The mechanisms causing metal binding in the cement matrix are not well understood, but it is believed to be due to a combination of entrapment of insoluble metal precipitates (metal hydroxides or silicates) in pore spaces within the cementitious materials, and to binding onto the cemented lattice by the surface related mechanisms such as ion exchange and adsorption (Brown and Bishop, 1985).

Comparison of the results of SIA blocks with those of particulate incineration residues should be considered in terms of particle size fractions used in the leaching tests. Two different particle size ranges of particulate residues, rather than whole ash samples, used in the leaching tests may not completely represent the whole residues which contain the particle of entire size ranges, whereas SIA blocks used were fabricated with the whole residues. Elemental analysis of particulate residues, however showed that smaller particles contained more metals (Table 3.2) and the results of the four leaching tests indicated that metal leaching from SIA blocks was far lower than that of smaller particle sizes. Despite the above limitation it can be concluded that stabilization of incineration residues considerably reduces metal leachability.

#### 7.2.3c Comparison of Leaching Results with EPA Regulatory Limit for EP Toxicity and Drinking Water

Metal concentrations in the EP, TCLP, and Seawater Shaking leachates from SIA blocks are comparable to U. S. EPA Drinking Water Quality Standards and Hazardous Waste EP Toxic Criteria (Table 7.6). Metal concentrations in the leachates did not exceed the EPA regulatory limit for toxicity. Metal concentrations in all leachates of SIA blocks were lower than the EPA Drinking Water Quality Standards with the exception of Cd in EP and TCLP leachates from COB and Mn in TCLP leachate from COB. This, when compared with unstabilized particulate residues, supports the efficiency of stabilization of incineration residues. Taking into account of the surface area to volume ratio of finely-powdered block materials (<1.0 mm, see Table 3.4), these results provide a worst case scenario, i.e. the maximum amount of metal that can be leached from SIA blocks in seawater and acidic solutions.



Table 7.6 Comparison of EP, TCLP and Seawater Shaking leachate concentrations from stabilized incineration ash blocks with EPA regulatory limits for EP Toxicity and Drinking Water.

		Fe <sup>a</sup>	Cu	Pb	Zn	Cd	Mn	Cr	As	Hg
Drinking Water <sup>b</sup>		0.05	3.0	--	5.0	0.05	0.05	1.0	1.0	0.002
Toxic Criteria <sup>b</sup>		--	--	5.0	--	1.0	--	5.0	5.0	0.2
EP:	WOB	0.004	0.14	<0.001	0.047	<0.001	0.001	0.17	<0.001	<0.002
	HOB	0.019	0.92	<0.001	0.044	<0.001	0.001	0.11	0.005	<0.002
	COB	0.002	<0.001	0.003	0.054	0.11	0.004	0.16	0.002	<0.002
TCLP:	WOB	0.003	0.13	<0.001	0.038	0.002	0.028	0.17	<0.001	<0.002
	HOB	0.038	0.85	<0.001	0.029	<0.001	0.037	0.098	0.005	<0.002
	COB	<0.001	<0.001	0.022	0.24	0.35	0.063	0.16	0.002	<0.002
Seawater:	WOB	<0.001	0.21	<0.005	NA <sup>d</sup>	<0.001	<0.002	0.33	<0.001	<0.002
	HOB	0.003	2.7	<0.005		<0.001	<0.002	0.39	0.002	<0.002
	COB	<0.001	0.005	0.009		0.005	0.027	0.59	0.006	<0.002

<sup>a</sup> Unit of concentration is mg L<sup>-1</sup> and detection limits for each metal are listed in Table 7.3 through 7.5.

<sup>b</sup> Data from Federal Register (May, 1980).

<sup>d</sup> NA means not analyzed.

### 7.3 SEAWATER TANK DISSOLUTION STUDY

Calcium release from stabilized incineration ash (SIA) blocks may be an important indicator of a blocks' expected lifetime in the marine environment. Calcium is a major element in SIA blocks and participates in cementitious reactions contributing to overall block strength development. Over long time periods, a high rate of calcium release from the blocks may ultimately lead to structural failure either through increased porosity and/or chemical dissolution.

SIA blocks as well as particulate incineration residues are enriched in copper, lead, and cadmium (Table 3.2 and 7.1). The leaching behavior of potentially toxic metals in seawater from SIA blocks is of environmental interest.

Seawater tank leaching studies were conducted to measure the release rate of major (Ca and Mg) and minor elements (Cu, Pb and Cd) from SIA blocks suspended in seawater.

#### 7.3.1 Materials and Methods

##### 7.3.1a Experimental Design

Cylindrical cores, with different geometrical surface areas (200 and 400  $\text{cm}^2$ ), were taken from each of three different optimum SIA blocks (Table 7.7). Each core was suspended with a monofilament line in an acid-washed polyethylene tank containing 1 or 2 liters of filtered (0.45  $\mu\text{m}$ ) seawater, holding a constant ratio of block surface area to seawater volume of 200:1 ( $\text{cm}^2 \text{L}^{-1}$ ). Seawater was collected from the Flax Pond Laboratory (salinity 27 ppt) and filtered through 0.45  $\mu\text{m}$  Millipore<sup>®</sup> filters. The tank seawater was continuously mixed with magnetic stirrers. Lids were placed in the tanks to prevent outside contamination. An opening in the lid was covered with a 0.45  $\mu\text{m}$  Millipore<sup>®</sup> filter paper to allow exchange of gases. A separate tank containing 2 L seawater only was used as a control.

Table 7.7 Formulation and bulk characteristics<sup>a</sup> of stabilized incineration ash blocks.

	WOB <sup>b</sup>	HOB	COB
<b>Formulation</b>			
Ash type	Westchester composite ash (WCA)	Huntington composite ash (HCA)	New York City fly ash (NYCFA)
Ash content (%) <sup>c</sup>	68	67	62
Cement <sup>d</sup> (%)	15	15	15
Moisture (%)	17	18	23
Curing temp. (°C)	49	23 (air)	49
Curing time (day)	1	7	3
<b>Characteristics</b>			
Comp. strength (psi)	1231	455	228
Wet density (g cm <sup>-3</sup> )	1.97	1.77	1.64
Porosity (%)	36.5	39.4	47.7
Permeability coeff. (cm s <sup>-1</sup> )			
Top	2.17 x 10 <sup>-8</sup>	1.05 x 10 <sup>-7</sup>	1.26 x 10 <sup>-7</sup>
Bottom	2.53 x 10 <sup>-8</sup>	3.54 x 10 <sup>-5</sup>	1.06 x 10 <sup>-5</sup>

<sup>a</sup> Data from Roethel *et al.* (1986).

<sup>b</sup> WOB; Westchester optimum block, HOB; Huntington optimum block, and COB; New York City optimum block.

<sup>c</sup> % based on the dry weight.

<sup>d</sup> Portland cement, Type I.

The experiments were conducted at room temperature and extended over 104 days. Duplicate samples (50 ml each) were removed during each sampling period using acid-washed syringes. Samples were filtered through 0.45  $\mu\text{m}$  Millipore<sup>®</sup> filters, acidified to pH <2 with Ultrex<sup>®</sup>  $\text{HNO}_3$ , and stored at 5°C prior to analysis. pH of the tank waters was also measured during each sampling interval. Sampling was conducted at intervals of 1, 2, 4 and 6 days, then weekly for 3 weeks, and bi-weekly for 4 weeks. Subsequent samples were taken at 3-week intervals. After sample removal, the seawater volume was readjusted to 1 or 2 L by adding 100 ml of fresh seawater. Seawater in the tanks was periodically exchanged with fresh seawater (Table 7.8).

#### 7.3.1b Leachate Analysis

Calcium and magnesium in the seawater leachates were analyzed by flame Atomic Absorption Spectrophotometry [AAS] (Section 3.1.2).

Copper, lead and cadmium were analyzed using flameless AAS (Section 3.2.2). Standards were serial dilutions of Fisher Certified atomic absorption standards and were prepared in the same matrix present in the samples to be analyzed; for Cu, Pb and Cd, (1+10) diluted seawater with 0.2% Ultrex<sup>®</sup>  $\text{HNO}_3$ .

#### 7.3.1c Leachable Fraction Analysis

Leachable fractions of calcium and copper were determined for use in a model analysis of the Ca and Cu leaching behavior in the tank leaching study (van der Sloot *et al.*, 1985). The leachable fraction ( $f$ ) is defined as the fraction of the total concentration of the element that can be leached from crushed block material at high dilution. Portions of unreacted SIA blocks were ground using mortar and pestle to achieve a size of less than 0.5 mm. Approximately 2 g of each block type was placed into acid-washed polyethylene bottles along with 400 ml of filtered (0.45  $\mu\text{m}$ ) seawater (salinity 27 ppt). After mechanically shaking for 3 days, samples were filtered through a 0.45  $\mu\text{m}$  Millipore<sup>®</sup> filter paper and acidified to pH <2 with Ultrex<sup>®</sup>  $\text{HNO}_3$ . The leachates were then analyzed for calcium and copper (Section 3.1.2 for Ca and 3.2.2 for Cu).

Table 7.8 Sampling intervals and measured pH values in tank study.

Cumulative Time (day)	pH of Tank Seawater						
	WOB1 <sup>a</sup>	WOB2 <sup>b</sup>	HOB1	HOB2	COB1	COB2	Blank <sup>c</sup>
START							
1	9.11	9.27	8.86	8.99	9.44	10.2	8.14
3	8.97	9.08	8.84	8.58	9.41	10.2	8.15
7*	9.18	9.23	8.84	8.61	9.92	11.2	8.15
13	9.05	9.12	8.73	8.71	9.37	9.8	8.14
20*	9.04	9.06	8.70	8.69	9.33	9.8	8.07
27	8.86	8.82	8.42	8.49	8.82	9.2	8.13
34*	8.64	8.85	8.41	8.48	9.02	NA	8.14
48	8.71	8.76	8.39	8.47	8.72	NA	8.21
62*	8.28	8.71	8.31	8.35	8.62	NA	8.24
83	8.24	8.58	8.28	8.22	8.36	NA	8.21
104	8.24	8.56	8.23	8.21	8.31	NA	8.22
125	8.20	8.54	8.20	8.21	8.25	NA	8.32

<sup>a</sup> Optimum mix designs are listed in Table 7.7.

<sup>b</sup> Experimental conditions are:  
 (block surface area in cm<sup>2</sup>, volume of seawater in liter)  
 - (200, 1) for Block 1 (WOB1, HOB1 and COB1),  
 - (400, 2) for Block 2.

<sup>c</sup> Seawater filtered through 0.45 µm Millipore<sup>®</sup> filter papers.

\* indicates change of tank seawater after sampling.

NA : data not available (COB2 fell apart after 27 d of exposure in seawater).

### 7.3.1d Estimation of Pore Water pH

An estimation of pore water pH of SIA blocks in seawater was determined over time by measuring the pH of a powdered SIA-seawater slurry. Unreacted SIA blocks were ground to a particle size less than 0.5 mm and mechanically shaken in seawater at a 1:4 (w/v) ratio for 48 hours. The pH of the solution was measured using a Digital Ionalyzer<sup>®</sup> Model 701-A pH/mv meter at 10 min, 0.5, 1.5, 3, 7, 24 and 48 hour intervals.

## 7.3.2 Results

### 7.3.2a Determination of Metal Fluxes

Calcium, magnesium and copper fluxes were calculated by dividing the incremental increase of metal (millimoles) by the leaching period (day) and by the geometric surface area ( $\text{cm}^2$ ) of the blocks. The following equation was used for calculating metal fluxes:

$$J = (C_t - C_0) \times V / (A \times t) \quad (7.1)$$

where  $J$  = ion flux ( $\text{moles mm}^{-2} \text{d}^{-1}$ ),

$C_t$  = ion concentration in tank water at time  $t$  ( $\text{moles L}^{-1}$ ),

$C_0$  = ion concentration in a control tank ( $\text{moles L}^{-1}$ ),

$V$  = volume of water in a test tank (1 or 2 L),

$A$  = surface area of blocks ( $2$  or  $4 \times 10^4 \text{ mm}^2$ ), and

$t$  = time since water was last replaced (days).

The calculated fluxes are not instantaneous rates but are averaged over a finite time period.

### 7.3.2b Calcium Release

Results of the calcium dissolution experiment are presented in terms of measured concentration (Table 7.9), calculated flux (Table 7.9) and cumulative calcium release (Figure 7.1). Two different geometrical surface areas were

Figure 7.1 Cumulative release of calcium from stabilized incineration ash blocks in seawater.  
(□) WOB1; (+) WOB2; (◇) HOB1; (△) HOB2; (×) COB1.

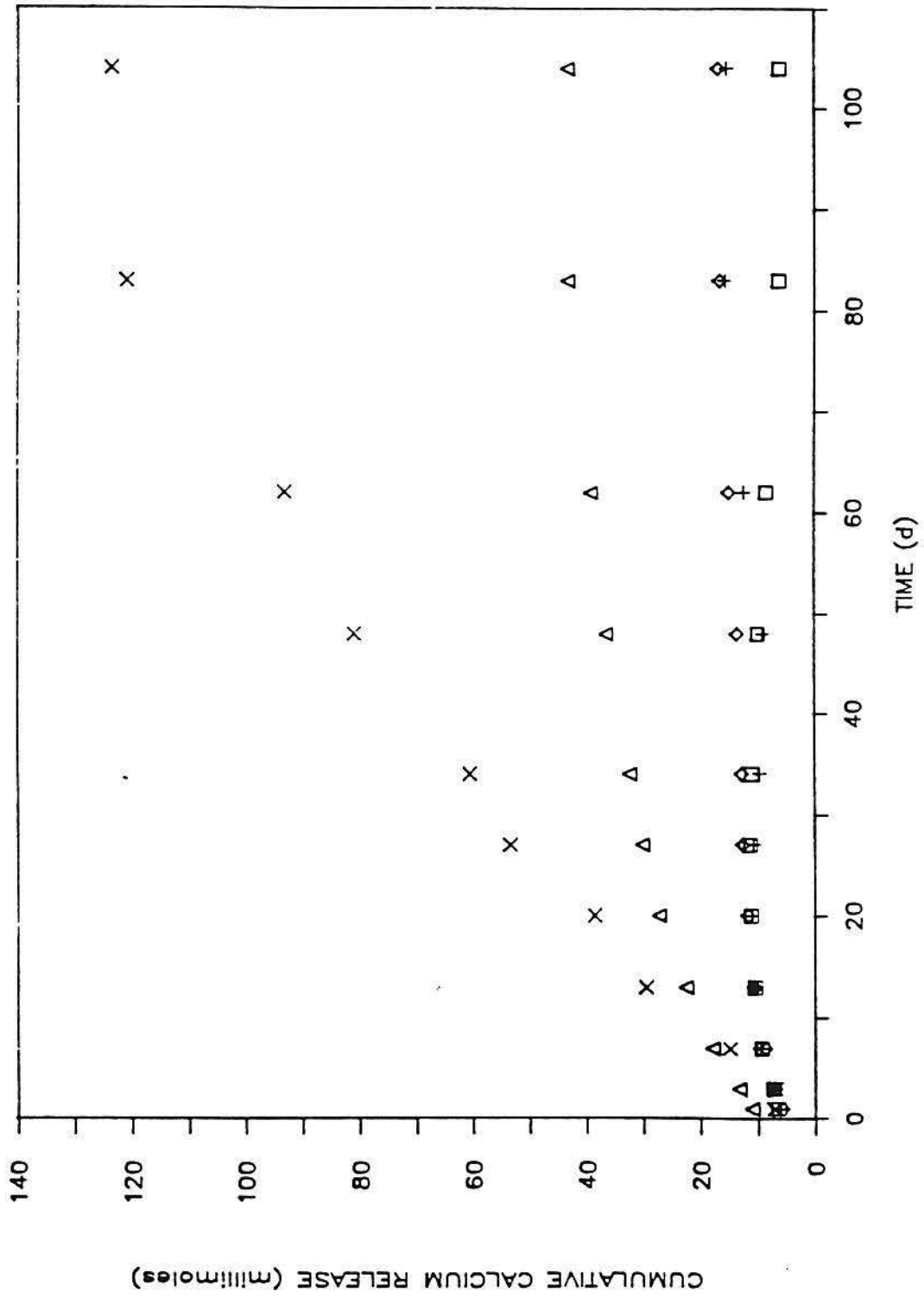




Table 7.9 Measured concentration and calculated flux of calcium in tank study.

Cumulative Time (day)	Concentration (millimoles) <sup>a</sup>					
	<u>WOB1</u> <sup>b</sup>	<u>WOB2</u>	<u>HOB1</u>	<u>HOB2</u>	<u>COB1</u>	<u>COB2</u>
1	6.44	6.05	5.59	11.0	7.20	12.9
3	7.30	7.07	6.92	13.3	6.84	22.1
7 *	9.25	9.56	8.64	17.9	14.9	18.9
13	1.23	0.93	1.93	4.70	14.6	44.8
20 *	1.93	1.47	3.08	9.41	23.7	45.1
27	0.15	-0.31	0.85	2.93	14.9	79.7
34 *	-0.18	-1.35	1.00	5.10	22.1	NA
48	-1.14	-0.61	0.79	4.13	20.3	NA
62 *	-2.70	2.70	2.17	6.78	32.5	NA
83	-2.08	3.29	1.73	4.07	27.8	NA
104	-2.30	3.04	1.92	4.12	30.3	NA
	Flux ( $\times 10^{-8}$ moles $\text{mm}^{-2} \text{d}^{-1}$ ) <sup>c</sup>					
1	29.9	30.0	26.3	54.2	34.6	63.6
3	11.3	11.7	10.8	21.8	10.9	36.4
7 *	6.14	6.78	5.81	12.6	10.2	13.4
13	0.96	0.77	1.51	3.85	11.7	21.3
20 *	0.69	0.56	1.12	3.55	8.74	9.95
27	0.10	-0.22	0.57	2.05	10.2	24.4
34 *	-0.06	-0.48	0.34	1.79	7.57	NA
48	-0.38	-0.22	0.27	1.45	6.96	NA
62 *	-0.45	0.48	0.37	1.19	5.57	NA
83	-0.46	0.78	0.39	0.95	6.34	NA
104	-0.25	0.36	0.22	0.48	3.46	NA

<sup>a</sup> Concentrations provided reflect subtracting the blank and negative sign means the concentration lower than the blank.

<sup>b</sup> Optimum mix designs are listed in Table 7.7 and experimental conditions in Table 7.8.

<sup>c</sup> Flux calculated using equation 7.1 and negative sign means the uptake of calcium from tank seawater.

\* indicates change of tank seawater after sampling.

NA means data not available (COB2 fell apart).

examined to assess the effect of block's surface area exposed to seawater on calcium release.

Calcium leaching from the Huntington and New York City blocks (HOB and COB) was observed to be continuous throughout the sampling period (Figure 7.1). Calcium release for Huntington blocks began to level off after 83 days, releasing 17 millimoles for HOB1 and 43 millimoles for HOB2 in 104 days. Calcium release from New York City block No.1 (COB1) approached an asymptotic value after 84 days, releasing a total of 124 millimoles in 104 days. New York City block No.2 (COB2) released 80 millimoles in 27 days. However, COB2 fell apart after 27 days' exposure to seawater and thereafter sampling of seawater was discontinued.

Removal of calcium from the tank seawater was observed for the Westchester blocks (WOB). During the initial 27 day leaching period, 11 millimoles of calcium were released from each of WOB1 and WOB2. Subsequently, removal of calcium from the tank seawater was observed for both of WOB1 and WOB2, at the same time a white precipitate formed on the surfaces of the blocks. For the remainder of the experiment, the release-uptake of calcium fluctuated in WOB1 and WOB2. As a result, lower cumulative amounts of calcium were released from these blocks; 6 and 15 millimoles for WOB1 and WOB2 after 104 days, respectively.

### 7.3.2c Calcium Flux

Calcium fluxes were calculated using equation 7.1 and are presented in Table 7.9. Generally, calcium fluxes were highest initially and decreased with time. COB1 showed the highest initial calcium flux of  $3.5 \times 10^{-7}$  moles  $\text{mm}^{-2} \text{d}^{-1}$  which decreased to  $3.5 \times 10^{-8}$  moles  $\text{mm}^{-2} \text{d}^{-1}$  after 104 days' exposure. The rate of calcium loss decreased from  $2.6 \times 10^{-7}$  to  $2.2 \times 10^{-9}$  moles  $\text{mm}^{-2} \text{d}^{-1}$  for HOB1 and from  $5.4 \times 10^{-7}$  to  $4.8 \times 10^{-9}$  moles  $\text{mm}^{-2} \text{d}^{-1}$  for HOB2 in 104 days.

Removal of calcium from tank seawater was observed for WOB1 and WOB2. WOB1 had an initial calcium flux of  $3.0 \times 10^{-7}$  moles  $\text{mm}^{-2} \text{d}^{-1}$ . After 104 days, WOB1 had calcium removal flux rate of  $2.5 \times 10^{-9}$  moles  $\text{mm}^{-2} \text{d}^{-1}$ . WOB2 also showed both the calcium release and uptake causing calcium flux to remain low

and variable throughout the experiment, decreasing from  $3.0 \times 10^{-7}$  at 1 day to  $3.6 \times 10^{-9}$  moles  $\text{mm}^{-2} \text{d}^{-1}$  after 104 days' leaching.

#### 7.3.2d Magnesium Uptake

Ion exchange has been thought to be one of the physico-chemical processes affecting the calcium release from the blocks in seawater, magnesium replacing calcium in the blocks (Edwards and Duedall, 1985). Thus, seawater samples removed from the tanks were analyzed for magnesium to determine if the loss of calcium was compensated for by the uptake of magnesium.

Results of magnesium analysis in tank seawater (Table 7.10) indicate that for HOB2 and COB1, where a continuous calcium release was observed, removal of magnesium occurred throughout the tank studies. The cumulative release of calcium and the subsequent cumulative uptake of magnesium from the seawater by SIA blocks is presented in Figure 7.2. Only HOB1, HOB2 and COB1 appear in Figure 7.2 since a continuous calcium release and magnesium uptake were observed for these blocks. During 104 day sampling period, HOB2 and COB1 respectively removed 42 and 109 millimoles of magnesium from the tank seawater while 43 and 124 millimoles of calcium was released to seawater, respectively. HOB1 released both calcium and magnesium, 17 and 5.6 millimoles, respectively, after 104 days.

The mole ratios of calcium release:magnesium uptake in HOB2 and COB1 are found to be very constant throughout the leaching period, with the mole ratios averaging 1.15 ( $\pm 0.09$ ) for HOB2 and 1.05 ( $\pm 0.09$ ) for COB1.

#### 7.3.2e Magnesium Flux

The magnesium uptake flux calculated using equation 7.1 are listed in Table 7.10. Only HOB2 and COB1 showed a persistent magnesium removal flux throughout the sampling period. Like calcium, magnesium fluxes were highest initially and decreased with time. For HOB2, the magnesium removal flux of  $3.6 \times 10^{-7}$  moles  $\text{mm}^{-2} \text{d}^{-1}$  at 1 day decreased to  $6.5 \times 10^{-9}$  moles  $\text{mm}^{-2} \text{d}^{-1}$  at 104 days. The uptake flux by COB1 also decreased from  $4.0 \times 10^{-7}$  moles  $\text{mm}^{-2} \text{d}^{-1}$  at 1 day to  $3.0 \times 10^{-8}$  moles  $\text{mm}^{-2} \text{d}^{-1}$  after 104 days. HOB1 had magnesium release

Table 7.12 Variables used in equation 7.6 and 7.7 for calculating effective diffusion coefficients for calcium.

Block Mix	$J^a$ ( $10^{-4}$ mmoles $\text{cm}^{-2}$ $\text{d}^{-1}$ )	$f^b$	$S_o^c$ (mmoles $\text{cm}^{-3}$ )	Density <sup>d</sup> ( $\text{g cm}^{-3}$ )	$D'^e$ ( $10^{-10}$ $\text{cm}^2$ $\text{s}^{-1}$ )
WOB	0.52	0.31	6.75	1.97	0.02
HOB	3.49	0.32	5.74	1.77	1.36
COB	34.6	0.38	5.26	1.64	113

<sup>a</sup> Calcium flux from experimental results (Table 7.9): average value between Block 1 and Block 2 at  $t = 104$  d was used for WOB and HOB, and flux value of COB1 at  $t = 104$  d for COB.

<sup>b</sup> Leachable fraction = (result from Section 7.3.1c / total Ca conc.) (van der Sloot *et al.*, 1985).

<sup>c</sup> Total Ca concentration in SIA blocks determined by a  $\text{HF-H}_3\text{BO}_3$ -AAS method (Table 7.1).

<sup>d</sup> Wet density from Roethel *et al.* (1986).

<sup>e</sup> Effective diffusion coefficient calculated from equation 7.6 with  $t = 104$  d.

used for calculating  $D'_{Ca}$ . For New York City block (COB), the flux value for COB1 at 104 days was used for calculating  $D'_{Ca}$  (Table 7.9). Total ion concentration in SIA blocks ( $S_o$ ) are given in Table 7.1 and the wet density of blocks are from Roethel *et al.* (1986). The leachable fraction,  $f$ , was calculated from the total amount of ion, TA, from Table 7.1 and the amount of the ion leached (AL) in Section 7.3.1c,  $f = AL/TA$ . Effective diffusion coefficients for calcium ranged from  $0.02 \times 10^{-10} \text{ cm}^2 \text{ s}^{-1}$  for WOB to  $113 \times 10^{-10} \text{ cm}^2 \text{ s}^{-1}$  for COB (Table 7.12).

Using the diffusion coefficients and equation 7.7, the effective distance of diffusion was calculated for calcium over a wide range of time periods to estimate the change of the effective depth of diffusion over time (Table 7.13). The model predicts that during 100 years of exposure in seawater, less than 1 cm of outer surface of WOB and HOB blocks would be affected by the loss of calcium.

### 7.3.3c Copper Diffusion Coefficients

Results of tank dissolution study for copper were also applied to the same diffusion model to evaluate the depletion of copper at the surface of the blocks. Effective diffusion coefficient for copper ( $D'_{Cu}$ ) were calculated (equation 7.6) for each stabilized block. The results are shown in Table 7.14 along with the variables used to calculate  $D'_{Cu}$ . Values were from  $2.38 \times 10^{-10} \text{ cm}^2 \text{ s}^{-1}$  for HOB and  $21.4 \times 10^{-10} \text{ cm}^2 \text{ s}^{-1}$  for WOB.

The effective distance of diffusion for copper (Table 7.15) was calculated for different exposure periods using equation 7.6. Table 7.15 shows that it will take more than a century of exposure in seawater for diffusion to deplete the copper content present at the outer 4 cm of WOB and 2 cm of HOB.

### 7.3.4 Calcium Discussion

Effective diffusion coefficient for calcium ( $D'_{Ca}$ ) for stabilized incineration ash (SIA) blocks may be affected by many factors including the source of leachable calcium, pH, magnesium content of seawater and temperature.

Table 7.13 Effective distance ( $X_c$ ) of the diffusion zone for calcium.

Time (day)	$X_c$ (cm) <sup>a</sup>		
	<u>WOB</u> <sup>b</sup>	<u>HOB</u>	<u>COB</u>
100	0.006	0.048	0.442
200	0.008	0.069	0.625
365 (1 y)	0.011	0.093	0.844
730 (2 y)	0.016	0.131	1.19
1095 (3 y)	0.019	0.160	1.46
1825 (5 y)	0.025	0.207	1.89
3650 (10 y)	0.036	0.293	2.67
10950 (30 y)	0.062	0.507	4.62
18250 (50 y)	0.079	0.655	5.97
36500 (100 y)	0.112	0.926	8.44

<sup>a</sup> Effective distance of the diffusion zone in the blocks, calculated with equation 7.7.

<sup>b</sup> Optimum mix designs are listed in Table 7.7.

Table 7.14 Variables used in equation 7.6 and 7.7 for calculating effective diffusion coefficients for copper.

Block Mix	$J^a$ ( $10^{-8}$ mmoles $\text{cm}^{-2}$ $\text{d}^{-1}$ )	$f^b$ (mmoles $\text{cm}^{-3}$ )	$S_o^c$ (mmoles $\text{cm}^{-3}$ )	Density <sup>d</sup> ( $\text{g cm}^{-3}$ )	$D'^e$ ( $10^{-10}$ $\text{cm}^2 \text{s}^{-1}$ )
WOB	3.16	0.0003	0.14	1.97	21.4
HOB	6.82	0.0068	0.04	1.77	2.38
COB	BDL <sup>f</sup>				

<sup>a</sup> Copper flux from experimental results (Table 7.11): average flux value between Block 1 and Block 2 at  $t = 104$  d was used for WOB and HOB.

<sup>b</sup> Leachable fraction = (result from Section 7.3.1c / total Cu conc.) (van der Sloot *et al.*, 1985).

<sup>c</sup> Total Cu concentration in SIA blocks determined by a HF- $\text{H}_3\text{BO}_3$ -AAS method (Table 7.1).

<sup>d</sup> Wet density from Roethel *et al.*, (1986).

<sup>e</sup> Effective diffusion coefficient calculated from equation 7.6 with  $t = 104$  d.

<sup>f</sup> Cu concentration in COB was below detection limit ( $1 \mu\text{g L}^{-1}$ ).

Table 7.15 Effective distance ( $X_c$ ) of the diffusion zone for copper.

Time (day)	$X_c$ (cm) <sup>a</sup>		
	<u>WOB</u> <sup>b</sup>	<u>HOB</u>	<u>COB</u>
100	0.192	0.064	BDL <sup>c</sup>
200	0.272	0.091	
365 (1 y)	0.367	0.123	
730 (2 y)	0.520	0.173	
1095 (3 y)	0.636	0.212	
1825 (5 y)	0.822	0.274	
3650 (10 y)	1.16	0.387	
10950 (30 y)	2.01	0.671	
18250 (50 y)	2.60	0.866	
36500 (100 y)	3.67	1.23	

<sup>a</sup> Effective distance of the diffusion zone in the blocks, calculated using equation 7.7.

<sup>b</sup> Optimum mix designs are listed in Table 7.7.

<sup>c</sup> Cu concentration in COB was below detection limit ( $1 \mu\text{g L}^{-1}$ ).



### 7.3.4a Source of Leachable Calcium

The higher calcium flux at the earlier stage of experiment and the subsequent exponential drop in rate may be explained in terms of the leachable calcium in the blocks.

According to Stumm and Morgan (1981), the relative solubility of calcium compounds in seawater at 25°C and 1 atm is;  $\text{Ca}(\text{OH})_2 > \text{CaSO}_4 \cdot 2\text{H}_2\text{O} > \text{CaCO}_3$ . X-ray diffraction analysis showed the presence of these calcium compounds in SIA blocks (Roethel *et al.*, 1986). The relatively higher calcium flux in the earlier stage of the tank study, therefore may be attributed to the dissolution of the free lime and gypsum present at the surface of the blocks.

After depleting the free calcium compounds at the block surface, the interior calcium diffuses outward to the surrounding seawater. Due to the small portion (only surface) of blocks being in direct contact with the seawater, tortuosity is an important factor controlling the diffusion of calcium from the inner part of the blocks to the block surfaces. Diffusion of calcium from the inner part of the blocks to seawater is retarded by the increase in the path length of the diffusing ions, with the net result of decreasing flux over time.

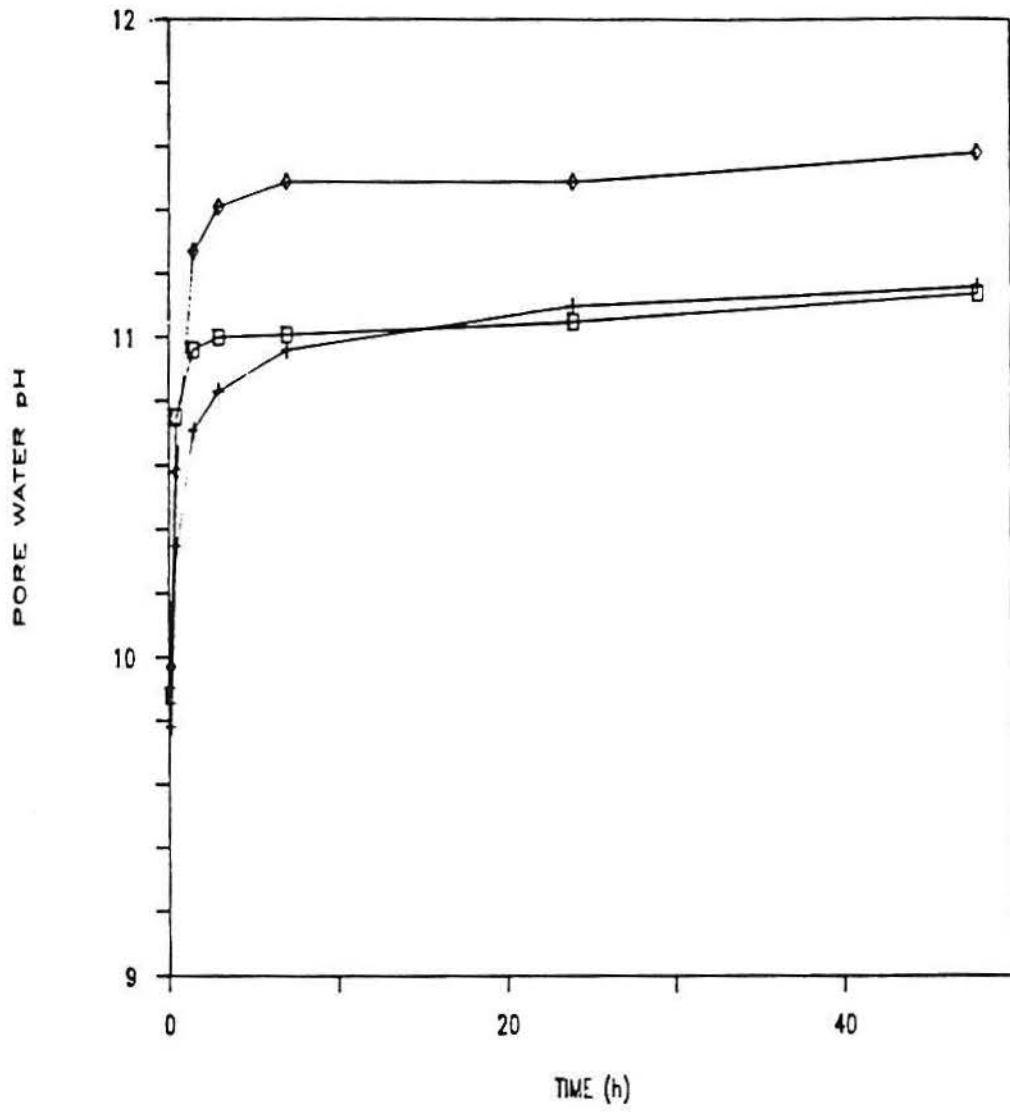
### 7.3.4b pH

Uptake of calcium with the formation of a white precipitate at the block surface was observed for WOB1 and WOB2, resulting in lower  $D'_{\text{Ca}}$ . This observation may be accounted for by pH, pore water pH (Figure 7.4) and tank water pH (Table 7.8). WOB, with a pore water pH of 11.1 after 3 hour shaking and a tank water pH of 9.19 after 1 day (Table 7.1), had a diffusion coefficient of  $0.02 \times 10^{-10} \text{ cm}^2 \text{ s}^{-1}$ . In contrast, with a pore water pH of 10.7 and tank water pH of 8.92, HOB had a  $D'_{\text{Ca}}$  of  $1.36 \times 10^{-10} \text{ cm}^2 \text{ s}^{-1}$  (Table 7.12).

WOB blocks showed the formation of brucite [ $\text{Mg}(\text{OH})_2$ ] and aragonite ( $\text{CaCO}_3$ ) after 30 to 60 days exposure in seawater (Roethel *et al.*, in press). Precipitation of aragonite was also observed for oil ash blocks which had

Figure 7.4 Pore water pH versus time for stabilized incineration ash blocks in seawater.

(□) WOB; (+) HOB; (◇) COB.



relatively high pore water pH's and removed calcium from the seawater (Breslin, 1986). The calcium removed from the seawater precipitated on the surfaces of the suspended blocks, and thus calcium release from WOB blocks may be obstructed by the formation of brucite and aragonite in the pore spaces and on the surfaces of the blocks, resulting in lower  $D'_{Ca}$  of WOB.

For COB, both the largest calcium release and the highest pore water and tank water pH's were observed. This contradictory observations may be attributable to the block's surface area to volume ratio. COB lost its structural integrity after 27 days exposure in seawater, which was also observed in the Seawater Submersion Test (Roethel *et al.*, 1986). Extensive gypsum development via the hydration of anhydrite was found in X-ray Diffraction Analysis (Roethel *et al.*, 1986). Due to the larger molecular size of gypsum ( $CaSO_4 \cdot 2H_2O$ ) compared to that of anhydrite ( $CaSO_4$ ), the conversion resulted in an expansion of the block. As the expansion exceeded the available pore space volume, it created a pressure in the interior of the blocks finally resulting in the structural failure of the material and increase of surface area to volume ratio (Roethel *et al.*, 1983).

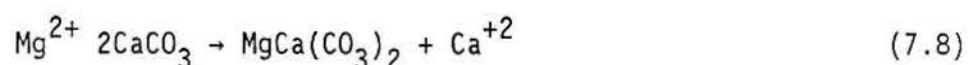
#### 7.3.4c Magnesium in Seawater

Magnesium analysis of seawater samples from the tank leaching study showed a constant removal of magnesium from the seawater by the blocks for HOB2 and COB1 but both magnesium uptake and release were observed fro WOB1, WOB2 and HOB1. The variability in the magnesium uptake/release for these blocks may be attributable to the fluctuation between release and uptake of calcium, and to the very low calcium release, which may be too small to show a distinct compensatory magnesium uptake. The calcium:magnesium mole ratio in HOB2 and COB1 are found to be very consistent throughout the leaching period, with the mole ratios averaging 1.15 ( $\pm 0.09$ ) for HOB2 and 1.05 ( $\pm 0.09$ ) for COB1. These values are lower than those of previous studies and closer to a ratio of 1. Edwards and Duedall (1985) observed a ratio of 1.27 to 2.40 for coal waste blocks, while Breslin (1986) had a ratio of 1.32 to 1.66 for oil ash waste blocks.

Several factors may be responsible for the magnesium uptake by SIA blocks.

From the previous tank dissolution tests, it is evident that diffusion is not the only process involved in calcium release from the blocks (Roethel, 1981; van der Sloot, 1983; Edwards and Duedall, 1985).

Substitution of magnesium for calcium observed on the leaching test of stabilized waste blocks in seawater was suggested as one possible mechanism of calcium release other than diffusion (Edwards and Duedall, 1985; Breslin, 1986). Edwards and Duedall (1985) provided evidence for an ion exchange process. They showed for coal waste blocks that the calcium flux is affected by the magnesium concentration in the surrounding water; calcium flux increased in freshwater with an addition of magnesium to values near that found in seawater. Breslin (1986) also showed that  $D'_{Ca}$  decreases as the salinity of the solution decreases and thus the magnesium content in the solution decreases. The presence of ion exchange was demonstrated by the shift in the main calcite ( $CaCO_3$ ) peak in X-ray Diffraction Analysis of coal waste blocks (Milliman, 1974), indicating some substitution of magnesium for calcium, via the equation:



Another mechanism that may contribute to the uptake of magnesium by the blocks is the precipitation of brucite [ $Mg(OH)_2$ ]. Brucite formation was observed in the pore spaces of SIA blocks and coal waste blocks after exposure to seawater (Parker *et al.*, 1981; Roethel *et al.*, in press). Since the pore water pH for all SIA blocks (Figure 7.4) exceeds the equilibrium pH (9.55) of brucite (Pytkowicz *et al.*, 1966), magnesium may replace calcium during the dissolution of lime [ $Ca(OH)_2$ ] in the pore waters of the blocks resulting in the removal of magnesium from seawater.

From the mole ratio of calcium:magnesium, it is apparent that at least part of calcium release was compensated for by the magnesium uptake. If magnesium is laid down in forms which contribute to physical integrity, then the expected lifetime calculated using a diffusion model would be conservative and the actual lifetime of blocks in seawater would be longer than model prediction.

#### 7.3.4d Temperature

The model (Table 7.13) predicts that in 100 years, at  $-23^\circ C$  and salinity

of 26 ppt, less than 1 cm of outer surface of WOB and HOB would be affected by the loss of calcium. In coastal area, the seawater temperatures cycle annually between 1°C and 25°C while the experiments were conducted at room temperature (~23°C). Edwards (1983) has shown a temperature dependence of calcium release from coal waste blocks, where about 50% less calcium was released at 4°C than at room temperature (~23°C). Since the diffusivity (D) of ions decreases with decreasing temperature (Li and Gregory, 1974), the model predictions presented in Table 7.13 may represent the maximum values for the effective depth of the diffusion zone for the blocks exposed to seawater.

### 7.3.5 Copper, Lead and Cadmium Discussion

Copper was detectable in seawater leachates throughout the experiment, however the cumulative concentrations of copper after 104 days' of leaching were low (Table 7.10 and Figure 7.3). The rate of copper leaching ranged from  $0.3 \times 10^{-12}$  to  $0.7 \times 10^{-12}$  moles  $\text{mm}^{-2} \text{s}^{-1}$  after 104 days. For copper and cadmium, initial metal release to seawater was followed by readsorption of the metal from the tank seawater. The initial release of copper and cadmium was higher for those blocks with greater surface area, which may suggest that the copper and cadmium present at the outermost part of blocks were rapidly released to seawater. This initial metal pulse is probably due to leachable metals present at the block surface rather than a real diffusive copper release. Copper and cadmium, which were released on the first day, subsequently readsorbed onto the block surfaces. In case of cadmium, only 12% (COB1) and 1% (COB2) of cadmium released on the first day, still remained in the tank seawater after 7 days. After the first change of the tank water with fresh seawater after 7 days leaching, cadmium was no longer detected in seawater leachates.

Previous investigations on coal ash and oil ash blocks showed an enrichment of trace elements, as well as retention, in the surface of the blocks after being exposed to seawater for prolonged period (Seligman, 1978; Roethel et al., 1983; Breslin, 1986). Copper, lead and cadmium were effectively retained by SIA blocks. Factors including pH, cement content of SIA blocks and leachable fraction may account for the retention of trace elements.

### 7.3.5a pH

Dissolution of calcium compounds in SIA blocks in seawater results in a solution of high pH (Table 7.8 and Figure 7.4). High pH generally retards the mobility of trace elements such as copper, lead and cadmium in solution. Alkaline conditions may favor the formation of precipitates such as lead hydroxides and copper carbonates (Theis and Richter, 1979). Incineration residues used for fabricating SIA blocks were found to be enriched in iron and manganese (Table 3.2) and tank leaching conditions were alkaline (Table 7.8 and Figure 7.4). Precipitation of iron and manganese hydrous oxide phases at high pH levels may result in the coprecipitation/adsorption of other metal ions in solution (Swallow, 1978; Johnson, 1986). Therefore, the scavenging of copper, lead and cadmium by iron and manganese hydrous oxides and/or precipitation through the formation of metal hydroxides and carbonates may be an important factor in the retention of these metals by SIA blocks.

### 7.3.5b Cement

Cement is an important additive to improve strengths of SIA blocks and may also act to reduce the metal leaching (Section 7.2.3c). In this study, the incineration residues were stabilized with 15% Portland cement, Type I. Stabilization of wastes with Portland cement has been demonstrated to effectively retain the heavy metals within the blocks (Young *et al.*, 1984; Poon *et al.*, 1985; Shively *et al.*, 1986). Metal binding in the cement matrix may be due to a combination of entrapment of insoluble metal precipitates in pores in cemented material and within the cementitious matrix, and to adsorption to surfaces within the matrix (Brown and Bishop, 1985).



## 7.4 SEQUENTIAL EXTRACTION OF STABILIZED INCINERATION ASH

Samples of blocks fabricated using Westchester incineration ash at the Besser Company, Alpena, Michigan, were subjected to the sequential extraction procedure to determine the effects of stabilization on metal leachability.

### 7.4.1 Methods

Westchester investigation ash was stabilized using cement to form a solid block using conventional block making equipment (Section 4.4). Samples of the 6/1 Reef blocks were ground with a mortar and pestle and sieved to a particle size  $<425 \mu\text{m}$ . The sieved samples were then oven-dried at  $110^\circ\text{C}$  for 24 hours. The samples were then extracted using the sequential extraction procedure as given in (Section 3.3.2).

The total elemental concentration of the 6/1 Reef blocks was determined using the  $\text{HF-H}_3\text{BO}_3$  acid digestion (Section 3.3.2a).

### 7.4.2 Results and Discussion

The distribution of the seven elements in the five fractions of the stabilized incineration block is given in Table 7.16 and Figure 7.5. For each metal in the stabilized incineration ash the sum of the five extraction fractions is compared to the total elemental composition of samples of material as determined by the  $\text{HF-H}_3\text{BO}_3$  digest.

#### 7.4.2a Short-term and Long-term Leachability for Stabilized Incineration Ash

To assess potential environmental impacts of metal leaching, the results can be grouped into short-term and long-term leachable fractions. Short-term leachability estimates are based on the total metal extracted from the exchangeable and carbonate phases (Fractions A + B). Long-term leachability estimates are based on the total metal extracted from the exchangeable, carbonate, and Fe and Mn phases (Fractions A + B + C) Figure 7.5.

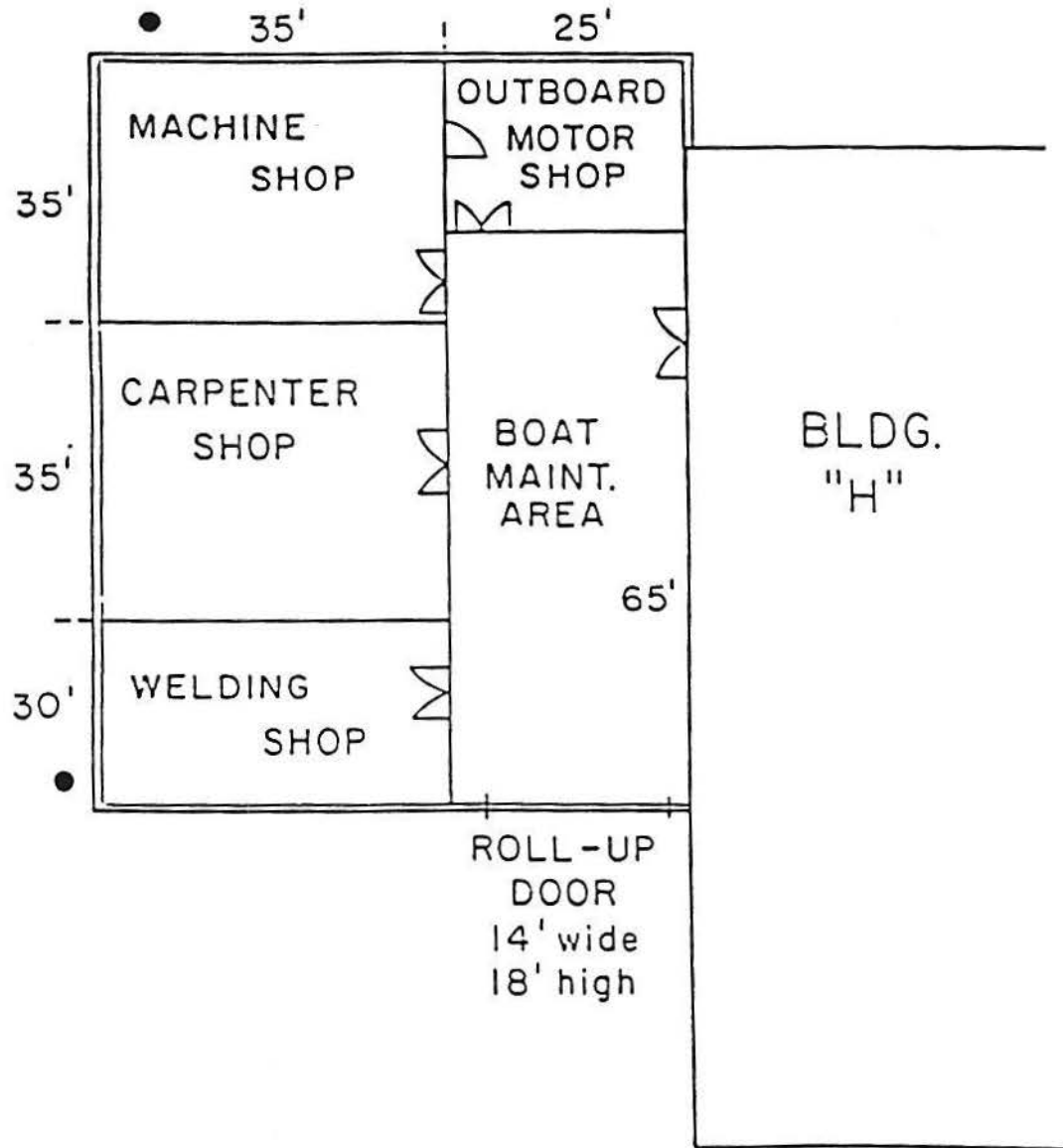
Results of the metal leaching show that less metal is available for



Table 7.16. Sequential extraction of metals from stabilized incineration ash.

Fraction	Concentration	(%)	Fraction	Concentration	(%)
<u>Fe</u>			<u>Pb</u>		
A	2 ± 0.5	0.1	A	9 ± 1	0.2
B	1192 ± 12	2.2	B	1450 ± 110	41.0
C	10360 ± 700	19.1	C	872 ± 100	23.2
D	28 ± 4	0.1	D	240 ± 48	6.4
E	42640 ± 280	78.5	E	1090 ± 13	29.2
Σ	54220 ±	100.0	Σ	3750 ± 220	100.0
M <sub>T</sub>	53080 ± 1570		M <sub>T</sub>	3690 ± 410	
<u>Mn</u>			<u>Ca</u>		
A	2 ± 0.5	0.2	A	56260 ± 3480	43.6
B	185 ± 15	22.4	B	51010 ± 3100	39.5
C	314 ± 21	38.0	C	1570 ± 432	1.2
D	6 ± 0.8	0.7	D	1274 ±	1.0
E	320 ± 6	38.7	E	19000 ± 9800	14.7
Σ	825 ±	100.0	Σ	142720 ± 9800	100.0
M <sub>T</sub>	861 ± 30		M <sub>T</sub>	149680 ± 5360	
<u>Zn</u>			<u>Cd</u>		
A	301 ± 19	7.3	A	6 ± 0.5	24.5
B	1790 ± 73	43.3	B	11 ± 1	43.7
C	753 ± 60	18.2	C	3 ± 0.1	10.8
D	79 ± 8	1.9	D	0.03 ± 0.007	0.1
E	1210 ± 21	29.3	E	5 ± 0.2	20.9
Σ	4080 ± 31	100.0	Σ	25 ± 0.7	100.0
M <sub>T</sub>	4410 ± 180		M <sub>T</sub>		
<u>Cu</u>					
A	390 ± 25	27.3			
B	146 ± 36	10.3			
C	42 ± 8	3.0			
D	530 ± 50	37.4			
E	310 ± 120	22.0			
Σ	1470 ± 350	100.0			
M <sub>T</sub>	1480 ± 35				

Figure 7.5 Sequential chemical extraction of stabilized incineration residue.



### 9.1.1b Results and Discussion

Results of the elemental analysis of the soil samples are presented in Table 9.1. The elemental concentrations in the soils were variable, with soil sample 1A having the highest metal content of the soils analyzed. Variations in the metal content of the spoils may be a result of differences in soil type.

In an attempt to determine elemental enrichment in the soil samples, the elemental concentrations were normalized to the iron concentration in each sample. The Fe/metal ratios are shown in Table 9.1 and Figure 9.2. Enrichment or depletion of an element would be indicated if the Fe:metal ratio of the samples (1A, 1B, 2A, and 2B) significantly differed from the control samples (3A, 3B). Figure 9.2 shows that Ni, Cu, Cr, and Zn are not significantly different from the control samples as a function of location or depth. Iron:lead ratios in the samples 1A, 1B, 2A and 2B are less than the control samples indicating a slight lead enrichment ( $\approx 4$  fold) for soil samples 3A and 3B. Iron:manganese ratios show considerable variation with possible enrichment in sample 2A.

Monitoring the Metal/Fe ratio in the soil after boathouse construction will allow a determination of the release of metals from the incineration ash blocks to the surrounding soil.

### 9.1.2 Radon Emanating from Incineration Ash: Results from City, Huntington, and Westchester Ashes and Blocks

#### 9.1.2a Introduction

Radon ( $^{222}\text{Rn}$ ) is a radioactive gas in the Uranium ( $^{238}\text{U}$ ) decay series. Recent discoveries of high levels of this gas in homes built over pegmatite or uranium contaminated soil have led to concerns about its presence in natural building materials as well. This study examined  $^{222}\text{Rn}$  emanation from incinerator ash, which has been proposed as an additive in cement blocks, as an alternative to burial in landfills.

Table 9.1. Elemental analysis ( $\mu\text{g/g}$ ) of soil.

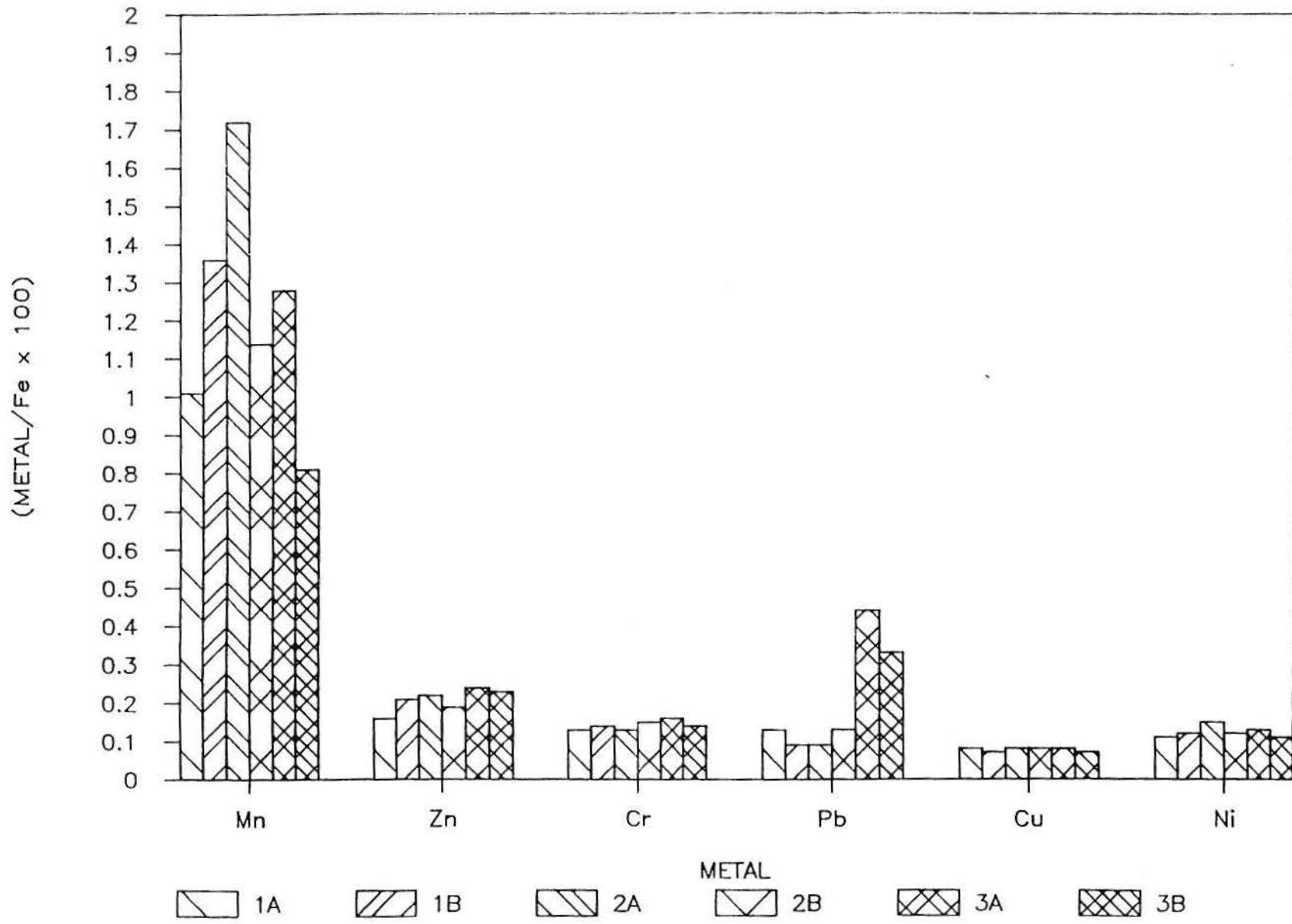
Element	1A	1B	2A	2B	3A	3B
Fe	10370 $\pm$ 2240	8780 $\pm$ 210	7770 $\pm$ 110	7900 $\pm$ 440	8190 $\pm$ 250	6450 $\pm$ 310
Mn	105 $\pm$ 3.6	119 $\pm$ 1.3	134 $\pm$ 2	90 $\pm$ 3.8	105 $\pm$ 16	52 $\pm$ 1.2
Mn (N)	1.01	1.36	1.72	1.14	1.28	0.81
Zn	17 $\pm$ 0.4	18 $\pm$ 4.3	17 $\pm$ 3.3	15 $\pm$ 0.5	20 $\pm$ 1.4	15 $\pm$ 1.3
Zn (N)	0.16	0.21	0.22	0.19	0.24	0.23
Cr	13 $\pm$ 1.4	12 $\pm$ 1.0	10 $\pm$ 1.2	12 $\pm$ 0.9	13 $\pm$ 0.9	9 $\pm$ 1.1
Cr (N)	0.13	0.14	0.13	0.15	0.16	0.14
Pb	13 $\pm$ 6.2	7.9 $\pm$ 0.2	7.1 $\pm$ 0.8	9.9 $\pm$ 0.2	36 $\pm$ 3.9	21 $\pm$ 1.3
Pb (N)	0.13	0.09	0.09	0.13	0.44	0.33
Cu	8.6 $\pm$ 2.9	6.3 $\pm$ 0.2	6.1 $\pm$ 0.1	6.0 $\pm$ 0.3	6.5 $\pm$ 0.9	4.3 $\pm$ 0.3
Cu (N)	0.08	0.07	0.08	0.08	0.08	0.07
Ni	10.9 $\pm$ 1.6	10.8 $\pm$ 0.3	11.5 $\pm$ 0.3	9.5 $\pm$ 0.1	10.6 $\pm$ 1.4	6.8 $\pm$ 1.1
Ni (N)	0.11	0.12	0.15	0.12	0.13	0.11
Cd <sup>a</sup>	BDL	BDL	20.3 $\pm$ 1.5	40.6 $\pm$ 2.0	BDL	BDL

Elements are normalized (N) to iron as  $(X/\text{Fe} \times 100)$ .

BDL - Below detection limits.

<sup>a</sup> Cadmium results are expressed in ng/g.

Figure 9.2 The metal:iron ratio for MSRC soil metals.



$^{222}\text{Rn}$  gas is produced directly by radioactive decay of radium ( $^{226}\text{Ra}$ ) in a solid (in this case incinerator ash). This decay is energetic and causes some of the radon to be ejected or recoiled out of the particles of the solid. The amount of radon which leaves the particle, or percent emanation, determines the magnitude of the material as a source for the radioactive gas. The  $^{222}\text{Rn}$  gas is in turn radioactive, and decays. The half-life, or time for one half of the  $^{222}\text{Rn}$  atoms to decay, is 3.82 days. If the sample is placed in a sealed container, in about five half-lives (16 days), a steady state is reached in which the activity (number of decays per unit time) of  $^{222}\text{Rn}$  in the container doesn't change with time. The ratio of this activity to the activity of  $^{226}\text{Ra}$  in the ash gives the percent emanation of radon from the ash.

#### 9.1.2b Sample Preparation

Ash from three operational facilities was analyzed for  $^{222}\text{Rn}$  emanation and  $^{226}\text{Ra}$  activity. The Southwest Brooklyn plant operated by the City of New York, the Signal-RESCO facility in Westchester County, and the Town of Huntington incinerator located in East Northport were selected. Each type of ash was analyzed in three forms: (1) pure ash, (2) powdered aggregate of 85 percent ash and 15 percent Portland cement binder for building blocks, and, (3) single chunks broken off building blocks formed from ash and cement aggregate. Blocks of ash aggregate (ash plus Portland cement) were freeze dried; single small chunks were broken off the blocks, weighed, and placed dry in the bottom of washed and dried 1 gallon acid bottles. Powdered aggregate was obtained by crushing ash aggregate blocks. Blocks containing these ashes were fabricated during phase I of this project (Roethel *et al.*, 1986). Pure ash and powdered aggregate samples were oven-dried (80°C) overnight, weighed, and suspended in distilled water in washed acid bottles. A powder made from a chunk of a cement block was treated in a similar fashion to the ash samples. In addition to the samples mentioned, blanks were run which included empty acid bottles, acid bottles with distilled water, and system blanks. The results of the blank analyses were subtracted from the sample analyses. Absolute efficiency of the system was checked using a  $^{226}\text{Ra}$  standard.



### 9.1.2c Methods

$^{222}\text{Rn}$  analysis calls for purging the sample container with helium to remove existing radon and waiting 2 weeks for the radon to be emitted and attain steady state (Mathieu, 1977). After two weeks the container is purged again with helium, which drives the radon emitted into an extraction board that removes the radon onto activated charcoal at dry-ice temperatures. The activated charcoal with the radon is heated to drive the radon gas off into counting vessels. Overall extraction and counting efficiency is 80-90 percent. In addition to the ash, and ash-cement aggregates, a cement block of the type used in building construction was powdered and analyzed for radon emanation for comparison with blocks formed from ash aggregate. To measure the  $^{226}\text{Ra}$  content of the ash, powdered ash, ash aggregate and powdered cement block were placed in sealed counting tins. Gamma emission from these powdered samples was measured using an intrinsic germanium detector.  $^{214}\text{Pb}$  is actually measured on the gamma detector because this product of  $^{226}\text{Ra}$  decay gives more accurate gamma peaks than  $^{226}\text{Ra}$ . If an ingrowth time of two weeks is allowed prior to counting, it is assumed that the activity of  $^{214}\text{Pb}$  is equal to the activity of  $^{226}\text{Ra}$ .

Gamma counting gives activity of  $^{226}\text{Ra}$ , the parent to  $^{222}\text{Rn}$ . If all of the  $^{222}\text{Rn}$  produced by  $^{226}\text{Ra}$  decay was recoiled from the ash into the container, the equilibrium activity of  $^{222}\text{Rn}$  would equal  $^{226}\text{Ra}$  activity in the solid. Since some fraction of radon produced is actually recoiled into the container, this fraction, or percent emanation, is the best measure of the material as a source of radon gas.

### 9.1.2d Results and Discussion

The  $^{222}\text{Rn}$  emanation from ash and aggregate samples along with the  $^{226}\text{Ra}$  gamma activities of ash and aggregate samples are shown in Table 9.2. Emanation of radon gas out of a sample is expected to increase as the surface area to volume ratio for that sample increases. Since solid chunks of material have low surface area to volume ratios relative to powders, and chunk size was restricted by the size of the opening to the container, no detectable radon emanated from the Westchester and Huntington block chunks. Percent emanation from a chunk of block made from City ash, obtained using gamma activity from

Table 9.2.  $^{222}\text{Rn}$  emanation from, and  $^{226}\text{Ra}$  gamma activity of, ash and aggregate samples.

Sample	Mass (grams)	Emanated $^{222}\text{Rn}$ (DPM/gm)	Gamma Activity (DPM/gm)		% Emanation (for $^{222}\text{Rn}$ )
			$^{210}\text{Pb}$	$^{214}\text{Pb}$	
<u>Ash</u>					
City	5.53	0.32±0.01	23.85	1.77	18.1
Westchester	41.80	0.07±0.01	1.09	0.84	8.3
Huntington	46.89	0.06±0.01	1.32	1.06	5.7
<u>Block powder</u>					
City	5.51	0.25±0.01	19.81	1.80	13.9
Westchester	8.42	0.05±0.01	1.06	0.96	5.2
Huntington	13.37	0.01±0.01	1.33	0.92	1.1
Cement	48.20	0.19±0.01	1.04	1.09	17.4
<u>Block chunks</u>					
City	5.49	0.08±0.01	ND <sup>b</sup>	ND	4.4 <sup>c</sup>
Westchester	8.41	0 <sup>a</sup>	ND	ND	
Huntington	13.35	0*	ND	ND	

<sup>a</sup> Blank value exceeded sample value.

<sup>b</sup> ND values for these samples were not determined.

<sup>c</sup> Obtained using City block powder gamma activity and emanated  $^{222}\text{Rn}$  value.

the corresponding powder, shows a value approximately one-third that of the powder.

Since the amount of radon emanated from a powder would be much greater than from a block of the same material (see City block powder and chunk values, Table 9.2), the values in the table represent an upper limit on radon emanation. Table 9.3 shows calculations for determining the total  $^{222}\text{Rn}$  activity for a room in a building built with the ash aggregate having the highest radon activity (City). A more realistic, but still upper limit value, can be obtained by using the emanation from a chunk of City block aggregate. It should be noted that  $^{222}\text{Rn}$  emanation from a standard cement block commonly used in construction is 3.8 times higher than emanation from Westchester block powder, and 19 times higher than Huntington block powder. Note also that the  $^{226}\text{Ra}$  ( $^{214}\text{Pb}$ ) activity of the cement is approximately equal to that of the ash. Therefore, based on the activities of the measured radionuclides, incinerator ash is as safe as cement for incorporation into building materials.

## 9.2 ARTIFICIAL REEF CONSTRUCTION

### 9.2.1 Model Estimate of Marine Disposal Impacts

Calculations were performed to make a potential estimation of the dispersion distance of metals released from a hypothetical artificial reef constructed from stabilized incineration ash blocks (Figure 9.3). Professor A. Okubo has developed a relationship for the dispersion and dilution of a leachate constituent from a source near the seafloor based on measurements of turbulent and dispersive processes near the seabed (Roethel and Woodhead, 1983). The downstream distance of dispersion for copper from WOB and HOB was calculated using the following equation:

$$L = \frac{q\lambda}{2\pi^{1/2} W S_p X} \quad (9.1)$$

where  $L$  = downstream distance of dispersion (m),  
 $q$  = source strength ( $\mu\text{g}$ ),  
 $\lambda$  = leaching rate of ion ( $\text{sec}^{-1}$ ),

Table 9.3. Approximate supported radon content of a building 60'x 90'x 20'.

---

Assuming block size of: 7.5" x 7.5" x 17.5"

6592 blocks total for 4 walls  
 x 15.4 kg/block weight  
 101,517 kg total mass of material  
 x 250 DPM/kg : City Block powder emanated  $^{222}\text{Rn}$  activity (0.25 DPM/g)  
 $2.5 \times 10^7$  disintegrations total per minute = total  $^{222}\text{Rn}$  activity

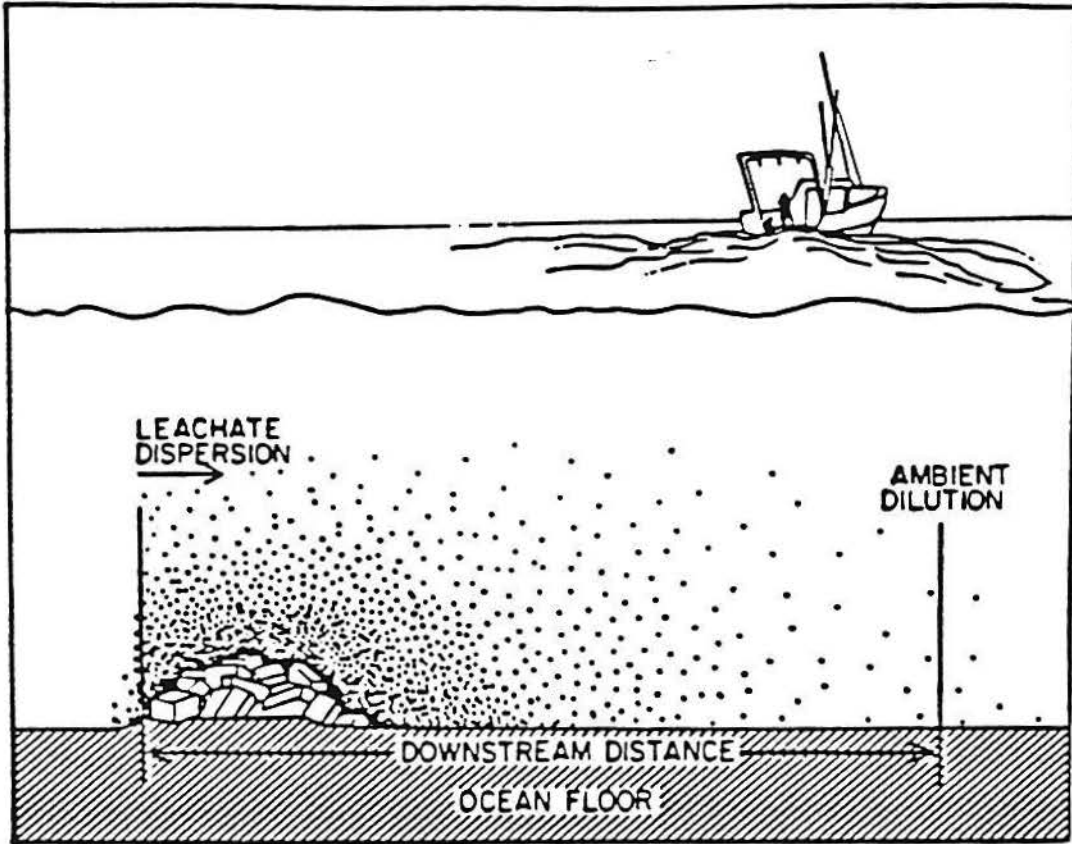
Volume of the room =  $2.67 \times 10^6$  liters

$^{222}\text{Rn}$  activity = 10 DPM/liter of air  
 = 0.16 Bequerels/liter of air  
 = 4.72 pCi/liter of air

$^{222}\text{Rn}$  activity if City block chunk value is used:  
 = 3.2 DPM/liter of air  
 = .05 Bequerels/liter of air  
 = 1.5 pCi/liter of air

---

Figure 9.3 Diagram showing the downstream dispersion of leachate from a stabilized incineration ash reef configuration.



- $W$  = diffusion velocity ( $\text{cm s}^{-1}$ )  
 $S_p$  = ambient concentration of ion in seawater ( $\text{g cm}^{-3}$ )  
 $X$  = mixing height from the bottom (cm).

Copper leaching rates ( $\lambda$ ), expressed as the fraction of copper leached per time, were determined from the tank leaching study using the copper flux for 1 and 104 days after placement of SIA blocks on the seafloor. The hypothetical reef is assumed to consist of 1,000 tons (metric) of SIA blocks. The reef would contain approximately 55,000 SIA blocks; size of 20 x 20 x 40 cm and weight of 18 kg. Assuming 35% pore space within the reef, the reef would occupy a volume of about 1188  $\text{m}^3$  (Figure 7.5). Source strength ( $q$ ) was obtained by multiplying the copper concentration in the block ( $\mu\text{g g}^{-1}$ ) by the total weight of the reef (g). A seawater diffusion velocity of  $1 \text{ cm s}^{-1}$  and a conservative height of diffusion of 5 m are assumed. Copper concentration in the New York Bight was reported  $1.2 - 7.8 \times 10^{-9} \text{ g cm}^{-3}$  (Segar and Cantillo, 1976). In this calculation, the lowest value ( $1.2 \times 10^{-9} \text{ g cm}^{-3}$ ) was used for the ambient water column concentration for copper to estimate the worst case.

Results in Table 9.4 show that the copper dispersion distance would be virtually undetectable after a few days of leaching. Distance ranged from 1.5 m for WOB to 8.7 m for HOB after 1 day, and decreased to 0.023 m and 0.047 m after 104 days for WOB and HOB, respectively.

#### 9.2.1a Limitations of the Model Estimate

Laboratory measurements of the calcium flux from SIA blocks predict that the blocks can have a potentially long lifetime in the ocean environment (Section 7). In addition, copper, lead and cadmium can be effectively retained by the blocks. Calculations of the plume length of copper from a hypothetical artificial reef show that the distances of copper dispersion decrease with time. These results, however, were obtained under controlled laboratory conditions. Therefore, the model predictions have limitations in their applicability to processes occurring in the real ocean environment.

Physical and biological processes are likely to impact the structural integrity and thus the leaching rates of the blocks in the ocean. Bioerosion

Table 9.4 Model calculations of dispersive distance (L) for copper<sup>a</sup>.

	WOB <sup>b</sup>	HOB
Total Cu Conc. <sup>c</sup> ( $\mu\text{g g}^{-1}$ ):	4700	1400
Leaching Rate <sup>d</sup> ( $\text{sec}^{-1}$ ):		
1 day	$6.83 \times 10^{-11}$	$1.33 \times 10^{-9}$
104 day	$1.03 \times 10^{-12}$	$7.22 \times 10^{-12}$
Downstream Distance (m):		
1 day	1.5	8.7
104 day	0.023	0.047

<sup>a</sup> Downstream distance calculated using equation 7.8 and constants used for equation 7.8 are

- :total weight of disposal reef = 1000 tons (metric),
- :diffusion velocity in seawater =  $1 \text{ cm s}^{-1}$ ,
- :ambient Cu concentration in water column =  $1.2 \times 10^{-9} \text{ g cm}^{-3}$   
(from Segar and Cantillo, 1976).

<sup>b</sup> Optimum mix designs are listed in Table 7.7

<sup>c</sup> Total Cu concentration in SIB blocks determined by a HF-H<sub>3</sub>BO<sub>3</sub>-AAS method (Table 7.1)

<sup>d</sup> Leaching rate is the fraction of Cu leached per time: from average flux value between Block 1 and Block 2 in Table 7.10.



processes caused by the colonization of the blocks by organisms may increase leaching rates by increasing exposed surface area. Earlier studies with blocks of fly ash and flue gas desulfurization sludge (Parker *et al.*, 1981; Humphries, 1985; Roethel *et al.*, 1983) show that the clam Zirfaea crispata and the barnacle Balanus improvisus were able to bore into or bioerode the block surfaces. On the other hand, encrusting organisms like bryozoans may reduce the calcium release by reducing the area of direct contact with the seawater. Physical erosion processes such as bottom currents and water movement due to storm action may move the blocks causing physical erosion of the blocks.

## Section 10

## REFERENCES

- American Society for Testing and Materials. 1975. Standard specification for fly ash and other pozzolans for use with lime - Procedure C593-69 In: 1975 Annual Book of ASTM Standards, Vol. 13 Philadelphia, Pa. pp. 340-344.
- American Society for Testing Materials (ASTM). 1980. Proposed method for leaching of waste materials, Part A: Water Shake Extraction Procedure. In: Annual Book of ASTM Standards, Part 31-Water, Philadelphia, PA. pp. 1369-1372.
- Annual Book of ASTM Standards, 1974. American Society for Testing Materials, Philadelphia, PA, 1974.
- B. A. Auld. 1973. Acoustic Fields and Waves in Solids (Wiley, New York)
- Barber, E. G. 1970. The Utilization of Pulverized Fuel Ash. Journal of the Institute of Fuels, 43, 4-9.
- Breslin, V.T. 1986. Chemical behavior of particulate and stabilized oil ash waste in seawater. Ph.D. Dissertation, Department of Oceanography and Ocean Engineering, Florida Institute of Technology, FL, 138 pp.
- Brown, T.M. and P.L. Bishop. 1985. The effect of particle size on the leaching of heavy metals from stabilized/solidified wastes. In: International Conference on New Frontiers for Hazardous Waste Management, Pittsburgh, PA, 1985.
- Carleton, H. R. and J. F. Muratore. 1985. "Effects of Exposure on the Physical Properties of Coal Waste Blocks in the Ocean", in Wastes in the Ocean, edited by I. W. Duedall et. al. (John Wiley & Sons, Inc. New York) Vol. 4, Ch. 29, pp. 667-690.
- Carleton, H. R. and J. F. Muratore. 1986. "Ultrasonic Evaluation of Concrete", in Proceedings of the 1986 IEEE Ultrasonics Symposium, Williamsburg, edited by B. R. McAvoy (IEEE, New York).
- Carpenter, E. J., and J. S. Lively, 1980. Review of estimates of algal growth using  $^{14}\text{C}$  tracer techniques. In: Primary productivity in the sea, P. G. Falkowski (Ed.). Plenum Press, New York, pp. 161-178.
- Cross, T. 1982. Trace metal uptake by mussels exposed to suspended coal waste particulates. M.S. Thesis, MSRC, SUNY at Stony Brook, N.Y., 81 pp.
- Duedall, I.W., J.S. Buyer, M.G. Heaton, S.A. Oakley, A. Okubo, R. Dayal, M. Tatro, F.J. Roethel, R.J. Wilke and J.P. Hershey. 1983. Diffusion of calcium and sulphate ions in stabilized coal wastes. In: Industrial and Sewage Wastes in the Ocean, I.W. Duedall, B.H. Ketchum, P.K. Park and D.R. Kester (Eds.), Wiley-Interscience, NY. pp. 375-395.
- Ediger, R.D., G.E. Peterson and J.D. Kerber. 1974. Application of the

- graphite furnace to saline water analysis. Atomic Absorption Newsletter, 13(3): 61-64.
- Ediger, R.D. 1975. Atomic absorption analysis with the graphite furnace using matrix modification. Atomic Absorption Newsletter, 14(5): 127-130.
- Edwards, T. 1983. Dissolution rates of calcium in stabilized coal wastes in freshwater and seawater. Master Thesis, Marine Sciences Research Center (MSRC), State University of New York (SUNY) at Stony Brook, NY, 69 pp.
- Edwards, T. and I.W. Duedall. 1985. Comparison of dissolution processes of stabilized coal wastes in freshwater and seawater systems. In: Wastes in the Ocean, Vol. 4: Energy Wastes in the Ocean, I.W. Duedall, D.R. Kester, P.K. Park and B.H. Ketchum (Eds.). Wiley-Interscience, NY. pp. 467-498.
- Garrels, R. M. and C. L. Christ. 1965. Solutions, Minerals and Equilibria. Freeman, Cooper and Company, San Francisco, California, 450 pp.
- Goldberg, E. D. 1978. The mussel watch. Environ. Conser. 5:101-125.
- Greenberg, R.R., W.H. Zoller and G.E. Gordon. 1978. Composition and size distributions of particles released in refuse incineration. Environmental Science & Technology, 12(5): 566-573.
- Guillard, R. R. L., and J. H., Ryther. 1962. Studies on marine planktonic diatoms. I: Cyclotella nana Hustedt and Detonula confervacea (Cleve) Gran. Canadian Journal of Microbiology, 8, 222-239.
- Humphries, E. M., Duedall, I. W. and S. J. Jordan. 1985. Stabilized coal combustion wastes as a fouling substrate in estuarine waters. In: Wastes in the Ocean, Vol. 4: Energy Wastes in the Ocean, Chapter 27. I. W. Duedall, P. K. Park, D. R. Kester and B. H. Ketchum (eds.). John Wiley & Sons, Inc., New York.
- Landreth, R. and J. Mahloch. 1977. Chemical fixation of wastes. Industrial Water Engineering, 14(4): 16-19.
- JCPDS. 1979. Powder Diffraction File, Inorganic materials Alphabetical Index, Joint Committee on Powder Diffraction Standards, International Center for Diffraction Data, Swathmore, Pennsylvania.
- Johnson, C.A. 1986. The regulation of trace element concentrations in river and estuarine waters contaminated with acid mine drainage: The adsorption of Cu and Zn on amorphous Fe oxyhydroxides. Geochimica et Cosmochimica Acta, 50(11): 2433-2438.
- Law, S.L. and G.E. Gordon. 1979. Sources of metals in municipal incinerator emissions. Environmental Science & Technology, 13(4): 432-438.
- Lawrence, W.F., W.H. Buttermore and R.B. Muter. 1972. Characterization, beneficiation and utilization of municipal incineration flyash. In: Proceedings of the 3rd Mineral Waste Utilization Symposium, Chicago, Ill, 1972.

- Milliman, J.D. 1974. Marine Carbonates. Springer-Verlag New York Inc., NY, 375 pp.
- Muratore, J. F. and H. R. Carleton. 1981. "The Ultrasonic Properties of Impregnated Graphite", in Proceedings of the 1981 IEEE Ultrasonics Symposium, Chicago, edited by B. R. McAvoy (IEEE, New York) pp. 940-944.
- Muratore, J. F. and H. R. Carleton. 1982. "Ultrasonic Spectra of Porous Composites", in Proceedings of the 1982 IEEE Ultrasonics Symposium, San Diego, edited by B. R. McAvoy (IEEE, New York) pp. 1049-1053.
- Muratore, J. F. and H. R. Carleton. 1985. "Phase Spectroscopy on Lossy Media", in Proceedings of the 1985 IEEE Ultrasonics Symposium, San Francisco, edited by B. R. McAvoy (IEEE, New York) pp. 1047-1051.
- Muratore, J. F. 1987. "Ultrasonic Spectroscopy of Inhomogeneous Media", Ph.D. Dissertation, State University of New York at Stony Brook.
- Murphy, L. S., E. M. Haugen, and J. F. Brown. 1983. Phytoplankton: comparison of laboratory bioassay and field measurements. In: Wastes in the Ocean, Vol. 1: Industrial and Sewage wastes in the Ocean, I. W. Duedall, B. H. Ketchum, P. K. Park, and D. R. Kester (Eds.) Wiley-Interscience, New York, 219-233.
- Neal, H.A. and J.R. Schubel. 1987. Solid Waste Management and the Environment: The mounting garbage and trash crisis. Prentice-Hall, Inc. Englewood Cliffs, NJ, 240 pp.
- Neville, A.M. 1983. Properties of concrete. Halsted Press, Div. of Wiley & Sons, New York, NY.
- Parker, J.H., P.M.J. Woodhead and I.W. Duedall. 1981. Coal-Waste Artificial Reef Program, Phase 3, Vol. 2: Comprehensive report. EPRI Report CS-2009, Electric Power Research Institute, Palo Alto, CA, 404 pp.
- Parker, J.H., P.M.J. Woodhead, I.W. Duedall, J. Colussi, R.G. Hilton and L.E. Pfeiffenberger. 1985. Coal-waste blocks for artificial-reef establishment: A large scale experiment. In: Wastes in the Ocean, Vol. 4: Energy Wastes in the Ocean, I.W. Duedall, D.R. Kester, P.K. Park and B.H. Ketchum (Eds.). Wiley-Interscience, NY. pp. 537-555.
- Poon, C.S., A.I. Clark, C.J. Peters and R. Perry. 1985. Mechanisms of metal fixation and leaching by cement based fixation processes. Waste Management and Research, 3: 127-142.
- Pytkowicz, R.M., I.W. Duedall and D.N. Connors. 1966. Magnesium ions: activity in seawater. Science, 152: 640-642.
- Roethel, F.J. 1981. Interactions of stabilized power plant coal wastes with the marine environment. Ph.D. Dissertation, MSRC, SUNY at Stony Brook, NY, 349 pp.
- Roethel, F. J., Duedall, I. W., and P. M. J. Woodhead. 1983. Coal Waste

- Artificial Reef Program: Conscience Bay Studies. Electric Power Research Institute, May 1983. pp. 4.63-4.65.
- Roethel, F.J. and P.M.W. Woodhead. 1983. Feasibility of marine disposal of urban wastes, sewage sludge and fly ash; A Rationale in support of second phase funding. MSRC, SUNY at Stony Brook, NY, 82 pp.
- Roethel, F.J., I.W. Duedall and P.M.J. Woodhead. 1983. Coal-Waste Artificial Reef Program: Conscience bay studies. Electric Power Research Institute, Palo Alto, CA, 304 pp.
- Roethel, F.J., V. Schaeperkoetter, K. Park and R. Gregg. 1986. The fixation of incineration residues: physical and leachate properties. Final report to the New York State Legislative Commission on the Water Resource Needs of Long Island, 200 pp.
- Segar, D.A. and A. Cantillo. 1976. Trace metals in the New York Bight. In: Middle Atlantic Continental Shelf and the New York Bight, Special Symposium, Vol. 2, M.G. Gross (Ed.). American Society of Limnology and Oceanography, Lawrence, Kansas. pp. 171-198.
- Seligman, J.D. 1978. Chemical and physical behavior of stabilized scrubber wastes and fly ash in seawater. Master Thesis, MSRC, SUNY at Stony Brook, NY, 82 pp.
- Shively, W., P. Bishop, D. Gress and T. Brown. 1986. Leaching tests of heavy metals stabilized with portland cement. Water Pollution Control Federation, 58(3): 234-241.
- Silberman, D. and G.L. Fisher. 1979. Room-temperature dissolution of coal fly ash for trace metal analysis by atomic absorption spectrometry. Analytica Chimica Acta. 106: 299-307.
- Sokal, R. R., and F. T. Rohlf. 1981. Biometry, 2nd Edition, W. H. Freeman and Company, San Francisco.
- Strickland, J. D. H., and T. R. Parsons. 1977. A Practical Handbook of Seawater Analysis. Bulletin No. 167 of the Fisheries Research Board of Canada, Ottawa, Canada, 311 pp.
- Stumm, W. and J.T. Morgan. 1981. Aquatic Chemistry, 2nd Edition. Wiley-Interscience, NY, 780 pp.
- Swallow, K.C. 1978. Adsorption of trace metals by hydrous ferric oxide in seawater. Ph.D. Dissertation, Massachusetts Institute of Technology, MA.
- Surgi, R. 1986. Residues from resource recovery facilities: current research. Presented for Signal Environmental Systems, May 1986 at MSRC, SUNY at Stony Brook, NY, 16 pp.
- Theis, T.L. and R.O. Richter. 1979. Chemical speciation of heavy metals in power plant ash pond leachate. Environmental Science and Technology, 13(2): 219-224.



- Thompson, R. B. and D. O. Thompson. 1985. "Ultrasonics in Non destructive Evaluation", Proceedings of the IEEE 73, 1716-1755.
- Thorn, D. J. and J. D. Watt. 1965. Composition and Pozzolanic Properties of Pulverized Fuel Ashes II. Pozzolanic Properties of Fly Ashes as Determined by Crushing Strength Tests on Lime Mortar. Journal of Applied Chemistry, 15, 595-604.
- U. S. Environmental Protection Agency. 1978. Bioassay Procedures for the Ocean Disposal Permit Program. EPA 600/9-78-010, Office of Research and Development, U. S. Environmental Protection Agency, Gulf Breeze, Florida, pp. 121.
- U.S. Environmental Protection Agency (EPA). 1980. Hazardous waste management system: Identification and listing of hazardous waste, Toxicity Test Extraction Procedure (EP). Federal Register, 45(98): 33063-33285, May 19, 1980.
- U.S. EPA. 1986. Hazardous waste management system: Land disposal restrictions, Proposed rule-Toxicity Characteristic Leaching Procedure (TCLP). Federal Register, 51(9): 1750-1758, January 14, 1986.
- van der Sloot, H.A. 1983. Similarities in the leaching characteristics of coal ash and coal ash products in freshwater and seawater. (Abstract) 4th International Ocean Disposal Symposium, 11-15 April, Plymouth, England.
- van der Sloot, H.A., E.G. Weyers, D. Hoede and J. Wijkstra. 1985. Physical and chemical characterization of pulverized coal ash with respect to cement-based applications. SL85/754DVH.1, Netherlands Energy Research Foundation, Petten, The Netherlands, 248 pp.
- van der Sloot, H.A., J. Wijkstra, C.A. Van Stigt and D. Hoede. 1985. Leaching of trace elements from coal ash and coal-ash products. In: Wastes in the Ocean, Vol. 4: Energy Wastes in the Ocean, I.W. Duedall, D.R. Kester, P.K. Park and B.H. Ketchum (Eds.). Wiley-Interscience, NY. pp. 467-498.
- Venuto, C. J. and J. H. Trefry. 1983. Frequency distribution patterns and partitioning of copper, iron and zinc in selected tissues of the black mullet (Mugil cephalus) Florida Scientist, 46 (3/4):346-355.
- Vincent, R. D., M. Mateos, and D. T. Davidson. 1961. Variation in Pozzolanic Behavior of Fly Ashes. In: Proceedings 61. American Society for Testing and Materials, Philadelphia, Pennsylvania, pp. 87-126.
- Yentch, C. S.. 1965. Distribution of chlorophyll and phaeophytin in the open ocean. Deep Sea Research, 12, 653-666.
- Young, H.W., J.C. Young, M. Boybay and T. Demirel. 1983. Effect of chemical treatment of fly ash on the leaching of metals. In: Hazardous and Industrial Waste Management and Testing, Third Symposium, L.P. Jackson, A.R. Rohlik and R.A. Conway (Eds.). ASTM Publication Code No. 04-851000-16. American Society for Testing and Materials, Philadelphia, PA, pp. 10-117.